7-22-2014 12:00 AM

Understanding the role of cholinergic tone in the pedunculopontine tegmental nucleus

Kaie Rosborough
The University of Western Ontario

Supervisor
Dr. Vania Prado
The University of Western Ontario

Graduate Program in Anatomy and Cell Biology
A thesis submitted in partial fulfillment of the requirements for the degree in Master of Science

UNDERSTANDING THE ROLE OF CHOLINERGIC TONE IN THE PEDUNCULOPONTINE TEGMENTAL NUCLEUS

Thesis format: Monograph Article

by

Kaie Rosborough

Graduate Program in Anatomy and Cell Biology

A thesis submitted in partial fulfillment
of the requirements for the degree of
Masters of Science

The School of Graduate and Postdoctoral Studies
The University of Western Ontario
London, Ontario, Canada

Abstract

To better understand the role of cholinergic signaling in specific regions of the brain, several genetically modified mice targeting the vesicular acetylcholine transporter (VAChT) gene have been generated (Prado et al., 2006; Guzman et al., 2011; de Castro et al., 2009). VAChT stores acetylcholine (ACh) in synaptic vesicles, and changes in this transporter expression directly interferes with ACh release. Here, we use a mouse line with VAChT deletion in the pedunculopontine tegmental nucleus (PPT) to evaluate the consequences of decreased cholinergic signaling from the PPT *in vivo*. Based on the efferent connectivity from the PPT, our hypothesis is that decreased cholinergic signaling from the PPT will affect specific behavioural outputs. It was determined that these mice have strong deficits in spatial and goal-directed learning as well as an antidepressive-like phenotype. Mild phenotypes include gait abnormalities, anxiety-like behavior and decreased compulsivity. Improving our understanding of cholinergic signaling from the PPT and how it relates to behavioural abnormalities may lead to the development of novel treatments for the symptoms of neurological diseases such as PD and PSP, which show degeneration of PPT neurons (Hirsch et al. 1987).

Keywords

Pedunculopontine tegmental nucleus, acetylcholine, genetically modified mice

List of Abbreviations

5CSRTT	5-choice serial reaction time task
7N	Facial nerve
Ach	Acetylcholine
ARAS	Ascending reticular activating system
ATN	Anteroventral thalamic nucleus
ChAT	Choline acetyltransferase
CHT1	High-affinity choline transporter 1
CNS	Central nervous system
CPu	Caudate/putamen
CuN	Cuneciform nucleus
DA	Dopamine
DR	Dorsal raphe
GABA	Gamma-aminobutyric acid
GAD	Glutamic acid decarboxylase
GPe/GPi	External globus pallidus/ Internal globus pallidus
FST	Forced swim test
LDT	Lateral dorsal tegmentum
mAChRs	Muscarinic acetylcholine receptors
MD	Mediodorsal thalamic nucleus
Mo5	Motor trigeminal nucleus
MWM	Morris water maze
NAc	Nucleus accumbens
nAChRs	Nicotinic acetylcholine receptors
PD	Parkinson's disease
PNS	Peripheral nervous system
PPN	Pedunculopontine nucleus (humans)
PPT	Pedunculopontine tegmental (rodents)
PSP	Progressive supranuclear palsy
REM	Rapid eye movement
SC/IC	Superior colliculus/ Inferior colliculus
Ser	Serotonin
SNc/SNr	Substantia nigra pars compacta/ Substantia nigra pars reticulata
STN	Subthalamic nucleus
TAN	Tonically active neurons
TST	Tail suspension test
VAChT	Vesicular acetylcholine transporter
VGluT	Vesicular glutamate transporter
VP	Ventral pallidum
VTA	Ventral tegmental area

Acknowledgments

I would like to thank my lab members, Ashbeel Roy, Mohammed Al-Onaizi, Dr. Monica Guzman, Dr. Flavio Beraldo, Ben Kolisnyk, Gustavo Parfitt, Jue Fan and Sanda Raulic for their invaluable assistance over the course of my study.

I would also like to thank my supervisors, Drs. Marco and Vania Prado, for their support and guidance. Their encouragement and suggestions have been instrumental in my completion of this thesis.

Finally, I would like to thank my supervisory committee members, Dr. Shawn Whitehead, Dr. Susanne Schmid and Dr. Arthur Brown for their mentorship and constructive input.

Table of Contents

List of Figures

List of Tables

Chapter 1

1 The Cholinergic System

Acetylcholine (ACh) was the first neurotransmitter to be discovered. This neurotransmitter, described by Otto Loewi in 1921 (Mesulam et al., 1984), is one of the major neurotransmitters in the central nervous system (CNS), and it is also the main neurotransmitter in the peripheral nervous system (PNS) In the CNS, there are two primary sources of acetylcholine: local interneurons or projection neurons that innervate distal targets. Tonically active cholinergic interneurons are located mainly in the dorsal striatum and the nucleus accumbens (reviewed by Picciotto et al., 2012). Projection neurons originate mainly from two brain regions: the pedunculopontine nucleus and lateral dorsal tegmentum nuclei (together known as the mesopontine tegmentum) located in the brainstem (Mesulam et al., 1995), and also from the basal forebrain (Zaborszky et al., 2008). Mesulam and colleagues (1984) utilized immunohistochemistry to divide all the cholinergic neurons into six major categories based on their connectivity patterns in the rat and primate brain. The Ch1 and Ch2 groups of neurons provide the major cholinergic input to the hippocampus. The Ch3 group project to the olfactory bulb and the Ch4 group of cholinergic neurons topographically innervate the entire neocortical mantle. The Ch5 and Ch6 groups are the major source of cholinergic innervation of the thalamus. Each of the Ch categories are also delineated by distinct nuclear boundaries (Mesulam et al., 1984).

ACh can act as a neuromodulator in the CNS by changing the state of neurons so their response to subsequent stimulation is altered (Picciotto et al., 2012). The actions of ACh are mediated through receptors on a large number of neuronal subtypes, both pre- and post-synaptically. These receptors fall into two classes: metabotropic acetylcholine receptors (mAChRs) and ionotropic nicotinic acetylcholine receptors (nAChRs) (reviewed by Picciotto et al., 2000; Wess 1996).

There are five unique subtypes of the mAChR receptor (M1-M5), all of which are G-protein-coupled receptors (Wess 1996). mAChR are linked to either G_q or $G_{i/o}$ type G-

proteins. The M1, M3 and M5 receptors are linked to the G_q protein, whereas the M2 and M4 receptors are coupled to $G_{i/o}$ type G-proteins (Wess 1996). The G_q proteins activate phospholipase C, while $G_{i/o}$ proteins negatively couple to adenylate cyclase (Wess 1996).

The nAChRs are non-selective cation channels with a molecular mass of 290 kDA that cause depolarization of the neuron (Changeux et al., 1998; Picciotto et al., 2001). These allosteric receptors respond to ACh and nicotinic agonists by quickly (μs to ms range) opening the channel that is permeable to Na^+, K^+ and sometimes Ca^{2+} ions (Changeux and Edelstein, 2005). nAChRs are transmembrane oligomers made up of five subunits symmetrically arranged around a central ionic channel. The combinations of subunits have distinct expression patterns in specific neuronal types (Gotti et al., 2007). The nAChR subunits, encoded by 12 genes, have been classified into two subfamilies of proteins: nine α-subunits (α2-α10) and three β–subunits (β2-β4) (Gotti et al., 2007). The nAChRs can also be classified based on their pharmacological properties into groups of receptors that are sensitive to α-Bungarotoxin (homomeric and heteromeric receptors consisting of α7, α8, α7-8, α9 and/or α10 subunits) and receptors that are insensitive to α-Bungarotoxin (heteromeric receptors consisting of α2-α6 and β2-β4 subunits) (Gotti and Clementi, 2004). The various nAChRs subunit combinations differ in their cellular localization in the brain. There are two main types of nAChRs in the brain: the α7 homo-oligomer and the α4β2 hetero-oligomer (Changeux and Edelstein, 2005). The α7 nAChR is characterized by fast activation and desensitization, a low affinity for ACh and a high Ca^{2+} permeability (Gotti et al., 2007) and it is located presynaptically (Jones and Wonnacott, 2004). The α4β2 nAChR is characterized by a low desensitization, a high affinity for ACh and nicotinic agents, and it is strongly upregulated by nicotine exposure (Changeux and Edelstein, 2005, Picciotto et al., 2001; Reviewed by Buisson and Bertrand, 2002). β2-containing nAChRs and α7 nAChRs are widely expressed in the brain (Gotti et al., 2007) whereas other subtypes have a more restricted expression. Interestingly, chronic exposure of nAChRs to ACh or nicotinic agonists results in a gradual decrease in the rate of response to the ligand and ultimately a high-affinity, desensitized, closed state of the receptor (Changeux and Edelstein, 2005).

1.1 Acetylcholine

To synthesize ACh, the precursor choline must be brought into the cell by the high-affinity choline transporter (CHT1) or SLC5A7 (solute carrier family 5 member 7) (reviewed by Ribeiro et al., 2006). Once in the cytoplasm of nerve terminals, choline is used to synthesize ACh by the enzyme choline acetyltransferase (ChAT) (Prado et al., 2002; Parsons 2000). The vesicular ACh transporter (VAChT) or SLC18A3 (solute carrier family 18 member 3) loads ACh into synaptic vesicles (Prado et al., 2002; Parsons 2000). Thousands of molecules of ACh are packaged into a synaptic vesicle to form a quantum so ACh can be released by exocytosis.

1.2 The High-Affinity Choline Transporter

In the CNS, cholinergic neurons are incapable of synthesizing ACh *de novo*, so their ability to signal with this neurotransmitter depends on the neurons ability to uptake choline (Tucek 1985). To do this, neurons have two carrier-mediated transport systems for choline uptakewhich are located in the pre-synaptic nerve terminal (Haga 1971). The concentrations of available choline in the extracellular space determines which system is used for choline transport. At high concentrations, choline is transported into the neuron by a low-affinity system that is Na^+-independent, whereas at low concentrations, the high-affinity Na^+-dependent system predominates. The high-affinity transporter is distinguished from the low-affinity transporter by its inactivation by hemicholinium-3 as well as its dependence on extracellular Na^+ and Cl^- levels (Yamamura and Snyder, 1972). Okuda and Haga (2000) were the first to isolate the cDNA encoding CHT1 in the rat brain. CHT1 is unique to cholinergic neurons because choline is specifically converted into ACh only when the high-affinity transporter is used, whereas choline taken up with the low-affinity transporter is not converted to ACh (Yamamura and Snyder, 1972). Choline uptake is believed to be the rate-limiting step in ACh synthesis (Okuda and Haga, 2000). In order to maintain ACh synthesis, CHT1 is used to recover choline from the synapse after ACh hydrolysis by AChE (Birks and MacIntosh, 1961). While CHT1 function is predominantly at the plasma membrane, it has been demonstrated that this protein is located on the plasma membrane, as expected, but also on presynaptic vesicles that were positive for VAChT (Ribeiro et al., 2003; Ferguson et al., 2003).

Depolarization leads to an increase in the V_{max} for high-affinity choline uptake as well as an increase in the density of CHT proteins in the plasma membrane (Ribeiro et al., 2003; Ferguson et al., 2003). These results suggest that large intracellular stores of CHT1 are available to be delivered to the plasma membrane when the rate of ACh release is increased.

1.3 The Enzyme Choline Acetyltransferase

ChAT is a single-stranded globular protein that mediates the transfer of an aceyl group from acetyl coenzyme A (acetyl-CoA) to choline at the synaptic terminals of cholinergic neurons to generate ACh (Oda 1999). The enzyme is synthesized in the perikaryon of cholinergic neurons and is transported to the nerve terminal through axoplasmic flow (Oda 1999). There, it can exist in two forms: a soluble form (80-90% of total enzyme activity) and an insoluble membrane-bound form (10-20% of total enzyme activity). Smith and Carroll (1993) demonstrated that in the rat hippocampal tissue, ChAT can be fractionated with synaptic vesicles, suggesting that a portion of the membrane-bound ChAT may be attached to cholinergic synaptic vesicles by a glycosyl-phosphatidylinositol anchor.

Genomic studies by Misawa et al. (1992) have identified a number of ChAT mRNA species that are transcribed from different promoter regions and produced by differential splicing. Interestingly, the genomic structure of ChAT is unique in addition to being complex: the VAChT gene is embedded in the first intron of the ChAT gene (Erickson et al., 1994), which was subsequently named the “cholinergic gene locus” (Erickson et al., 1994; Eiden 1998). Inside the first intron there is a 1590 bp open reading frame (ORF) that encodes the VAChT protein, which is in the same transcriptional orientation as the ChAT gene (Bejanin et al., 1994). Alternative splicing of this single precursor mRNA gives rise to two proteins involved in sequential biochemical steps: synthesis and storage of ACh (Alfonso et al., 1994). Several studies have confirmed the coexpression of the ChAT and VAChT proteins. Benjanin et al. (1994) investigated whether signals (such as retinoic acid) that induced ChAT gene expression also induced VAChT gene expression, and found that the agents increased the mRNA and protein levels of both products, indicating a common regulatory mechanism of their transcription.

In *Drosophila*, VAChT and ChAT transcripts contain the same complete first exon and use a common promoter upstream of the ChAT first exon (Kitamoto et al., 1998). However, in vertebrates, the expression mechanisms are far more complicated. There are several different promoters in the 5' region of the cholinergic gene locus: a common promoter for R-type ChAT and VAChT mRNA (upstream of ChAT exon R), two promoters for VAChT mRNA between ChAT exon R and the VAChT ORF, and one promoter for M-type ChAT mRNA between ChAT exons N and M (Mallet et al., 1998). The different ChAT mRNA transcripts are summarized in Figure 1.

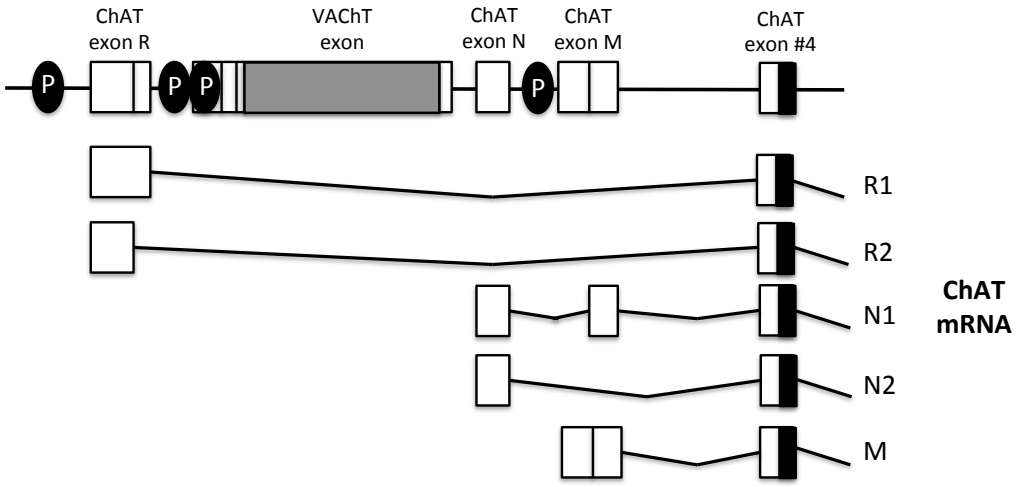

Figure 1. The vertebrate cholinergic gene locus and the five ChAT mRNA transcripts produced by differential splicing. P = promoter. Adapted from Mallet et al. 1998.

The primary structure for ChAT reveals a number of putative phosphorylation sites and short-term post-translational regulation of the ChAT enzyme by protein kinases has been demonstrated. For instance, Dobransky et al. (2001) demonstrated that phosphorylation of serine 440 by protein kinase C (PKC) increased enzyme activity, and may also alter subcellular localization (Dobransky et al., 2001). It is likely that phosphorylation influences whether the protein will be soluble or membrane-bound and as well as the enzyme's catalytic activity, which in turn alters the biosynthesis of ACh (Cooke and Rylett, 1997).

1.4 The Vesicular Acetylcholine Transporter

VAChT is also critical to the functioning of the cholinergic system as it is required for ACh storage. The importance of VAChT is emphasized by VAChT knockout mice that cannot survive after birth due to respiratory dysfunction and atrophied skeletal muscle (de Castro et al., 2009). The consequences of reduced VAChT expression have been demonstrated using genetically modified mice with a knockdown of VAChT gene expression. The homozygous VAChT knockdown mice (VAChT-KD^{HOM}) have a 62% decrease in VAChT protein levels and present severe muscular fatigue and cognitive alterations. However, heterozygous VAChT knockdown mice (VAChT-KD^{HET}) have a 40% decrease in VAChT expression but they survive into adulthood with no muscular dysfunction but similar cognitive changes to those seen in the VAChT-KD^{HOM} mice (Prado et al., 2006).

VAChT is a 12-transmembrane domain protein with a 75 kDa molecular mass that is part of the Major Facilitator Superfamily of transporters (Alfonso et al., 1994; Erikson et al., 1994; Vardy et al., 2004). The exact three-dimensional structure of VAChT is not known, but a model has been proposed based on the structure of two other members of this family: lactose permease and glycerol 3-phosphate (Vardy et al., 2004). The 12 transmembrane helices are suggested to form two bundles, one composed of helices I-IV and the other composed of helices VII-XII (Khare et al., 2010), with both the N- and C-terminus regions projecting into the cytoplasm. It is helix X that contains Trp331 and Asp398 which are the amino acids involved in ACh binding and proton translocation, respectively (Fritz et al., 2001; Kim et al., 1999). VAChT has been localized to the perinuclear region in the cell bodies of ChAT-positive neurons, as well as to the nerve terminals (Roghani et al., 1998). Of the two types of secretory vesicles in the cholinergic nerve terminal (synaptic vesicles and large-dense core vesicles, LDCVs), immunogold studies indicate that VAChT is found in the synaptic vesicle population (Gilmore et al., 1996). The C-terminal of VAChT contains a di-leucine motif required for clathrin-mediated endocytosis, and this is the site of regulation for its trafficking within the neuron (Varoqui and Erickson 1998; Barbosa J Jr et al., 2002; Ferreira et al., 2005). The amino acid sequence of the C-terminal tail of VAChT reveals a consensus

phosphorylation site for PKC, suggesting that post-translational modification of VAChT could change ACh storage, and subsequently release (Erickson et al., 1994, Roghani et al., 1994). Specifically, Krantz et al. (2000) identified serine 480 as the major phosphorylation site in the protein and PKC as the kinase involved. Krantz et al. (2000) also demonstrated in stable transfected PC12 cells that a S480E mutation increases VAChT expression in LDCVs by diverting VAChT trafficking away from endosomes.

VAChT utilizes the electrochemical gradient created by V-type proton ATPase (Parsons 2000) to bring ACh into the synaptic vesicle by exchanging two luminal protons for a cytoplasmic ACh molecule (Nguyen et al., 1998). The impermeability of the secretory vesicles provides a large proton-motive force that drives the accumulation of ACh inside the vesicle so that the vesicular ACh concentration is 100-fold greater than the cytoplasmic concentration (Eiden 1998). However, the electrochemical potential created by the ATPase is sufficient to concentrate ACh 3000-fold greater in synaptic vesicles than in the cytoplasm, suggesting that there are regulatory mechanisms that arrest the vesicular ACh filling (Parsons 2000). Varoqui and Erickson (1996) demonstrated that VAChT is a very slow transporter, and that in PC12 cells that overexpress human VAChT, the transport of [^{3}H]ACh is saturable, suggesting that VAChT is likely the rate-limiting step for ACh release from the nerve terminal. The level of expression of VAChT thus has a great influence on the release of this neurotransmitter. Song and colleagues (1997) over-expressed VAChT in xenopus neurons and found that it increased the amount of ACh released by the synaptic vesicles. As well, they found that the neuron had an increase in the number of miniature EPSPs, which suggests that more synaptic vesicles were becoming competent to store and release ACh than usual (Song et al. 1997). Synaptic vesicles themselves do not regulate the amount of ACh stored within them, but the level of VAChT expression on the vesicle dictates the amount of neurotransmitter released (Prado et al., 2002).

1.5 ACh-Glutamate Co-transmission

Recent studies have shown that some cholinergic neurons in the brain express a vesicular glutamate transporter (VGluT) in addition to VAChT, and thus have the potential to release both ACh and glutamate. For example, cholinergic neurons in the

striatum co-express VGluT3 (Schafer et al., 2002; Gras et al., 2008; Guzman et al., 2011). Basal forebrain cholinergic neurons projecting to the amygdala also co-express VGluT3 (Nickerson et al., 2006). While the mechanisms of regulation of VAChT are unknown, it has been shown that ACh loading into the synaptic vesicles can be influenced by the VGluT3 activity through a process called vesicular synergy (Gras et al., 2008). It has been suggested by Hnasko and collegues (2012) that accumulating the negatively charged glutamate inside these cholinergic neurons changes the pH value to increase VAChT transport activity.

In a number of studies, animal models of cholinergic deficiency have generated by using electrolytic or excitotoxic methods, as well as cholinergic immunolesion, to ablate cholinergic neurons (Schliebs and Arendt, 2006). These studies often destroy non-cholinergic neuron in addition to the cholinergic neurons, or they do not fully deplete the cholinergic neurons. More importantly, lesions destroy neurons that may be co-releasing glutamate and ACh, which prevents researchers from distinguishing the behavioural effects of these two neurotransmitters. The use of genetically modified mice with VAChT knockouts restricted to a unique brain region provides a means to elucidate the role of cholinergic deficiency specifically (Guzman et al., 2011; Martyn et al., 2012; Kolisnyk et al., 2013).

The comparison of striatal VGluT3-KO mice with striatal VAChT-KO mice ($VAChT^{D2\text{-}Cre\text{-}flox/flox}$ mice) highlights the effect of ACh/glutamate co-transmission, and also the importance of separating the physiological role of each of these neurotransmitters (Guzman et al., 2011). For instance, mice with a lesion of cholinergic neurons in the striatum have been found to be hyperactive and more responsive to cocaine than controls (Hikida et al., 2001; Kitabatake et al., 2003), so this phenotype was initially attributed to the loss of cholinergic signaling from striatal interneurons. Two genetically modified mouse lines were created to differentiate the behaviours controlled by the glutamateric and cholinergic neurotransmission. VGluT3-KO mice did not have glutamate release from the striatal cholinergic interneurons, and behavioural analysis of these VGluT3-KO mice revealed that they are also hyperactive and more responsive to cocaine than controls (Gras et al., 2008). The $VAChT^{D2\text{-}Cre\text{-}flox/flox}$ mice do not release acetylcholine from

striatal cholinergic interneurons but the behavioural analysis of these mice revealed that they are not hyperactive and they do not have altered cocaine-induced behaviour (Guzman et al., 2011). This comparison suggests that it was the glutamate release from the cholinergic neurons, not the ACh release that was responsible for the phenotype observed in the lesion studies.

2 Pedunculopontine Tegmental Nucleus

Integrity of the proteins involved in ACh synthesis, storage and release, functioning muscarinic and nicotinic receptors and intact neurons are all critical for the functioning of the cholinergic system. Dysfunction of the cholinergic system has been implicated in a number of diseases, such as Alzheimer's disease (Prado et al., 2013). The potential role of altered cholinergic signaling in neurobiological disease has brought the pedunculopontine nucleus (PPN, in humans) or pedunculopontine tegmentum (PPT, in rodents) into the scientific spotlight. Significant loss of cholinergic neurons of the PPT has been demonstrated in post-mortem studies of patients with Parkinson's disease (PD) and progressive supranuclear palsy (PSP), a Parkinson's-like syndrome (Jellinger 1988, Warren et al., 2005). It has been shown that 40-50% of PPN cholinergic neurons degenerate in Parkinson's patients and over 60% degenerate in patients with PSP (Jellinger 1988). Understanding the behaviours regulated by this cholinergic nucleus is fundamental in determining how degeneration in this area leads to the symptoms observed in PD and PSP patients.

2.1 PPT Anatomy

The PPT is composed of a highly heterogeneous population of neurons that differ by their connectivity, behaviours they regulate, and their discharge properties (Martinez-Gonzalez 2012). The three major neuron types in the PPT are cholinergic, GABAergic and glutamatergic (Martinez-Gonzalez 2012). Not only are the types of neurons and their function heterogeneous, but so is the distribution of these neuronal subtypes across the PPT. The pedunculopontine tegmental nucleus has two subdivisions based on the cell density and distribution of the Ch-5-group cholinergic neurons: the pars compacta (PPTc) and pars dissipates (PPTd) (Papahill et al., 2000). However, these two subdivisions may

best be considered anatomically as a two-component structure, with each component being responsible for distinct behavioural and psychological functions (Winn 2006).

Immunolabeling has identified a rostro-caudal distribution of ChAT-labeled cholinergic neurons, with more of these neurons in the caudal portion of the PPT (Martinez-Gonzalez 2012). GABAergic neurons are more concentrated in the rostral PPT and glutamatergic neurons are more concentrated in the caudal PPT (Martinez-Gonzalez 2012). The rostro-caudal distribution of the different neuronal subtypes is highlighted by the changes in cytoarchitecture and organization of the cholinergic neurons along this axis (Martinez-Gonzalez et al., 2011). Where there is low GABAergic neuron density (caudal PPT) the cholinergic neurons are bipolar-shaped and organized in a layer like structure; where GABAergic neuron density is high, the cholinergic neurons are round-shaped and in a random distribution (Martinez-Gonzalez et al., 2011). The unique distribution of each neuron subtype is related to the distinct connectivity of the rostral and caudal portions of the PPT, which suggests that the two regions might be functionally distinct. Neurochemically, the rostral and caudal sections of the PPT each have distinct and diverging projections that innervate distant structures (Martinez-Gonzalez et al., 2011).

In addition to the two shapes of the cholinergic neurons in the PPT, they have also been shown to have two types of firing patterns: slow-firing and fast-firing (Martinez-Gonzalez et al., 2011). Mena-Segovia et al. (2008) demonstrated that the slow-firing neurons correlate to the cortical upstate during slow oscillations and the fast-firing neurons correlate to the cortical downstate during slow oscillations.

Understanding the different roles each neuronal subtype of the PPT plays in regulating behaviour is further complicated by the fact immunohistochemistry studies revealed that 40% of cholinergic neurons in this region also show glutamate immunoreactivity (Lavoie and Parent, 1994), suggesting that these neurons can co-release acetylcholine and glutamate. Immunolabeling studies also suggest that some cholinergic neurons of the PPT coexpress GABA markers as well (Wang and Morales, 2009). However, when mRNA transcripts of ChAT and glutamic acid decarboxylase (GAD;

required for production of GABA) were evaluated using *in situ* hybridization, they found that only 2% of PPT cholinergic neurons expressed GAD mRNA (Wang and Morales, 2009).

2.2 PPT Connectivity

2.2.1 Efferent Connectivity

A fundamental characteristic of the PPT is the long axons of the cholinergic neurons that project to very distant structures and have as many as five or six collaterals (Mena-Segovia et al. 2008).

Numerous tracer experiments have shown that the PPT projects to unique regions within the basal ganglia system. The subthalamic nucleus (STN) receives cholinergic, GABAergic and glutamatergic input from the caudal PPT in the monkey (Lavoie and Parent, 1994; Bevan and Bolam, 1995; Martinez-Gonzalez et al. 2009). The internal globus pallidus (GPi) in monkeys receives projections from the rostral PPT, of which 40% of the neurons are cholinergic (Woolf and Butcher, 1986; Edley and Graybiel, 1983). The external globus pallidus (GPe) receives only a small input from the PPT (Charara and Parent, 1994). The dopaminergic neurons of the substantia nigra (SN) receive input from the rostral PPT, specifically the *pars compacta* region (SNc) (Futami et al., 1995; Charara et al., 1996). In monkeys, 25% of these neurons are cholinergic (Lavoie and Parent, 1994). The ventral tegmental area receives significant cholinergic input from the caudal PPT in primates (Charara et al., 1996). The thalamus is one of the primary output centres of the PPT and it is heavily innervated by cholinergic neurons from the caudal PPT in the monkey (Parent et al., 1988, Takakusaki et al., 1996). Additionally, the striatum also receives direct projections from the PPT (Nakano et al., 1990; Dautan et al., 2014).

Until recently, it was believed that cholinergic interneurons were the only source of ACh in the striatum, and that the PPN only influenced the striatum indirectly through one of two routes: (1) innervation of midbrain dopaminergic neurons (Bolam et al., 1991) leading to increased dopamine release onto the striatum (Blaha and Winn, 1993) and (2) through innervation of the intralaminar and midline thalamus (Mena-Segovia et al., 2008)

which then project to the striatum (Erro et al., 1999). However, Dautan et al. (2014) used a Cre-driven mouse line to express the fluorescent protein YFP in cholinergic neurons (immunolabeled for ChAT) to reveal direct cholinergic innervation of both the dorsal striatum and nucleus accumbens from the PPT and LDT. These authors showed that the rostral PPT innervates the dorsolateral striatum, and the caudal PPT innervates the dorsomedial striatum and nucleus accumbens. Additionally, electron microscopy analysis of cholinergic synapses revealed that the 74% of synapses from rostral PPN contacted dendritic shafts, suggesting they contact striatal interneurons, and 26% made contact with the medium spiny neurons.

Additional areas that have been shown to receive cholinergic inervation from the PPT are: the inferior and superior colliculi which receive fibers from the caudal PPT (Mena-Sogovia et al., 2008); the basal forebrain (specifically the magnocellular preoptic area and the nucleus basalis magnocellualris) which also receives input from the caudal PPT (Semba et al., 1988; Losier and Semba, 1993; Mena-Segovia et al., 2008); the posterior lateral hypothalamus (Ford et al., 1995) as well as lower brainstem, pons, medulla and spinal cord (Martinez-Gonzalez et al., 2009) (Martinez-Gonzalez et al., 2009). PPT projections to the spinal cord that are thought to be directly involved in locomotion are primarily non-cholinergic (Skinner et al., 1990). Several studies have also shown that there is collateralization of targets by the same PPT neurons. For instance, Takakusakai et al. (1996) demonstrated that one individual cholinergic neuron will project to the SN, thalamus as well as caudal regions in the brainstem. The efferent connections from the PPT are summarized in Figure 2.

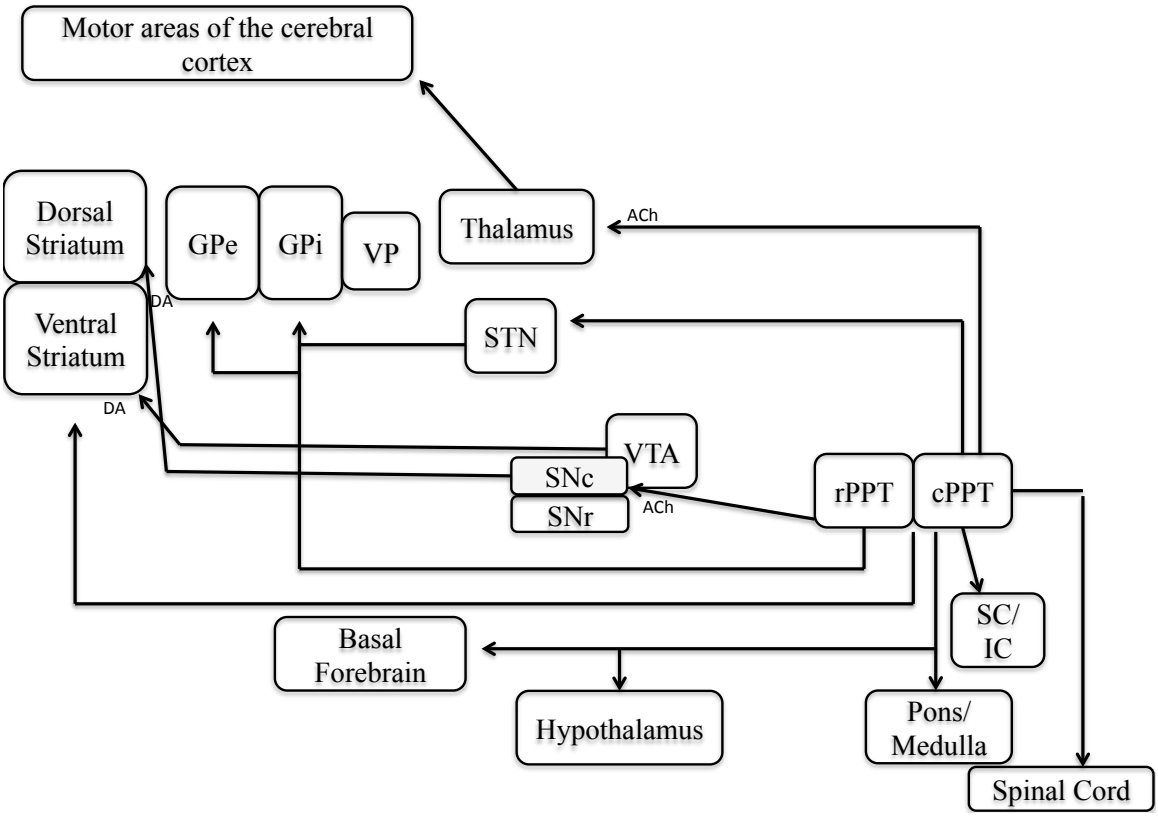

Figure 2. Summary of efferent connections of the PPT. GPe = external globus pallidus, GPi = internal globus pallidus, VP = ventral pallidus, SNc = substania nigra *pars compacta*, SNr = substantia nigra *pars reticulate*, VTA = ventral tegmental area, rPPT = rostral pedunculopontine tegmental nucleus, cPPT = caudal pedunculopontine tegmental nucleus, SC = superior colliculus, IC = inferior colliculus.

2.2.2 PPT Afferent Connectivity

There is not as detailed information regarding the afferent innervation of the PPT, but it is known that there are direct afferents from the cerebral cortex, thalamus, hypothalamus, pons, cerebellum, medulla, spinal cord and basal ganglia (Saper and Loewy, 1982; Semba and Fibiger, 1992).

In monkeys, the prefrontal and frontal lobe areas of the cerebral cortex that are involved in motor control have direct excitatory projections to the PPT (Matsumura et al., 2000; Martinez-Gonzalez et al., 2011). As well, tracer studies in primates have shown the basal ganglia system sends direct projections to the PPT. The STN directly targets neurons in the PPT with an excitatory input (Nauta and Cole, 1978; Martinez-Gonzalez

2011) and also indirectly though the SN (Florio et al., 2007). Additionally, the SN *pars reticulata* (SNr) has direct projections to the rostral PPT (Nakamura et al., 1989; Semba and Fibiger, 1992; Spann and Grofova, 1991). The enteropeduncular nucleus (rodents) or GPi (humans) sends GABAergic projections to the rostral PPT (Morizumi and Hattori, 1992). The ventral striatum was shown to project GABA-releasing neurons to the PPT in monkeys (Haber et al., 1990).

The PPT receives afferents from deep cerebellar nuclei (Hazarati and Parent, 1992) and receives fast sensory input from superior colliculi in the rat tectum (Woolf and Butcher, 1986; Semba and Fibiger, 1992). In tracer studies of the rat brainstem, it has been shown that the dorsal raphe neurons innervate the caudal PPT providing a serotonergic input (Steininger et al., 1992). The PPT also receives input from the laterodorsal tegmental nucleus (LDTg) and the contralateral PPT (Semba and Fibiger, 1992).

As a result of these connections, the PPT receives both sensory and motor inputs, as summarized in Figure 3.

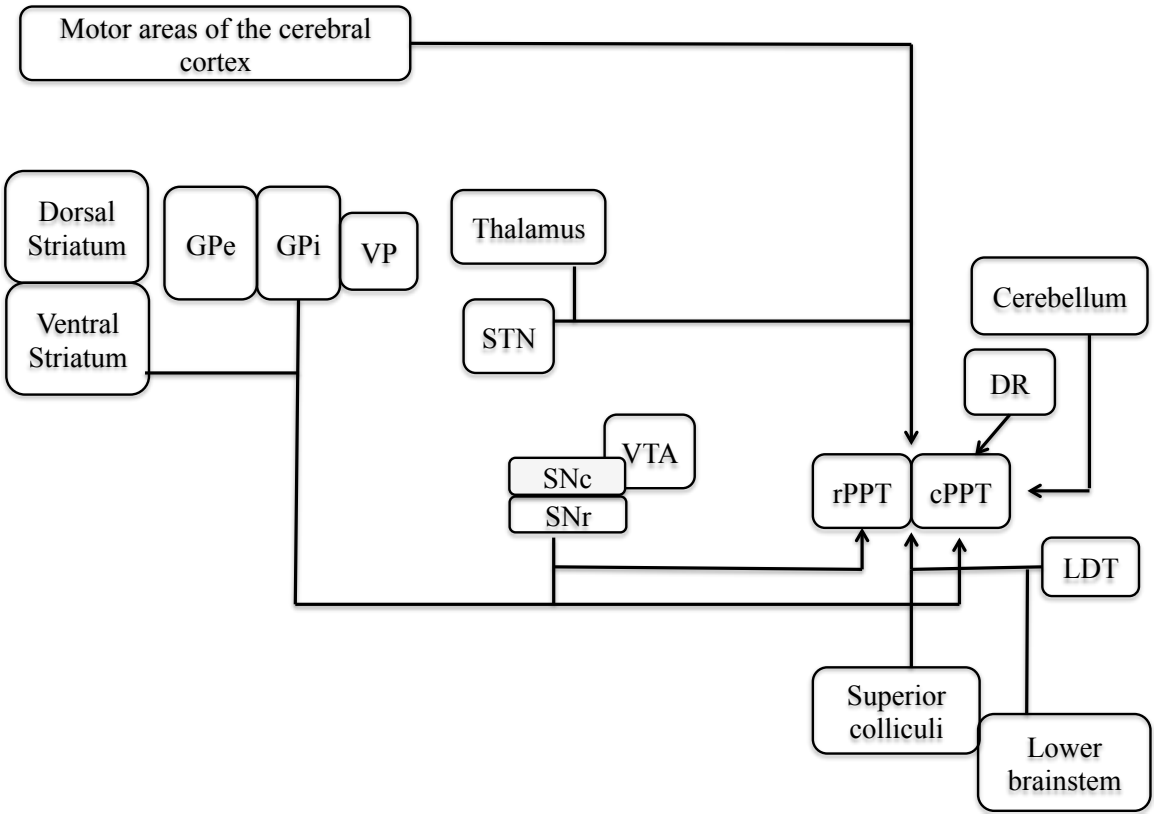

Figure 3. Summary of afferent connections to the PPT. GPe = external globus pallidus, GPi = internal globus pallidus, VP = ventral pallidus, SNc = substania nigra *pars compacta*, STN = subthalamic nucleus, SNr = substantia nigra *pars reticulate*, VTA = ventral tegmental area, DR = dorsal raphe, rPPT = rostral pedunculopontine tegmental nucleus, cPPT = caudal pedunculopontine tegmental nucleus, LDT = laterodorsal tegmentum.

2.3 PPT Function

The PPT, with its widespread-projecting neurons and heterogeneous neuronal subpopulations, is thought to have a complex role in a number of signaling networks in the brain. Many studies have investigated the possible functional role of the PPT, and to date, this nucleus is thought to be involved in locomotion and gait, REM sleep/brain state transitions, and cognitive functions such as attention and reward learning (Winn et al., 2011).

2.3.1 Locomotion and Gait

Strong reciprocal connections have been shown between the PPT and structures involved in the control of motor performance such as the basal ganglia; specifically, the STN, the SN and the GP (Bolam et al., 1991; Winn et al., 1997; Kita and Kita, 2011). Recent studies with retrograde and anterograde tracing have identified neuronal circuitry that is likely to be responsible for the control of locomotion, posture and muscle tone. Rolland et al. (2011) proposed that the SNr-PPT-reticulospinal circuit could control posture and axial muscle tone, and the GPi-PPT-reticulospinal circuit could control gait and locomotion (Rolland et al., 2011). Hikosaka et al. (2000) expanded on the role of the basal ganglia in the control of movements by suggesting that the basal ganglia has two kinds of outputs: the thalamocortical network to control volitional movement, and the outputs to the PPT to control autonomic movements such as saccades and locomotion.

Literature confirming the role of the PPT in locomotion is mixed, however. While the PPT is considered to be part of the mesencephalic locomotor region, bilateral excitotoxic lesions of the whole PPT failed to show any effects on locomotion (Inglis et al., 1994) while bilateral lesions of just the anterior PPT causes a reduction of locomotion in rats (Alderson et al., 2008). Takakusaki (2008) suggested that the PPT is required for the initiation and maintenance of motion, and in primates, lesioning the PPT with high frequency stimulation causes akinesia (Nandi et al., 2002).

Neuropathalogical studies have shown that in humans, 40%-60% of the cholinergic neurons in the PPT degenerated in PD and PSP patients, respectively (Jellinger 1988; Bohnen and Albin, 2011). This degeneration of PPT cholinergic neurons results in cortical and thalamic cholinergic denervation, which is related to gait and balance issues in these individuals with PD (Bohnen et al., 2009). The AChE inhibitor donepezil reduced the number of falls in patients with PD by 50% (Chung et al., 2010). Interestingly, in a rat model of PD (created with 6-hydroxydopamine lesions of the medial forebrain), analysis of firing patterns of neurons in the basal ganglia system and PPT following lesion revealed that the resulting increased oscillatory activity in the STN and SNr is transmitted to the PPT as inhibitory oscillatory output (Aravamuthan et al.,

2008). These results emphasize the relationship between the PPT, basal ganglia and motor disturbances in PD.

2.3.2 Cognitive functioning

In addition to the locomotor and gait abnormalities observed in individuals with PD or PSP, the loss of cholinergic PPT neurons in both diseases is also thought to play a role in the attentive and cognitive impairments seen in patients (Scarnati and Florio, 1997).

2.3.2.1 Arousal and Attention

Electroencephalography (EEG) has been used to monitor the electrical activity in the cortex, and there is a pattern of electrical potentials corresponding to an arousal state (McCormick 1989). For instance, during slow-wave sleep there is a synchrony of cortical activity, but during wakefulness and alertness there is a desynchronization of the electrical activity (McCormick 1989). It is known that the thalamus mediates these brain state transitions by coordinating the neuronal changes from a slow firing rate to phasic burst firing (Mena-Segovia et al., 2008). The connection between the intralaminar thalamic nuclei and the PPT has been associated with arousal and attention (Steriade et al., 1988). Electrical stimulation of the PPT results in this desynchronized EEG, which supports the role of the PPN in thalamocortical process like arousal (McCormick 1989). Kobayashi and Isa (2002) found that increased excitability of thalamic neurons increases visual acuity by decreasing the signal-to-noise ratio of the incoming sensory information. Behaviourally, this increases alertness and awareness of sensory information from the environment.

The interaction between the PPT and the thalamus is also thought to influence attention. Attention involves the ability to detect sensory stimuli, maintain readiness to respond to stimuli (sustained attention), discriminate significant from insignificant stimulus (selective attention) and to select and perform the appropriate motor response (executive control) (Inglis et al., 2000). The 5-choice serial reaction time task (5CSRTT) is frequently used to evaluate attentional processes in rodents. In the 5-CSRTT paradigm, animals are required to detect brief flashes of light presented pseudorandomly

in one of five locations on a screen and to make a nose-poke response in the correct spatial location in order to receive a food reward (Bari et al., 2008). The accuracy of the animal's response to the light stimulis provides an index of attentional capacity (Bari et al., 2008). Inglis et al. (2000) lesioned the PPT in mice and evaluated the resulting affects on attention using this task. Mice with bilateral PPT lesions showed decreased accuracy and a very high percentage of trials on which no response was made (omissions) when attentional demands of the task were increased by decreasing the stimulus duration. These results suggest that the mice are not vigilant to the stimuli, which emphasizes the importance of the integrity of PPT signaling in attentional processes.

2.3.2.2 Working memory

The PPT-thalamus circuit has been suggested to be involved in working memory. Cholinergic innervation to the anteroventral thalamic nucleus (ATN) were shown to be responsible for spatial- and context-dependent memory (Mitchell et al., 2002). Additionally, lesions of the ATN in rats led to significant spatial memory deficits in the radial maze (Sziklas and Petrides 1999). The ATN receives one of the highest numbers of cholinergic terminals in all of the thalamus from the PPT (Van Groen and Wyss, 1993), supporting the inclusion of PPT cholinergic signaling in the regulation of spatial memory.

2.3.2.3 Reinforcement learning

Stimulus-response and action-outcome associations are thought to be mediated by the basal ganglia, specifically due to the input from tonically active neurons in the striatum that respond to salient sensory events during behavioural conditioning (Schulz and Reynolds, 2012). These tonically-active neurons (TANs) are cholinergic interneurons that exhibit a tonic spike discharge (Schulz et al., 2011). Lapper and Bolam (1992) showed that most of the excitatory inputs to the TANs come from the intralaminar nuclei of the thalamus, which drives the spiking of the TANs. Electrical stimulation of the thalamus evoked the spiking of the striatal TANs (Schulz et al., 2011). Schulz and Reynolds (2013) proposed that regulation of TANs signaling is due to a glutamatergic input from the thalamus that is triggered by a an early sensory structure, such as the SC or

the PPT, to ensure that the dopamine burst is uninhibited and delivers a strong reinforcement signal for the event. In response to salient stimuli, and also to cues that predict magnitude of reward outcome, PPT neurons become phasically active (Pan and Hyland, 2005) (Okada et al., 2009), so it is been suggested that PPT outputs, or its projections to the SC, could be modulating thalamic control of striatal interneurons.

Condé et al. (1992) proposed a learning process model involving the PPT input to the midbrain dopaminergic neurons as a carrier of reinforcement information. Stimulation of the PPT results in excitation of the dopaminergic neurons of the SNc and the VTA (Lacey et al., 1990), which is essential for burst firing in dopaminergic neurons. Acetycholine acts on nicotinic receptors to depolarize the dopaminergic neurons and alter their firing rate (Calbresi et al., 1989; Lacey et al., 1990). Rats with lesions in the posterior PPT (pPPT) have been shown to perform worse than those with anterior PPT lesions (aPPT) or sham lesion mice in a level-release paradigm, as they were slower to learn the association between the lever release and the reward (Wilson et al., 2009), suggesting the PPT-ventral striatal circuitry connection is key for reward-reinforcement learning. Lesions of the PPT also blocked the reward effects of morphine, amphetamine or food as measured in the conditioned place preference test (Olmstead and Franklin 1993, 1994). Studies suggest that the PPT is involved in the process of forming as well as strengthening or maintaining rewarded behaviours through the regulation of dopamine-releasing neurons in the SNc and the VTA (Allen and Winn, 1995).

Recent research using a saccade task in monkeys has also focused on the interplay between the PPT-Dorsal raphe-Basal ganglia systems and their combined effect on reinforcement learning (Okada et al., 2011). These studies suggest that the PPT neurons may be involved in reward prediction. They proposed that the reward prediction information from the PPT and the actual information about the value of the reward from the dorsal raphe are integrated to evaluate the errors in reward prediction and signal to midbrain dopaminergic neurons to reinforce the learned behaviours that elicit the reward, as summarized in Figure 4.

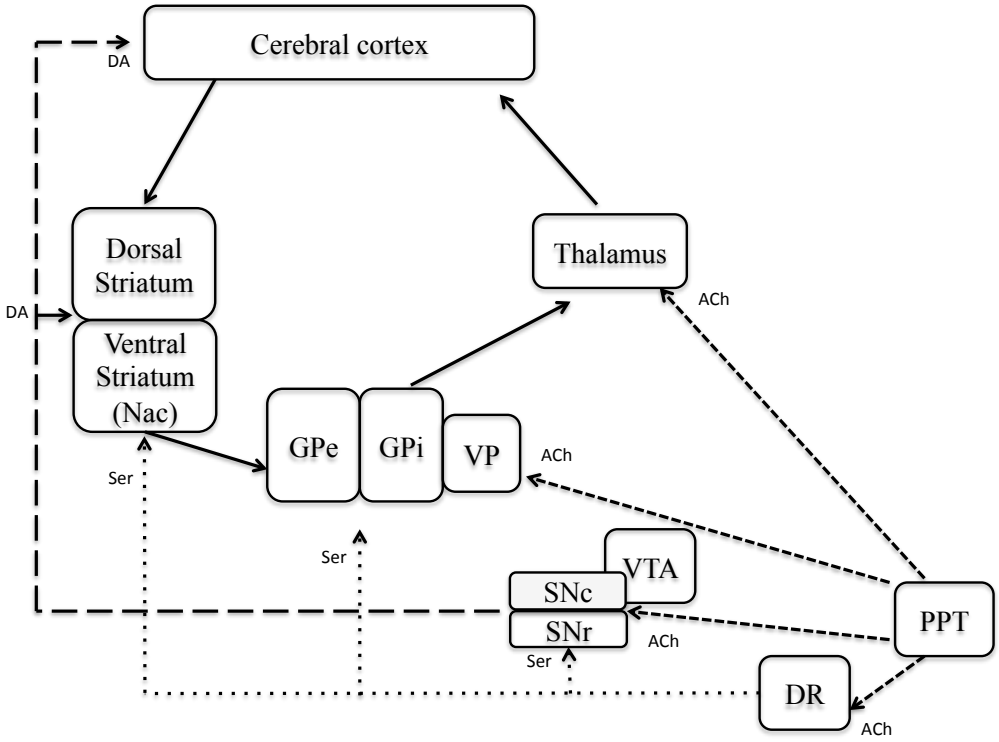

Figure 4. Summary of PPT-Dorsal raphe-Basal ganglia reinforcement learning circuitry. Nac = nucleus accumbens, GPe = external globus pallidus, GPi = internal globus pallidus, VP = ventral pallidus, SNc = substania nigra *pars compacta*, SNr = substantia nigra *pars reticulate*, VTA = ventral tegmental area, PPT = pedunculopontine tegmental nucleus, Ser = serotonin, DA = dopamine. Adapted from Okada et al., 2011.

2.3.3 Sleep

The PPT is thought to be part of the reticular activating system that drives global brain-state transitions (Ros et al., 2010). This link between cortical brain state and the PPT is supported by studies that show increases in firing rate of cholinergic neurons during spontaneous and sensory-induced brain state transitions from slow-wave activity to activated brain states (fast-frequency, low amplitude; typical of wakefulness, arousal or REM sleep (Mena-Segovia et al., 2008).

It has been postulated for many years that the PPT is involved in the control of rapid eye movement (REM) sleep (Garcia-Rill 1991). This theory has been supported by the comorbidity of sleep disturbances and the later onset of motor and cognitive decline

seen in progressive neurodegenerative disorders such as Parkinson's disease and progressive supranuclear palsy (PSP), where there is selective loss of cholinergic neurons in the PPT as well as other neuronal populations (Raggi and Ferri, 2010). Additionally, this is supported by anatomical studies of the PPT. The PPT projects directly to the thalamocortical system and also to the basal forebrain, both of which cause cortical activation during waking and REM sleep (Petrovic et al., 2013).

To clarify the role of the PPT in REM sleep regulation, Petrovic et al. (2013) lesioned the PPT bilaterally in rats and evaluated the effect on sleep-wake states using EEG. These studies showed that the lesions did not affect the sleep/wake cycle, but it did alter the structure of the sleep-wake transitions. There was an increase in the number of Wake/REM and REM/Wake transitions that was sustained for 5 weeks after the surgeries. The EEG showed that the lesions increased the Wake theta amplitude and the REM beta amplitude, demonstrating increased cortical activation (Petrovic et al., 2013).

Robust firing of midbrain dopaminergic neurons have been observed during REM sleep, concurrent with ACh and glutamate release from the PPT onto nigrostriatal dopaminergic neurons (Dahan et al., 2009). It has been proposed by Lima (2012) that the release of glutamate and ACh from the PPT onto the substantia nigra and VTA causes a dopaminergic release onto the reticular formation causing the activation of REM sleep. Degeneration of cholinergic signaling from the PPT disrupts this pathway and leads to sleep pathologies, which is often comorbid with PD motor symptoms (Lima 2012).

3 Rationale and Hypothesis

The physiological role of ACh released from cholinergic neurons from the pedunculopontine tegmental nucleus (PPT) is still poorly understood. Here, we generated mice with VAChT deletion selectively from PPT cholinergic neurons to investigate how ACh signaling from this nucleus contributes to different brain functions. This provides the opportunity to evaluate the consequences of decreased cholinergic signaling from the PPT *in vivo*.

Based on the efferent connectivity from the PPT, our hypothesis is that decreased cholinergic signaling from the PPT will affect specific behavioural outputs such as gait, motor control and sleep.

Improving our understanding of cholinergic signaling from the PPT and how it relates to behavioural abnormalities may lead to the development of novel treatments for the symptoms of neurological diseases such as PD and PSP.

4 Methods

4.1 Ethics Statement

All experiments were carried out following guideline set by the Canadian Council of Animal Care (CCAC), with the protocol approved by the University of Western Ontario Institutional Animal Care and Use Committee (protocol 2008-127). Only male mice were used in the behavioural studies. Mice were housed two to four per cage in a room with a 14-hour light/10-hour dark cycle, and provided access to food and water *ad libitum*.

4.2 Animals

Pedunculopontine tegmental nucleus-specific VAChT knockout mice ($VAChT^{En1\text{-}Cre\text{-}flox/flox}$) were generated using a Cre recombinase/LoxP system. In short, $VAChT^{flox/flox}$ mice (Martins-Silva et al., 2011; mixed C57BL/6J x 129/SvEv background, backcrossed to C57BL/6J for five generations) were crossed with the En1-Cre mice (Jackson Laboratories, stock no. 007916; Kimmel et al., 2000; mixed 129S1/SvImJ background, backcrossed to C57BL/6J in our laboratory for at least two generations). We then intercrossed $VAChT^{En1\text{-}Cre\text{-}flox/wt}$ mice to obtain $VAChT^{En1\text{-}Cre\text{-}flox/flox}$. Control mice used in our experiments are littermates $VAChT^{flox/flox}$. Only male $VAChT^{En1\text{-}Cre\text{-}flox/flox}$ mice greater than three months of age were used in these experiments with male $VAChT^{flox/flox}$ age-matched controls.

Rosa26-tdTomato mice ($B6.Cg\text{-}Gt(ROSA)26Sor^{tm14(CAG\text{-}tdTomato)Hze/J}$, Jackson Laboratories, stock no. 007914; Madisen et al., 2010) have a loxP-flanked STOP cassette to prevent the transcription of the downstream red fluorescent protein variant, tdTomato.

These mice were bred to mice expressing Cre recombinase under the control of the En1 promoter (En1-Cre mice). The offspring generated as a result of this breeding express dTomato in all Cre-expressing tissues. These mice were analyzed by immunohistochemistry to determine the brain regions where En1-Cre is expressed in cholinergic neurons.

4.3 Immunohistochemisty and Western Blots

For the immunofluorescence experiments, mice were anesthetized with ketamine (100mg/kg)-xylene (20 mg/kg) then perfused transcardially with 4% paraformaldehyde (v/v) in phospho-buffered saline (PBS) (pH 7.4). Brains from VAChT$^{En1\text{-}Cre\text{-}flox/flox}$ mice and VAChT$^{flox/flox}$ mice were removed and incubated in 4% paraformaldehyde in PBS overnight at 4°C. Brains were sectioned in the sagittal plane using a vibratome (40 μm thick) and transferred into a six well plate with each well containing PBS. Slices were place one per well in a clockwise manner. All slices within only one well were selected for immunohistological analysis. These selected free-floating slices were then washed with Tris-buffered saline (TBS) (pH 7.6) 3 times for 15 minutes then blocked and permeabilized by incubation for 1 h at room temperature in TBS with 0.2% Triton X-100, 3% bovine serum albumin (w/v), and 5% normal horse serum. Sections were then incubated for 48 hours at 4°C with mouse anti-CHT1 (high-affinity choline transporter 1) (catalog #ab5966; Millipore) at a 1:500 dilution in 1:1 TBS and blocking solution. Slices were washed 3 times for 15 min in TBS with 0.1% Tween20 (TBST), brain slices were incubated with the seconday antibody (an Alexa488 dye-conjugated rabbit anti-mouse IgG; catalog #a6662; Abcam) in 1:1 TBS and blocking buffer overnight at 4°C. Sections were washed five times for 10 minutes in TBS then mounted on slides with Immunomount (Thermo Scientific, Massachusetts, USA) and visualized using Leica-SP5 laser-scanning microscope using an argon laser and HeNe1 laser. Images were taken using Leica SP5 fluorescence microscope with a 40x oil immersion objective (1.25 NA). For each mouse, one image of each brain region was quantified and the percent colocalization of tdTomato and CHT1-labelled neurons was quantified. This value was obtained for four mice from each genotype and averaged.

For Western blot analysis, fresh brain tissue was used from both VAChT$^{En1\text{-}Cre\text{-}flox/flox}$ mice and VAChT$^{flox/flox}$ control mice. To prepare extracts, tissues were homogenized in buffer containing 10 mM Tris-HCl pH 7.5, 150 mM NaCl, 1 mM EDTA, 1% Triton X-100 and protease inhibitor cocktail. Extracts remained at 4^{o}C for 20 minutes then centrifuged (10,000 x g x 20 min). Protein concentration of the supernatant was determined using the Bradford method. 50 µl of protein was loaded into precast 12% gels (Lonza; Basel, Switzerland) and run for 90 minutes at 120 volts. Protein was then transferred to PVDF membrane using Trans-Blot SD Semi-Dry Transfer Cell (Bio-Rad; Hercules, CA). For immunoblotting, membranes were washed with TBS with 0.05% Tween20 (TBST) for 10 minutes then incubated with blocking solution (5% milk in TBST) for one hour. Membranes were then incubated in primary antibody at 4^{o}C overnight diluted in blocking solution. Antibodies were rabbit anti-VAChT (catalog #139103; Synaptic Systems) at a 1:3000 dilution and mouse anti-Synaptophysin (catalog #S5768; Sigma-Aldrich) at a 1:500 dilution. After, membranes were washed with TBST three times for fifteen minutes each. Membranes were developed using Amersham ECL Plus reagent kit (GE Life Sciences; Pittsburgh, PA). Non-saturated autoradiographs were analyzed with ImageJ.

4.4 Grip Strength and Wire Hang

A Grip Strength Meter from Columbus Instruments (Columbus, OH) was used to measure forelimb grip strength (Prado et al., 2006; Deacon, 2013). Mice grasped the smooth pull bar of the apparatus with forelimbs only and then were pulled backwards by the tail horizontally. The force applied to the bar immediately before grasp was released was recorded. 3 measurements were recorded per animal and averaged. The inter-trial interval for each mouse was 30 seconds, during which the mouse was returned to its home cage.

For the Wire Hang test (Prado et al., 2006; Deacon, 2013), each mouse was placed on a metal wire-grid, which was slowly inverted and suspended 40 cm above a piece of foam. The time for each mouse to fall from the wire was recorded with a 60s cut-off. The inter-trial interval for each mouse was 30 seconds, during which the mouse was returned to its home cage.

4.5 Open Field Locomotion

To measure spontaneous locomotor activity in new environments (Pierce and Kalivas, 2007; de Castro et al., 2009), mice were placed in an open field arena (20 cm x 20 cm platform with 30 cm high walls) and movement in the arena was recorded by VersaMax Animal Monitoring System from AccuScan Instruments Inc. (Columbus, OH). Mice were placed in the centre of the apparatus and allowed to freely explore the novel environment for 120 minutes in the light followed by 120 minutes in the dark. VersaMax converts infrared beam breaks into movement (cm) per 5-minute interval. For intersession habituation, mice spent 120 min in the same open field apparatus for three consecutive days. Measurements of total activity were obtained.

4.6 Rotarod

For the rotarod task (Prado et al., 2006; de Castro et al., 2009), mice were placed on the accelerating rotarod apparatus (San Diego Instruments; San Diego, CA) for ten trials with an inter-trial time of 10 minutes during which mice were placed in their home cage. On the second day the animals underwent four more trials with the same conditions from the previous day. Animals were allowed to acclimate to the rod for 5 seconds before the trial started. For the first 100 seconds the revolutions per minute (RPM) was 5, then 15 RPM for the subsequent 100 seconds, then 25 RPM for the next 100 seconds and finally 35 RPM for the final 100 seconds. The software records latency to fall. Rod was cleaned with 70% ethanol between trials.

4.7 CatWalk Gait Analysis

The CatWalk XT system by Noldus (Leesburg, VA) was used to assess the gait of the animals (Koopmans et al., 2005). The apparatus is made of a 1.3 m long glass plate with dim fluorescent light beamed into the glass from the side. The paw in contact with the glass was recorded by a video camera underneath the walkway. Mice were allowed free exploration of the walkway for 1 min. Three correct runs (the mouse crossed the walkway with no interruption or hesitation) for each mouse was recorded. Runs were analyzed using the Noldus software. Stride length is defined as the distance between two successive prints of the same paw.

4.8 Metabolic cages

Oxygen consumption (VO2), carbon dioxide production (VCO2), respiratory exchange ratio (RER), food and water intake, and physical activity were simultaneously measured using the Comprehensive Lab Animal Monitoring System (CLAMS) interfaced with Oxymax software (Columbus Instruments; Columbus, OH) (Guzman et al., 2013). Mice were housed individually in the metabolic chambers maintained at 24 ± 1°C. Mice had free access to powdered standard rodent chow and water. Mice had a 24 h habituation period, after which measurements were taken every 10 min for 24 h (12-h light/ 12-h dark). VO2, CO2, RER, food and water intake, ambulatory activity, and sleep (periods of inactivity) measurements were obtained using the Opto-M3 Activity Monitor and Oxymax software algorithms (Columbus Instruments; Columbus, OH).

4.9 Forced Swimming Test and Tail Suspension Test

The forced swimming test (FST) and tail suspension test (TST) were used to measure depressive-like behaviour (Martyn et al., 2012). For FST, mice were placed in the testing room and allowed to habituate for one hour. Mice were placed in a 2 L beaker with 1.8L of 25-27^{o}C water for 6 min. A video monitor was placed above the beaker and using ANYmaze software (Stoelting Co., IL) the time spent immobile and distance swam were calculated. Only data taken from 2-6 minutes were analyzed. Water was changed every 2-3 mice.

For the TST, mice were suspended from a bar 30 cm above a table by their tail, using masking tape placed 1.5 inches from the base of the tail, for 6 min (Martyn et al., 2012). Sessions were recorded and immobility time and immobility episodes were quantified using ANY-Maze software (Stoelting Co., IL).

4.10 Elevated Plus Maze

The elevated plus maze is used to investigate murine anxiety (Martins-Silva et al., 2011). The elevated plus maze is a plus-shaped platform with two open arms and two arms with dark plastic walls. Mice were placed in the centre facing the open arm opposite the experimenter. Mice were allowed to explore the maze for 5 minutes then they were

returned to their home cage. A video monitor was placed above the maze and total amount of time spent in the open or closed arms of the maze, as well as total distance travelled, was calculated with the Any-maze software (Stoelting Co., IL). Mice were considered to be completely within an arm of the maze when its centre of gravity was in that section. All parts were cleaned between animals, first with soap and water followed by 70% ethanol.

4.11 Light/Dark Place Preference Test

The light/dark place preference test is used to evaluate anxiety-like behaviour (Martyn et al., 2012). A black plexiglass insert that is exactly half the area of the open field arena (20 cm x 20 cm platform with 30 cm high walls) is placed in the arena. The black insert has a small opening in the front to allow the mouse to move freely between the open half of the arena or the dark covered half inside the insert. The test is done with the mice 30 min into their wake cycle (19:30 h) in a bright room. Mice are placed in the centre of the arena and ambulatory activity in a 10 min session is recorded using the VersaMax Animal Activity Monitoring System (AccuScan Instruments, Inc.; Columbus, OH). All parts were cleaned between animals, first with soap and water followed by 70% ethanol.

4.12 Marble Burying Task

The marble burying task considered presently to be a measure of repetitive, compulsive-like behaviours in mice, although it is still commonly used as a measure of anxiety-like behaviour in rodents (Angoa-Perez et al., 2013; Thomas et al. 2009). 20 glass marbles are arranged evenly on the surface of clean cage partitioned in half with bedding that is 2 inches deep. The number of marbles buried in a 15 minute session is counted. A marble must be 2/3 covered in bedding to be considered buried.

4.13 Morris Water Maze

Spatial memory was assessed using the spatial version of the Morris water maze (MWM) (Vorhees and Williams, 2006; Martyn et al., 2012; Kolisnyk et al., 2013). External cues were placed around a circular tank, 120 cm in diameter, filled with water at

a temperature of 25°C. A circular, clear escape platform, 10 cm in diameter, was placed 0.5 cm below the surface, such that it was hidden underneath the waterline but still mountable. The tank was conceptually divided into four quadrants. Testing was done on five consecutive days. On the first four days, the platform was kept in a constant position for each mouse. The mouse underwent four trials on each day, starting once at the dividing line between each quadrant facing the edge of the tank. 90 s were given for the mouse to reach the platform, with its path analyzed using a video monitor placed over the tank and ANY-maze software (Stoelting Co., IL). If task was not completed in 90 s, the mouse was guided to the platform. The inter-trial interval was 15 minutes. On the fifth day, one trial was done for each mouse with the platform removed from the tank. The mouse was placed directly opposite of the where the platform used to be, and was given 60 s swim around the tank. Time spent in the target quadrant was measured using ANY-maze software (Stoelting Co., IL).

The cued version of the MWM was performed to assess goal-directed behaviour (Rossato et al., 2006). For this variation, the platform was at water level and visible with a plastic block cue placed on it, and spatial cues were removed from the room. Mice were tested over two days with novel platform and starting location combinations. Mice underwent 8 consecutive training trials with a 30 s inter-trial interval on day 1. After 24 h the mice are probed for their retention of the trials but undergoing 2 cued trials, this time starting from a position that was not used during training.

4.14 Spontaneous Alternations Y-Maze Task

Working memory is evaluated using the spontaneous alternations Y-maze task (Hughes 2004). Test was performed using a symmetrical Y-shaped maze (30 cm long by 6 cm wide by 20 cm high) following a protocol previously described (de Castro et al., 2009; Kolisnyk et al., 2013). Mice were placed at the end of one arm and allowed to freely explore the maze for 8 min. A spontaneous alternation occurred when the mouse visited all three arms of the maze in sequence without revisiting a previous arm. All sessions were recorded and the order and number of arm entries were measured by Any-maze software (Stoelting Co., IL). The effect was calculated as percentage alternation according to the formula: [total alternation/(total arms entered - 2)] x 100. Therefore, the

following hypothetical sequence of arms entered by a mouse: A,C,A,B,C,A,C,B,A,C would yield an alternation score of 75% ([6 alternations/(10-2) arms entered] x 100). A score of 50% means random selection of goals arms. Animals statistically reach more than 50% alternation, indicating no random arms selection. By this criterion, we would see 100% alternation score only if the animal had run consistently clockwise or anticlockwise.

4.15 5-Choice Serial Reaction Time Task

4.15.1 Pre-training Phase

The five-choice serial reaction time task (5-CSRTT) is used to determine attention in mice (Robbins 2002; Romberg et al., 2011). Mice were trained in the 5-CSRTT in automated Bussey-Saksida Mouse Touch Screen Systems model 81426 (Campden Instruments Limited; Lafayette, IN). Schedules were designed and data were collected using the ABET II Touch software v.2.15 (Lafayette Instruments; Lafayette, IN).

Mice first were gradually food restricted and reduced to 85% of their normal weight before undergoing a pre-training program that was previously described by Kolisnyk et al. (2013) that involved habituating the mouse to the testing chamber for 15 minutes. The following day, the mouse spent 20 min in the chamber, during which the reward tray was illuminated and primed with strawberry milkshake (Saputo Dairy Products). Whenever the mouse went to the reward tray, it received the reward paired with a tone. The mouse repeated this process for two more days, each with 40 min duration.

In the next pre-training phase, the mice learn to pair the reward with a stimulus (a flash of light in one of the 5 windows) on the touchscreen. The stimulus appeared at random and remained for 30 s, after which it was removed and a reward paired with a tone was given (one trial). Once the mouse collected the reward another trial was initiated. This phase was continued until the mouse successfully completed 30 trials within a 60 min session.

The third phase of pre-training involved teaching the mouse to touch the stimulus on the screen. If the mouse touched the stimulus on the screen it received the reward paired with the tone. If the mouse touched the screen in where there was no stimulus there was no response. This phase was repeated until the mouse consistently completed 30 trials in a 60 min session.

Phase 4 was the same as phase 3, which the difference that the mouse had to nose poke the reward tray to initiate the trial. This phase was repeated until the mouse completed 30 trials in a 60 min session.

In the final pre-training phase (phase 5), the mice underwent the same procedure as in phase 4, but if the mouse touched one of the 5 screens that did not display the stimulus (an incorrect screen), it received a 5 s timeout, which was indicated by the chamber light turning on during this time. Mice must perform this phase with a minimum of 80% accuracy (at least 23 correct responses within 30 trials) within the 60 min session. This level of accuracy must be sustained for 2 consecutive days in order for the mouse to progress to 5-CSRTT training phase.

4.15.2 5-CSRTT Training Phase

In this phase, mice learn to respond to flashes of light pseudo-randomly displayed in one of the 5 locations on the touchscreen. The mouse nose pokes the reward dispenser to initiate the trial. There is a variable 5-10 s delay period during which the mice must attend to the screen, after which the light stimulus appeared on the touch screen. There was a 5 s period after the stimulus presentation where the mouse could still respond to the location (holding period). If the mouse touched the screen during the delay period, the response was recorded as premature and the mouse was punished with a 10 s timeout. A response to the stimulus window during stimulus presentation or during the holding period was recorded as a correct response. Responses to any other window were recorded as incorrect. Correct response was rewarded with the milkshake and tone pairing and an incorrect response was punished with a 10 s timeout. Failure to make any response was recorded as an omission and the mouse was punished with a 10 s timeout. Perseverative responses to the screen after either a premature, correct, or incorrect choice was also

recorded. Each session lasted until 50 trials were completed to a maximum duration of 1 h. Once the mice reached the criterion at 4 s stimulus duration of a minimum of 30 trials, 80% accuracy, and 20% omissions for 3 consecutive days, the stimulus duration was reduced to 2 s. After mice reached this same criterion for the 2s stimulus duration, the mice were tested 2 more days, and the average of those measures was recorded as their baseline performance.

4.15.3 Probe trial

After the baseline measures had been recorded, the mice were probed for attentional deficits in the following probe trial schedule: 2 d at 1.5 s stimulus duration, 2 d at 1.0 s stimulus duration, 2 d at 0.8s stimulus duration and finally 2 d at 0.6 s stimulus duration (Kolisnyk et al., 2013). The order of these probe trial sessions were semi-randomized using a Latin square method.

4.15.4 5-CSRTT measurements

On all 5-CSRTT sessions, accuracy was defined as: [(number of correct responses)/(total number of correct and incorrect responses)]. Rate of omissions was defined as: [(number of omitted responses)/(total number of responses)]. Response latency was defined as the duration of time between the initiation of the trial and the first touch of the correct stimulus. Reward collection latency was the duration of time between the mouse touching correct stimulus and then returning to the reward tray. A premature response was counted when the mouse touched any one of the 5 windows before the stimulus onset. A perseverative response was any identical response that occurred after either a correct, incorrect, or premature response. (Kolisnyk et al., 2013)

4.16 Statistical analysis

Data are expressed as mean ± SEM. Prism 5 and SigmaStat 3.5 software was used for statistical analysis. Comparison between two experimental groups was made by Student's *t* test. When several experimental groups or treatments were analyzed, two-way ANOVA or two-way ANOVA with repeated measures was used as required. When appropriate, a

Bonferroni *post hoc* comparison test was used. In all comparisons, $p < 0.05$ was considered statistically significant.

Chapter 2

5 Results

5.1 Immunohistochemistry and Western blot analysis of VAChT$^{En1\text{-}Cre\text{-}flox/flox}$ mice

In order to selectively eliminate VAChT in the PPT, VAChT$^{En1\text{-}Cre\text{-}flox/flox}$ mice were generated using a Cre-loxP system under the control of the regulatory elements (homeobox transcription factor 1) encoded by the *En1* gene (Kimmel et al., 2000). The *En1* gene was selected to drive Cre recombinase expression because its expression is restricted to the mes/r1 (Kimmel et al., 2000). Previous studies using the En1-Cre driverline have found Cre activity in cholinergic neurons of the rostral brainstem (including the PPT) but no activity in the more caudal motor neurons in the brainstem (Machold 2013). To test whether Cre was expressed in PPT cholinergic neurons, a reporter mouse line was used to reveal the location of En1-cre expression. The reporter line used was the *Rosa-26*-tdTomato mice, in which the *Rosa26* locus expresses tdTomato once Cre-mediated recombination has occurred. En1-Cre mice were crossed *Rosa-26*-tdTomato mice and immunofluorescence analysis of En1-Cre:*Rosa-26*-tdTomato mice brain slices used to investigate location of Cre expression driven by the En1 promoter. The number of neurons revealing colocalization between tdTomato- (red) and CHT1-labelled neurons (green) was divided by the total number of cholinergic neurons in the PPT (shown in Table 1) to give a percentage of colocalization for each animal. Colocalization (Fig. 6a) was observed on average in 40% of cholinergic neurons in the PPT and in 10% of cholinergic neurons in the Mo5 motor nuclei, but no colocalization was observed in the 7N motor nuclei, the striatum, and the cortex (Fig. 5; Table 1). Sagittal brain slices were selected to reflect the cholinergic nuclei at approximately the same lateral position in each animal. It should be noted that the most medial slice of the PPT did not have any colocalization between td-Tomato- and CHT1-labelled neurons, so the percent colocalization may not be consistent throughout the entirety of the PPT. We subsequently intercrossed En1-Cre mice with VAChT$^{flox/flox}$ mice to generate mice with a selective elimination of VAChT in the PPT.

Table 1. Summary of the number of YFP-labeled neurons colocalizing with CHT1-labeled cholinergic neurons in the immunohistological analysis of the En1-Cre:*Rosa-26*-tdTomato mouse line. Values are expressed as the number of YFP- and CHT1-colabelled neurons out of total number of CHT1-labelled neurons in the image obtained for that brain region in each mouse.

Mouse	PPT	Mo5	7n	Striatum	Basal Forebrain
1	22/45	9/57	0/48	0/33	0/33
2	14/54	11/89	0/46	0/29	0/16
3	3/12	4/84	0/78	0/38	0/29
4	4/6	5/82	0/72	0/42	0/21

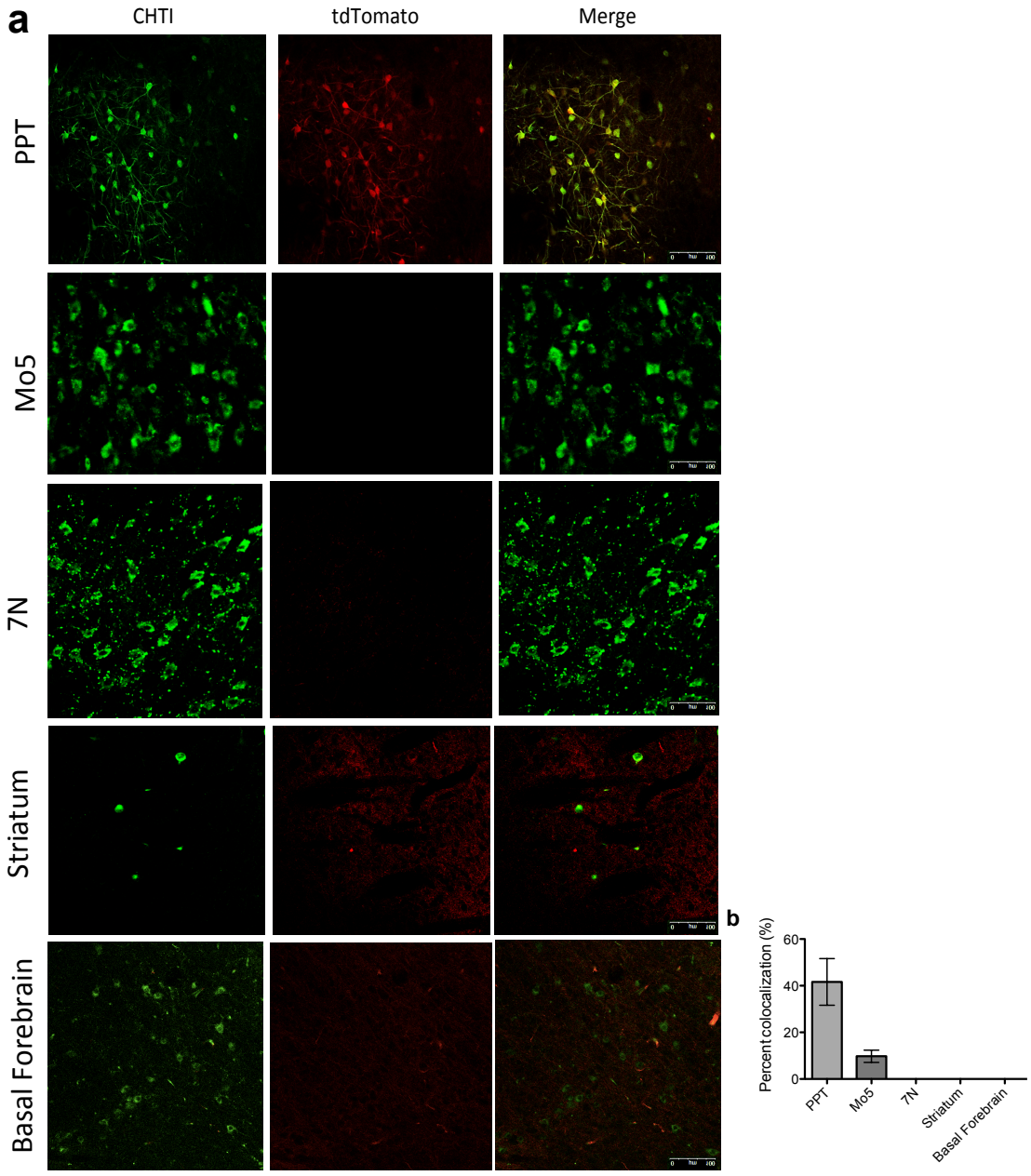

Figure 5. En1 promotor drives the expression pattern of Cre Recombinase in pedunculopontine tegmental nucleus cholinergic neurons. (a) Sections from reporter mouse line, En1-Cre:*Rosa-26*-tdTomato mice immunostained for CHT1 (green) and tdTomato (red). (b) summary of the average percent colocalization observed for each brain region; *n* = 4.

To indirectly assess the degree of Cre-mediated recombination, Western blot analysis of VAChT$^{\text{En1-Cre-flox/flox}}$ mice was performed to evaluate VAChT protein expression. In the brainstem, there was 50% decrease in VAChT protein levels ($t(6) = 5.123$, $p = 0.0018$; Fig. 6a). In the thalamus, the primary output centre of the PPT, there was 90% decrease

in VAChT protein levels ($t(6) = 3.369$, $p = 0.0151$; Fig. 6b), suggesting that most of the Cre-targeted neurons project to this brain area. The hippocampal blot shows a trend that suggests the $VAChT^{En1\text{-}Cre\text{-}flox/flox}$ mice have twice as much VAChT as controls, however this increase is not significant ($t(6) = 2.434$, $p = 0.0509$; Fig. 6d). VAChT protein levels in the striatum ($t(6) = 1.524$, $p = 0.1785$; Fig. 6c) and the cortex ($t(6) = 1.273$, $p = 0.2503$; Fig 6e) were not significantly affected.

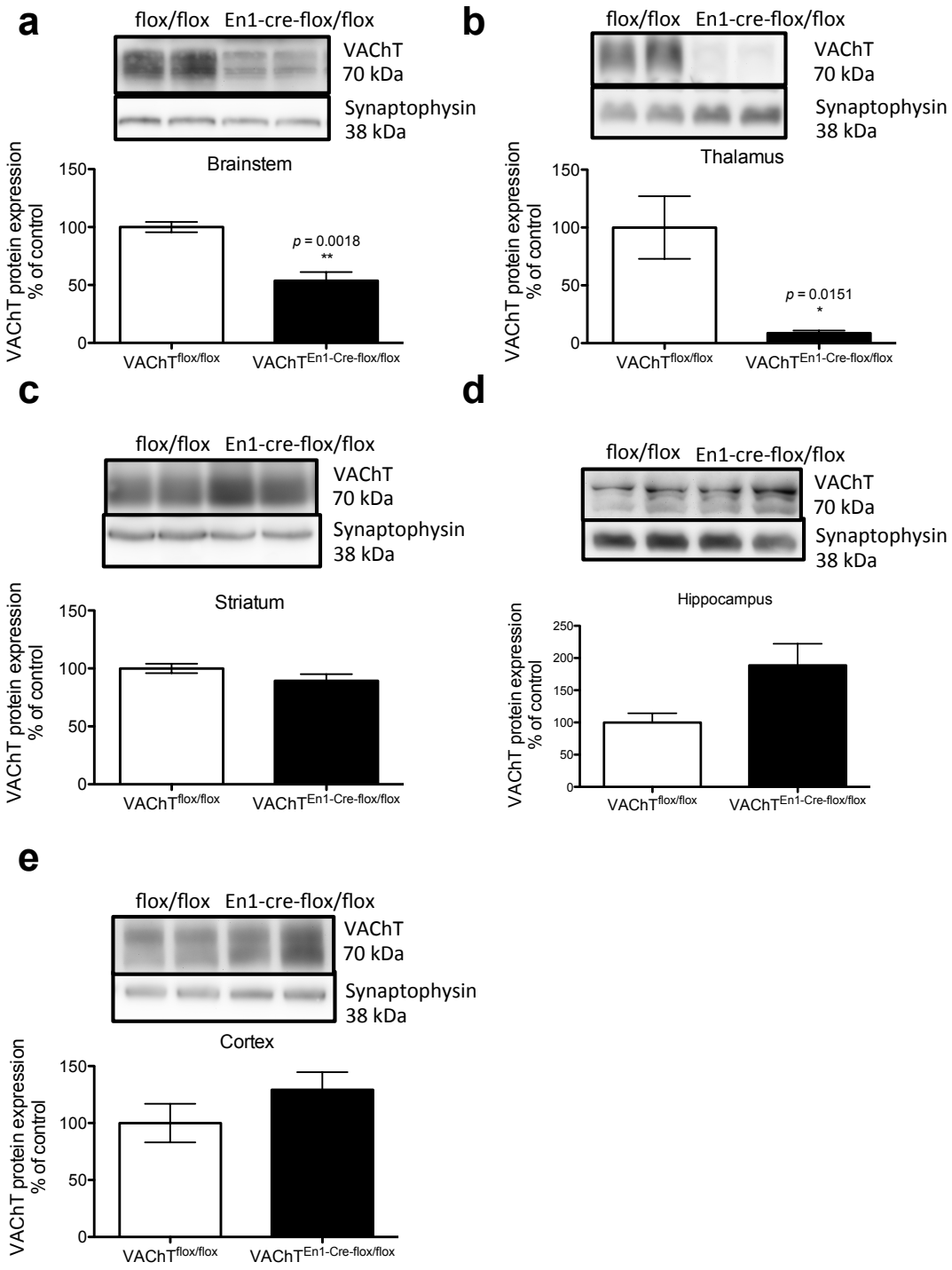

Figure 6. VAChT protein expression. Western blot analysis shows VAChT knockdown in (a) the brainstem, and (b) the thalamus. VAChT protein levels are not significantly changed in (c) the striatum, (d) the hippocampus and (e) the cortex; $n = 4$. Data analyzed using Student's t-test; *, $p < 0.05$, **, $p < 0.01$.

5.2 Behavioral analysis of En1-Cre mice

To test whether the presence of Cre recombinase under the control of the En1 promotor did not affect the behavioural phenotypes in the genetically modified mice, we compared the behaviours of wildtype (WT) mice with En1-Cre mice in a number of tasks.

First, we evaluated locomotor activity of these En1-Cre animals using automated locomotor boxes to evaluate spontaneous locomotor activity in a novel environment (Fig. 7) and habituation. En1-Cre mice were not different from wild-type controls in their short-term habituation to the novel locomotor boxes ($F_{(1,17)} = 0.15$, $p = 0.748$) (Fig. 7a) or in their total distance covered over the three days of testing ($F(1,17) = 0.17$, $p = 0.6859$) (Fig. 7b).

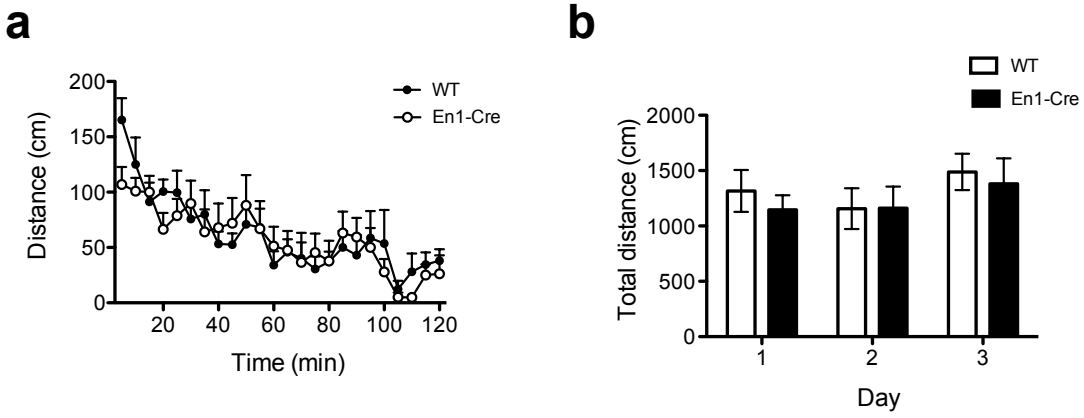

Figure 7. En1-Cre mice have normal spontaneous locomotor activity. (a) short-term habituation in locomotor boxes over two hours on day 1. (b) long-term habituation over three days, shown by total distanced travelled during each day. Data expressed as mean ± SEM and analyzed using repeated measures two-way ANOVA. WT *n* = 13, En1-Cre *n* = 9.

We also evaluated locomotor activity in a "familiar" environment during their wake (dark) and sleep (light) cycles (Fig. 8). No difference between controls and En1-Cre mice was observed in the distance travelled during the light and the dark phase ($F_{(1,21)} = 0.24$, $p = 0.6322$) (Fig. 8).

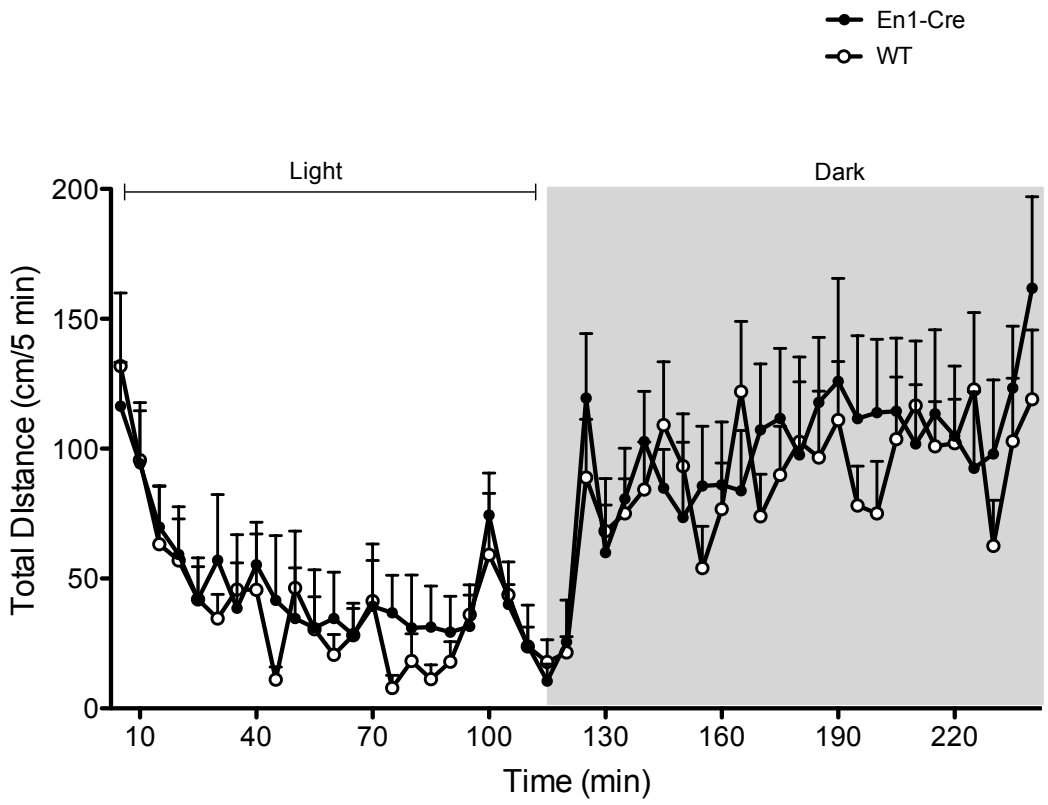

Figure 8. En1-Cre mice have normal spontanous locomotor activity during their sleep and wake cycles. Data expressed as mean ± SEM and analyzed using a repeated measures two-way ANOVA. WT *n* = 13, En1-cre *n* = 10.

We then used the grip strength test (Fig. 9) as well as the rotarod test to evaluate neuromuscular functioning (Fig. 10). In the grip strength test, there was no significant difference between the force applied to the grip strength apparatus by the forelimbs ($t(21) = 1.330$, $p = 0.1979$) (Fig. 9a) or by the hindlimbs ($t(21) = 0.5721$, $p = 0.5733$) (Fig. 9b).

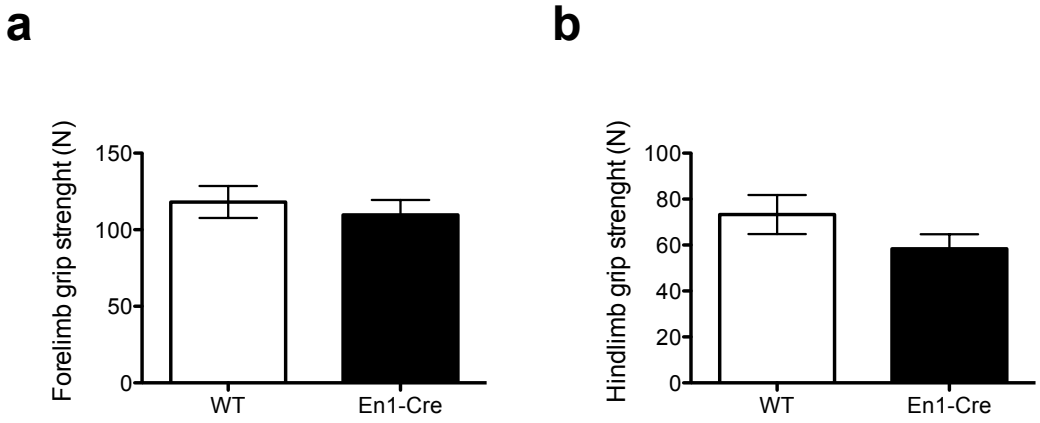

Figure 9. En1-Cre mice have no physical abnormalities in the grip strength. (a) Forelimb grip strength and (b) hindlimb grip strength. Data expressed as mean ± SEM and analyzed using a Student's t-test. WT *n* = 13, En1-cre *n* = 10.

During the rotarod task En1-Cre mice did not significantly differ from their controls in their latency to fall off the rod ($F_{(1,21)} = 2.37$, $p = 0.1383$) (Fig. 10a) or their distance travelled during the task ($F_{(1,21)} = 2.27$, $p = 0.1468$) (Fig. 10b). Together, these data suggest that the presence of Cre recombinase did not alter the neuromuscular functioning of the En1-Cre animals.

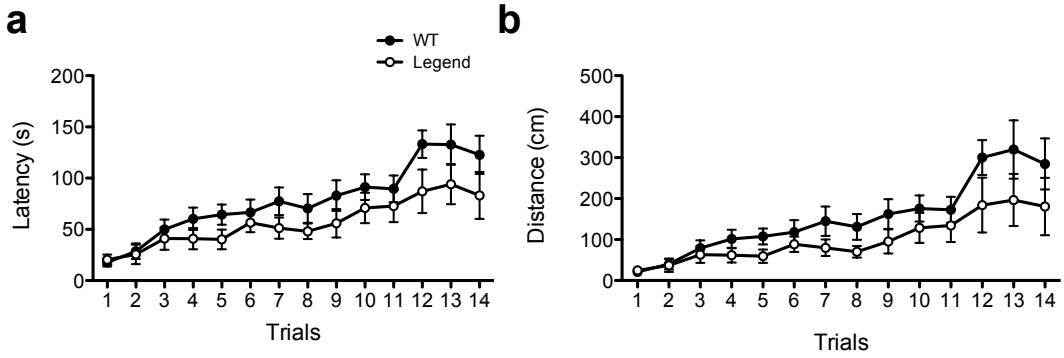

Figure 10. En1-Cre mice have normal neuromusclar functioning in the rotarod task. (a) Latency to fall of the rotating rod and (b) distance travelled on during the trial. Data expressed as mean ± SEM and analyzed using a repeated measures two-way ANOVA. WT *n* = 13, En1-cre *n* = 10.

Taken together, these data indicate that the En1-Cre mice are physically similar to control WT mice. We next tested the mice for the presence of psychiatric-like phenotypes such as depressive-like behaviour and anxiety-like behaviour. To look for the presence of psychiatric-like phenotypes in these animals, we used the forced swim test, the tail suspension test (Figure 11), and the elevated plus maze (Figure 12).

In the forced swimming test, the En1-Cre mice did not significantly differ from WT mice in time spent immobile during the final four minutes of the test ($t(12) = 0.8330$, $p = 0.4211$; Fig. 11a) or in their total distance swam during the test ($t(19) = 0.3285$, $p = 0.7461$; Fig. 11b). This was supported by the results from the tail suspension test, in which the En1-Cre mice again were not different from controls in the total time spent immobile during the test ($t(19) = 0.1814$, $p = 0.8579$; Fig. 11c) or in the number of immobility episodes ($t(18) = 1.011$, $p = 0.3254$; Fig. 11d). Thus, the presence of Cre recombinase under the control of the En1 promoter does not appear to cause a depressive-like phenotype in these animals.

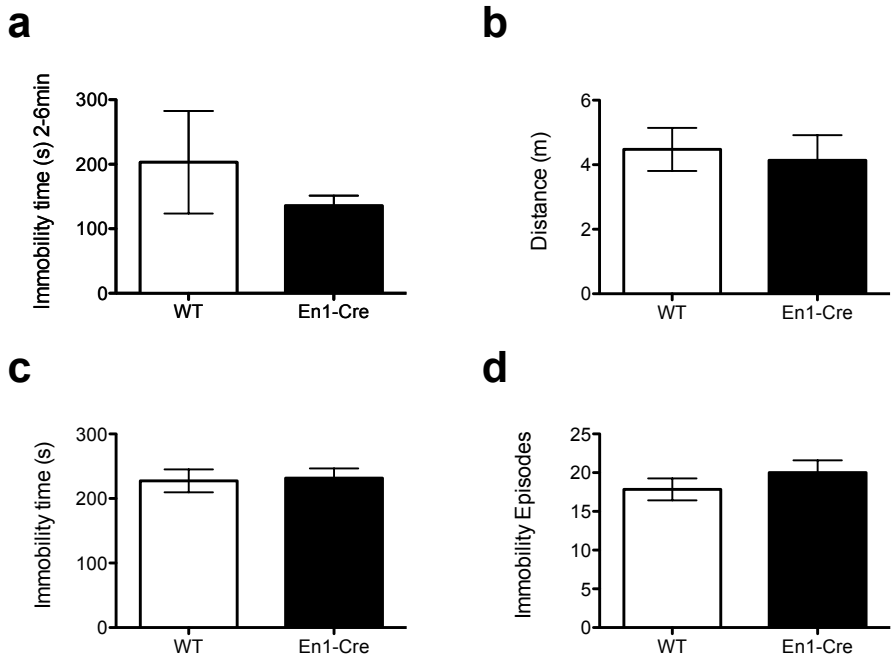

Figure 11. En1-Cre mice do not have a depressive-like phenotype in the forced swimming test or the tail suspension test. (a) Time spent immobile and (b) distance swam during the forced swimming test. (c) Time spent immobile and (d) number of immobility episodes in the tail suspension test. Data expressed as mean ± SEM and analyzed using a Student's t-test. WT *n* = 13, En1-cre *n* = 10.

The elevated plus maze was used to evaluate anxiety-like behaviour. En1-cre mice spent the same percentage of time on the closed and opened arms of the maze and in the centre of the maze as the WT controls ($F_{(1,63)}$ = 0.001, p = 0.9932; Fig. 12a). Additionally, the En1-Cre mice made the same number of entries into the open arms of the maze as the WT mice ($t(20)$ = 0.7555, p = 0.4587; Fig. 12b). This suggests that the En1-Cre mice do not demonstrate anxiety-like behaviour.

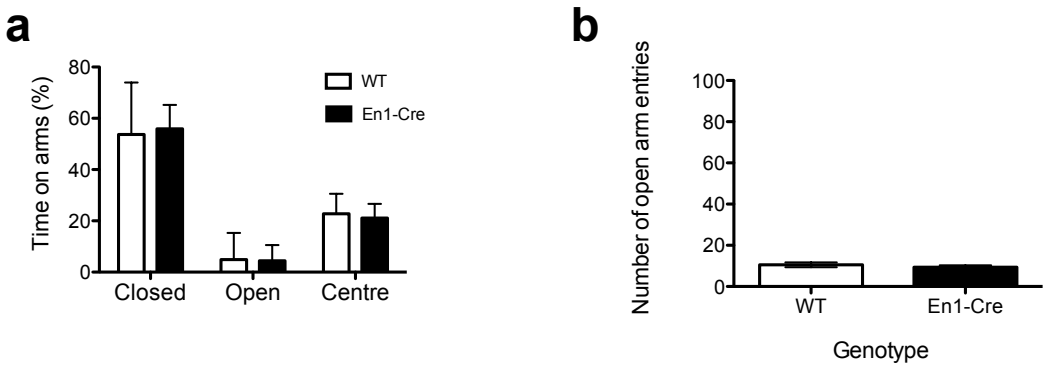

Figure 12. En1-Cre mice do not have anxiety-like behaviour in the elevated plus maze. (a) Percentage of time spent in the close and open arms as well as the centre of the elevated plus maze. (b) Total number of entries into the open arm of the elevated plus maze. Data expressed as mean ± SEM. (a) Analyzed using a two-way ANOVA and (b) analyzed using a Student's t-test. WT *n* = 13, En1-cre *n* = 10.

Finally, to assess cognitive functioning, we evaluated these mice in the Morris water maze (Figure 13) to assess changes to learning and memory. In the spatial version of the Morris water maze, the En1-Cre mice were not different from the WT mice in their latency to find the hidden platform over the four acquisition days of this test ($F(1,16) = 0.89$, $p = 0.3595$; Fig. 13a). During the probe trial, there was no significant difference between the two genotypes in their time spent in each quadrant during the probe trail ($F_{(1,16)} = 0.04$, $p = 0.8409$; Fig. 13b). Tukey *post hoc* analysis revealed the both the WT mice ($p = 0.0041$) and the En1-Cre mice ($p = 0.0125$) spent significantly more time in the target zone than the other three quadrants of the tank. Path tracings are representative of WT (Fig. 13c) and En1-Cre (Fig. 13d) mice during the probe trial. These data indicate that the En1-Cre mice have no deficits in spatial learning and memory.

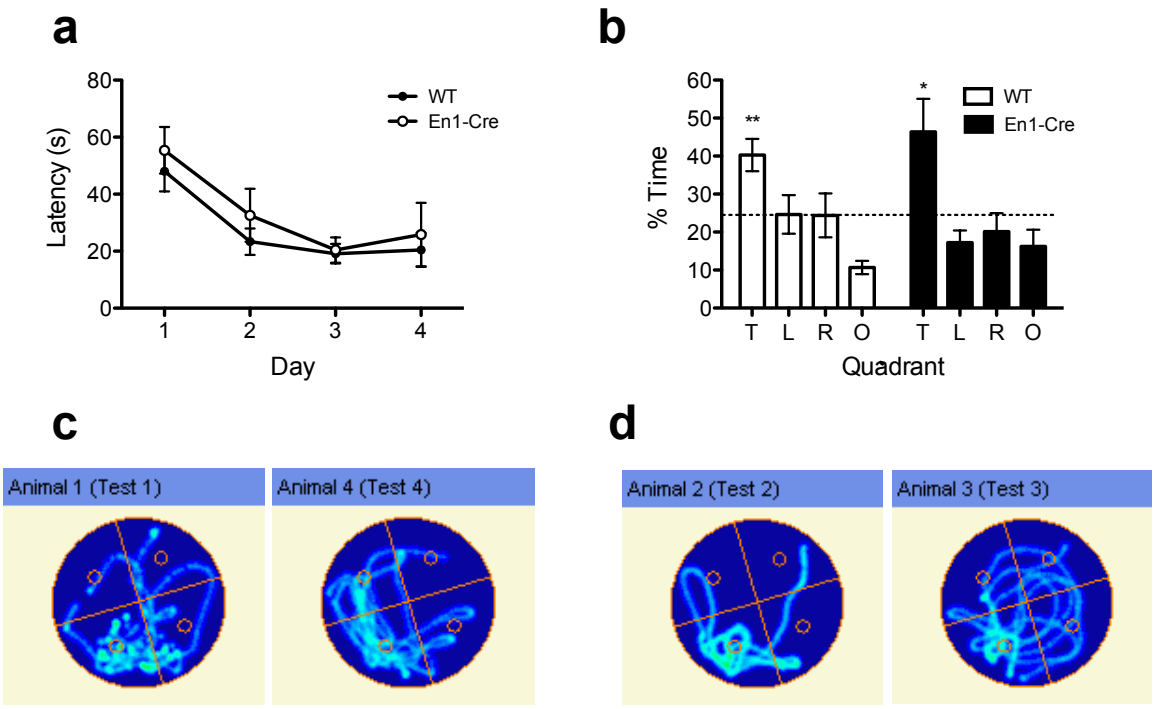

Figure 13. En1-Cre mice show normal learning and memory capabilities in the spatial version of the Morris water maze. (a) Latency to find the hidden platform during the four acquisition days and (b) percentage of time spent in each quadrant of the tank during the probe trial. T = target, L = left of target, R = right of target and O = opposite from target. (c) Representative path tracings of WT mice and (d) representative path tracings of En1-Cre mice. Target quadrant is the lower left segment of the path tracing image. Data expressed as mean ± SEM. (a) Analyzed using a repeated measures two-way ANOVA and (b) analyzed using a two-way ANOVA. *, $p < 0.05$, **, $p < 0.01$. WT $n = 11$, En1-cre $n = 8$.

Since En1-Cre mice were not different from controls in any of the behavioural parameters it was clear that the presence of Cre recombinase under the En1-Promotor did not impart any abnormalities on these animals. As such, we next assessed the $VAChT^{En1\text{-}Cre\text{-}flox/flox}$ mice for deficits resulting from the loss of cholinergic signaling from the PPT.

5.3 Behavior analysis of of VAChT$^{En1\text{-}Cre\text{-}flox/flox}$ mice

5.3.1 Locomotor activity and neuromuscular functioning

Since the PPT is thought to be involved in motor control (Alderson et al., 2008; Takakusaki 2008), a number of tests for locomotor activity and neuromuscular functioning were performed to test whether there will be any behavioural differences between control and VAChT$^{En1\text{-}Cre\text{-}flox/flox}$ mice.

Spontaneous locomotor activity was evaluated in an automated locomotor box. Mice were allowed to habituate in the box for two hours on Day 1 (short-term habituation). Long-term habituation was also measured in the locomotor box over two subsequent days. Total distance travelled over the two-hour period was calculated. There was no statistical difference between the distance travelled by VAChT$^{En1\text{-}Cre\text{-}flox/flox}$ mice and control littermates over the two-hour period on Day 1 ($F_{(1,23)} = 0.4546$, $p = 0.5055$; Fig. 14a) or between their ability to habituate to the locomotor boxes over three days ($t(1,79) = 1.74$, $p = 0.9430$; Fig. 14b). In summary, there were no apparent deficits in locomotor activity or habituation to a novel environment in the VAChT$^{En1\text{-}Cre\text{-}flox/flox}$ mice.

To further assess neuromuscular function in VAChT$^{En1\text{-}Cre\text{-}flox/flox}$ mice, two tests were used: the wire hang test and the grip strength test. For both the wire hang ($t(19) = 1.165$, $p = 0.2585$) and grip strength ($t(19) = 1.306$, $p = 0.2073$) tests there was no statistical difference between VAChT$^{En1\text{-}Cre\text{-}flox/flox}$ mice and control littermates (Fig. 14c-d).

The accelerating rotarod task was used to assess motor learning. Both VAChT$^{En1\text{-}Cre\text{-}flox/flox}$ mice and control littermates improved the time spent on the rotarod as well as distance traveled and there was no significant difference between genotypes in the latency to fall ($F_{(1,15)} = 0.88$, $p = 0.3618$) or distance travelled ($F_{(1,15)} = 0.56$, $p = 0.3302$) (Fig. 14e-f).

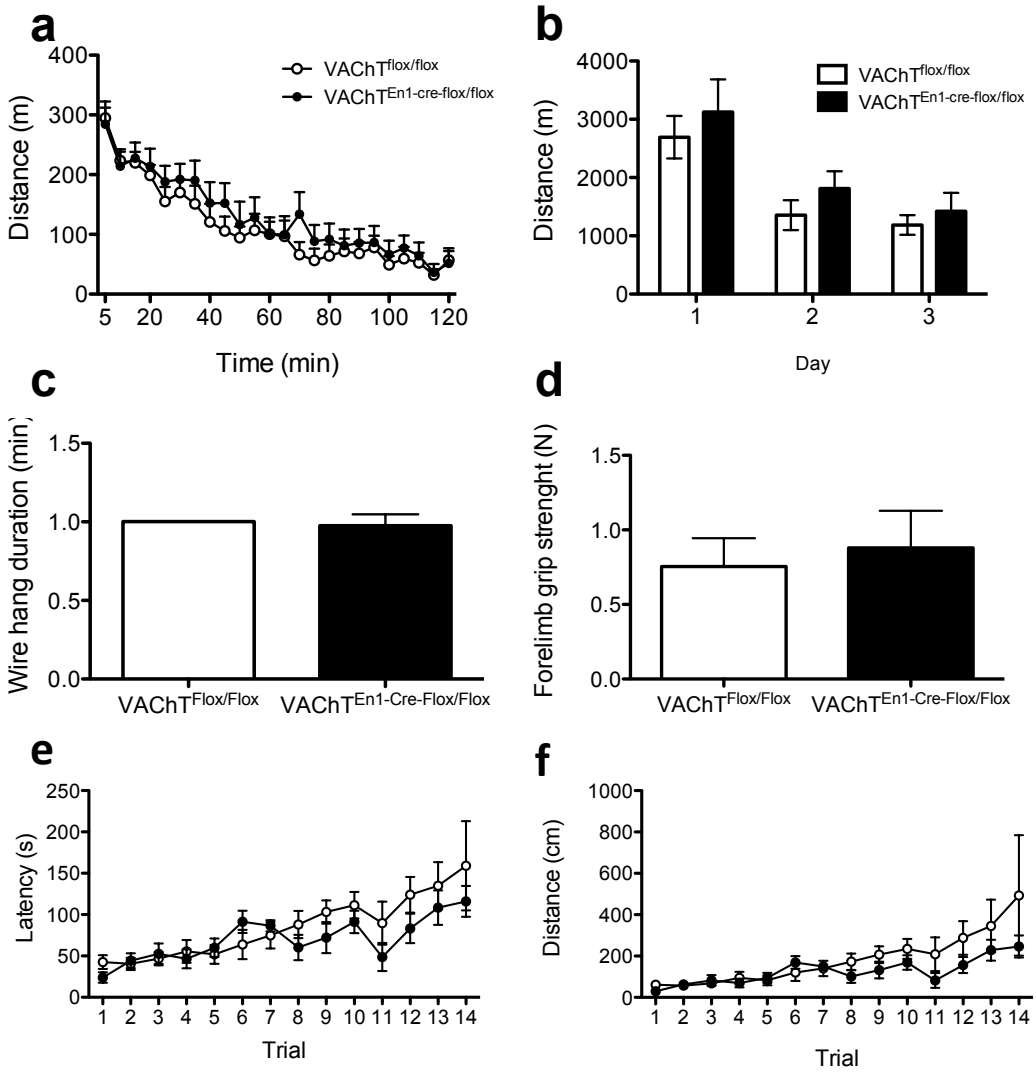

Figure 14. VAChT$^{En1\text{-}Cre\text{-}flox/flox}$ mice have normal spontaneous locomotor activity and neuromuscular functioning. (a) short-term habituation in locomotor boxes over two hours on day 1. (b) long-term habituation over three days, shown by total distanced travlled during each day. (c) duration of time on inverted wire mesh and (d) force applied by forelimbs to grip a wire. (e) latency to fall of rotarod and (f) distance covered during rotarod test. Data expressed as mean ± SEM. (a-b) analyzed using repeated measures two-way ANOVA, (c-d) analyzed using a Student's t-test, and (e-f) analyzed using repeated measures two-way ANOVA. (a-d) VAChT$^{flox/flox}$ *n* = 15, VAChT$^{En1\text{-}Cre\text{-}flox/flox}$ *n* = 12, (e-f) VAChT$^{flox/flox}$ *n* = 10, VAChT$^{En1\text{-}Cre\text{-}flox/flox}$ *n* = 7.

5.3.2 Metabolism and Sleep

Metabolic activity was measured using metabolic cages over a 48-hour period and data from the last 24 hours was analyzed. In these closed system chambers, mice were evaluated for oxygen consumption (Fig. 15a), carbon dioxide production (Fig. 15b), resting energy expenditure (RER) (Fig. 15c) and heat production (Fig 15d), as well as food and water intake (Fig. 15e-f). No significant difference was observed between $VAChT^{En1\text{-}Cre\text{-}flox/flox}$ mice and $VAChT^{flox/flox}$ controls in their VO2 ($F_{(1,30)} = 0.53$, $p = 0.4740$), VCO2 ($F_{(1,30)} = 0.54$, $p = 0.4667$), RER ($F_{(1,30)} = 0.12$, $p = 0.7301$) or heat production ($F_{(1,30)} = 1.57$, $p = 0.2202$), indicating that decreased VAChT expression in the PPT did not alter metabolism. Additionally, there was no significant difference between genotypes in food ($F_{(1,30)} = 0.88$, $p = 0.3568$) or water ($F_{(1,30)} = 0.25$, $p = 0.6189$) consumption.

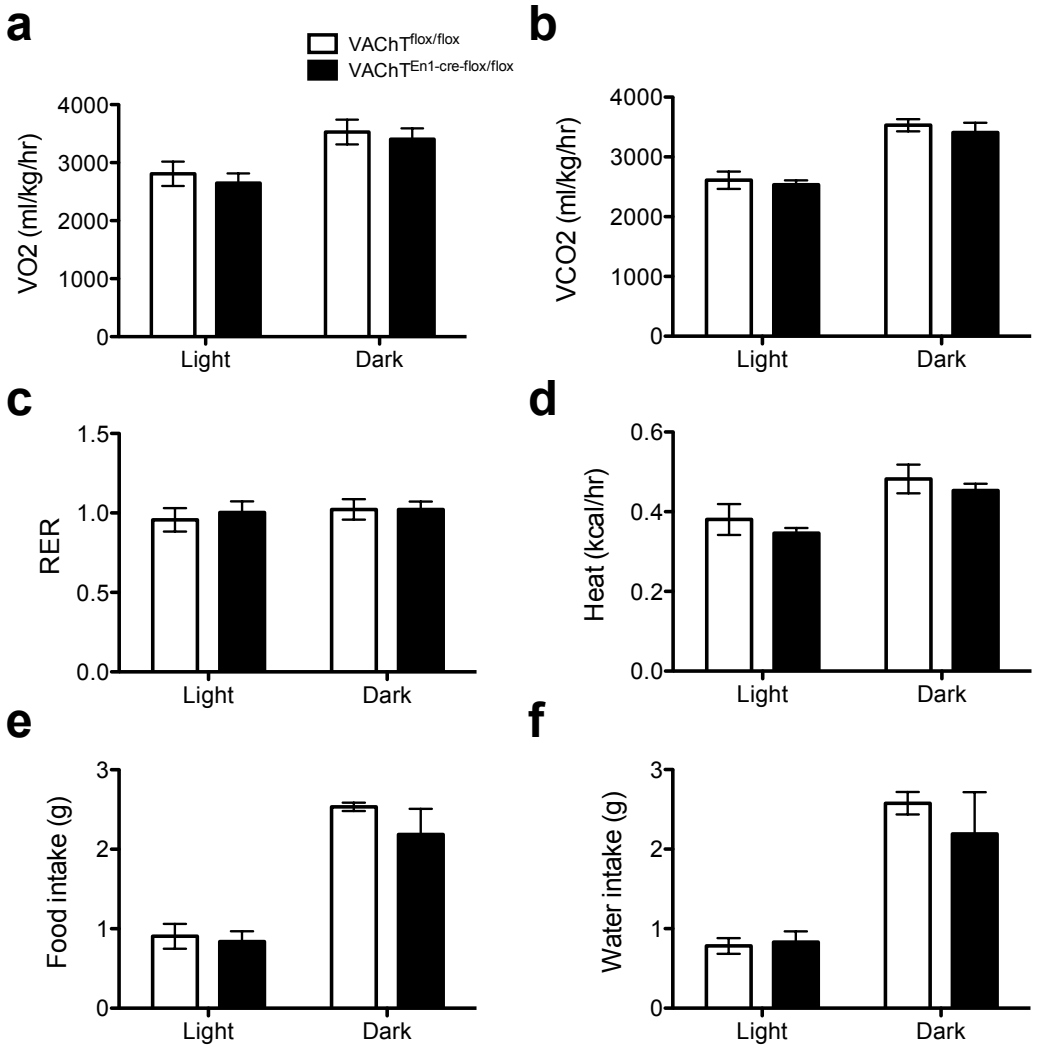

Figure 15. No difference in metabolism between VAChT$^{En1\text{-}Cre\text{-}flox/flox}$ mice and controls. Metabolic parameters were measured over a 48-hour period, with the data from only the last 24 hours analyzed. The light and dark periods are two consecutive 12-hour periods within those 24 hours analyzed. (a) oxygen consumption, (b) carbon dioxide consumption, (c) resting energy release (RER), (d) heat production, (e) food intake and (f) water intake. Data expressed as mean ± SEM, and analyzed using a two-way ANOVA. VAChT$^{flox/flox}$ *n* = 7, VAChT$^{En1\text{-}Cre\text{-}flox/flox}$ *n* = 10.

A feature of the metabolic cages is the ability to measure the animal's sleep through assessing time spent immobile in the cage versus time in motion (Guzman et al., 2013). The number of sleeping bouts, average duration of these bouts, and total time spent sleeping was measured for both the light and dark phases of the test. While there

was no significant different in the number of sleeping bouts ($F_{(2,45)} = 0.66$, $p = 0.5213$; Fig. 16a) or the average duration of these bouts ($F_{(1,45)} = 0.10$, $p = 0.9020$; Fig. 16c), Bonferroni *post hoc* revealed a significant decrease in the time spent sleeping during the dark phase of the test (the animal's wake cycle) ($F_{(1,45)} = 5.14$, $p = 0.0283$; Fig. 16b). This data suggests that there may be a role of PPT cholinergic signaling in the regulation of sleep-wake cycles.

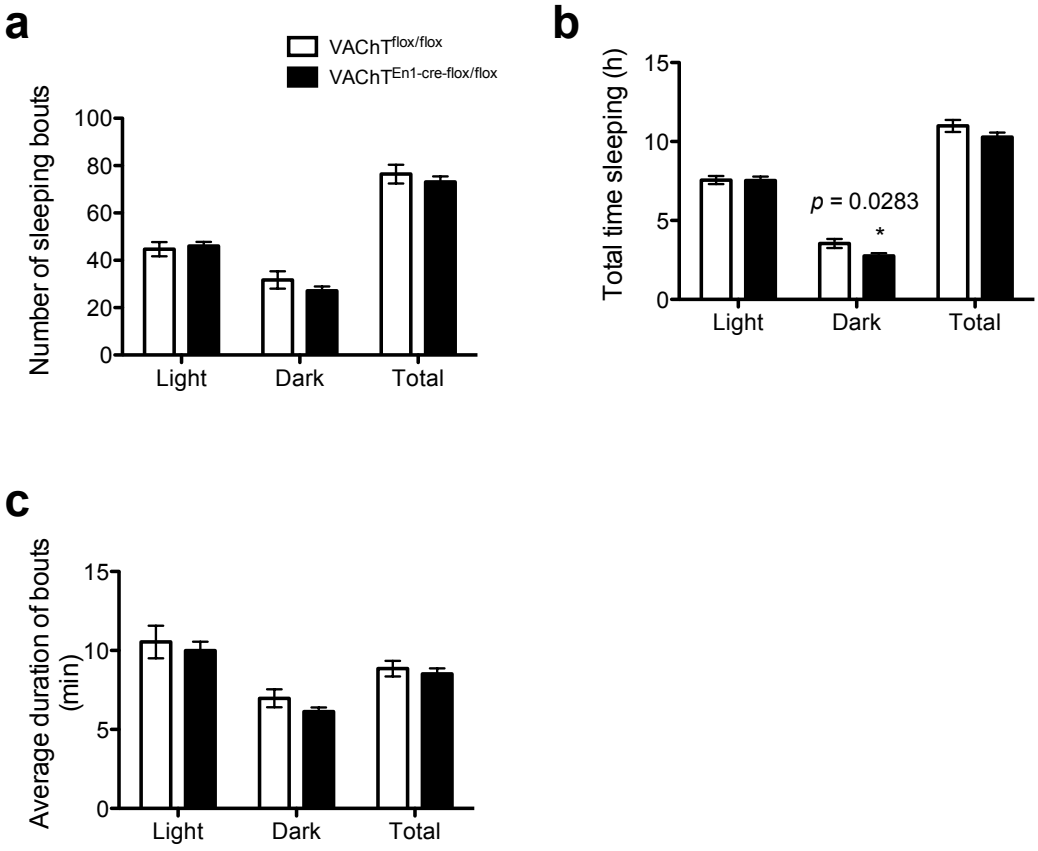

Figure 16. VAChT$^{\text{En1-Cre-flox/flox}}$ mice spend significantly less total time sleeping in the dark phase than controls. Sleep parameters were measured over a 48-hour period, with the data from only the last 24 hours analyzed. The light and dark periods are two consecutive 12-hour periods within those 24 hours analyzed. (a) number of sleeping bouts, (b) total time spent sleeping, and (c) average duration of sleeping bouts. Data expressed as mean ± SEM, and analyzed using a two-way ANOVA; *, $p < 0.05$. VAChT$^{\text{flox/flox}}$ $n = 7$, VAChT$^{\text{En1-Cre-flox/flox}}$ $n = 10$.

5.3.3 Gait

We used the CatWalk gait analysis to evaluate any subtle alterations in gait in these animals because the PPT is suggested to play a role in gait and posture (Rolland et al., 2011).

VAChT$^{En1\text{-}Cre\text{-}flox/flox}$ mice (aged 3-6 months) were not significantly different from VAChT$^{flox/flox}$ controls in terms of the intensity of their paw print ($F_{(1,56)} = 0.05$, $p = 0.8186$; Fig. 17a), the stride length ($F_{(1,56)} = 0.06$, $p = 0.8030$; Fig. 17c) and the overall normalcy of the gait ($t(14) = 1.269$, $p = 0.2251$; Fig. 17d). However, the VAChT$^{En1\text{-}Cre\text{-}flox/flox}$ mice demonstrated significantly smaller paw area than controls ($F_{(1,56)} = 10.32$, $p = 0.002$; Fig. 17b). Bonferroni postests did not reveal a significant difference between geneotypes for the paw area of a specific paw. Having a smaller paw print area suggests that the animals are walking either on the sides of the paws or on their toes, which may be indicative of slight postural instability.

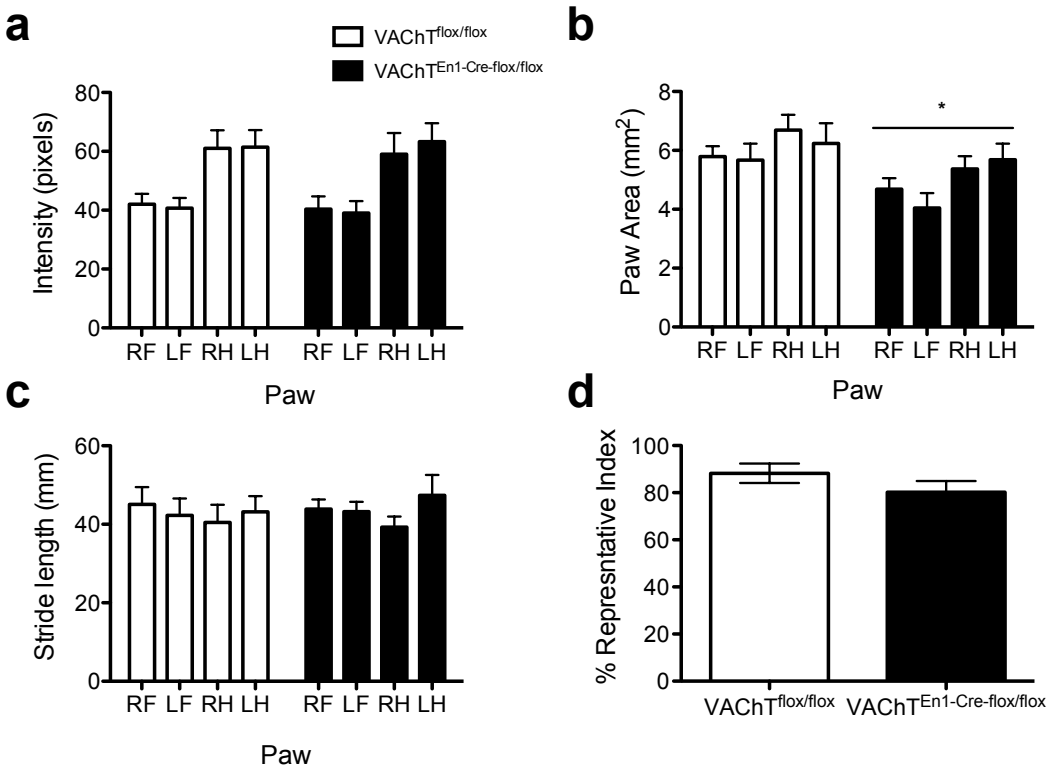

Figure 17. Young VAChT$^{\text{En1-Cre-flox/flox}}$ mice have abnormal gait. In young mice (aged 3-6 months), (a) intensity of paw print, (b) area of paw print, (c) distance between two prints from the same paw and (d) percent normalcy were measured. Data expressed as mean ± SEM and analyzed using two-way ANOVA except (d) was analyzed using a Student's t-test; *, $p < 0.05$. VAChT$^{\text{flox/flox}}$ $n = 8$, VAChT$^{\text{En1-Cre-flox/flox}}$ $n = 8$.

Because of this slight change in postural stability, we also followed with a gait analysis in older mice (12 months old). The results reflected those seen in the younger mice, but the abnormalities were even more profound. That is, old mutant mice showed a significant difference from controls in terms of paw area ($F_{(1,44)} = 9.34$, $p = 0.0038$; Fig. 18b) with the area of their print being smaller. Additionally, old VAChT$^{\text{En1-Cre-flox/flox}}$ mice were significantly different from age matched VAChT$^{\text{flox/flox}}$ controls ($F_{(1,48)} = 8.32$, $p = 0.0059$) in the intensity of their paw print (Fig. 18a). As for stride length, the old VAChT$^{\text{En1-Cre-flox/flox}}$ mice interestingly had a significantly longer stride length ($F_{(1,44)} = 7.58$, $p = 0.0086$) than the control mice (Fig. 18c). For intensity, paw area and stride length, Bonferroni *post hoc* did not reveal a significant difference between geneotypes for the paw area of a specific paw. However, when the representative index was compared

between genotypes, there was not a significant difference ($t(11) = 0.8566$, $p = 0.4099$). The representative index is a measure of interlimb coordination when compared to normal step sequence patterns (Neumann et al., 2009). In short, VAChT$^{En1\text{-}Cre\text{-}flox/flox}$ mice showed mild gait abnormalities in the CatWalk analysis, which is very sensitive to evaluating the gait parameters, but when compared to a representative normal murine gait, the overall gait of VAChT$^{En1\text{-}Cre\text{-}flox/flox}$ mice did not show to be significantly abnormal (Fig. 18d).

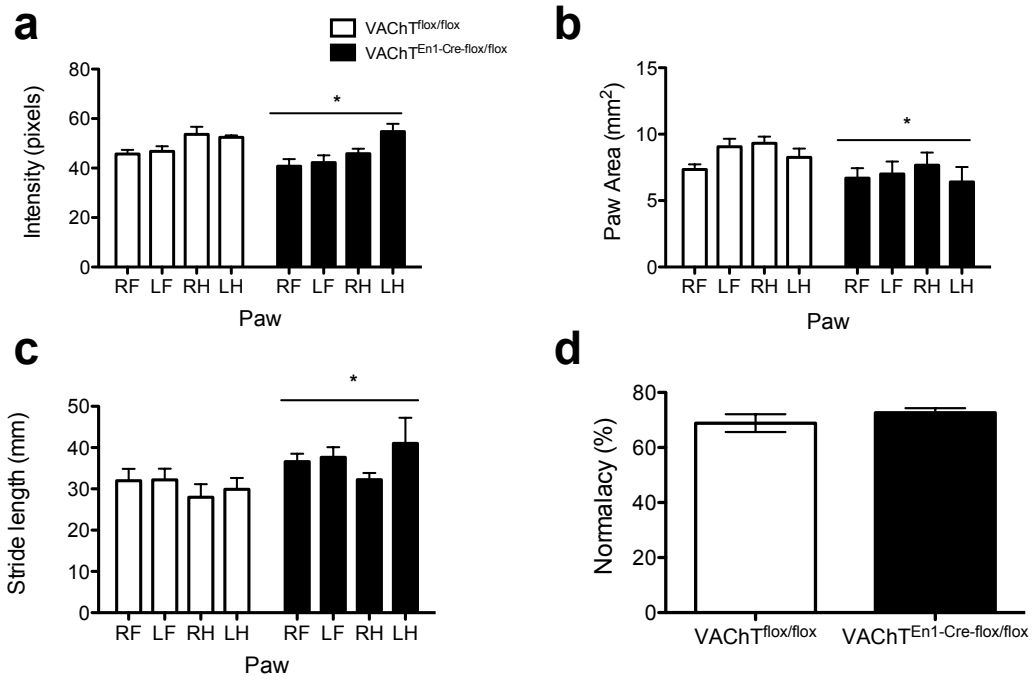

Figure 18. Old VAChT$^{En1\text{-}Cre\text{-}flox/flox}$ mice have abnormal gait. In old mice (aged 12 months) (a) intensity of paw print, (b) area of paw print, (c) distance between two prints from the same paw and (d) percent normalcy were measured. Data expressed as mean ± SEM and analyzed using two-way ANOVA except (d) was analyzed using a Student's t-test; *, $p < 0.05$. VAChT$^{flox/flox}$ $n = 8$, VAChT$^{En1\text{-}Cre\text{-}flox/flox}$ $n = 8$.

5.3.4 Psychiatric-like phenotypes

5.3.4.1 Depression

It has been proposed that depression is a result of dysregulation of the cholinergic system (Janowsky 1972) but to date, it is unclear which cholinergic nuclei in the brain

may be leading to depression symptoms when disturbed. Using the VAChT$^{En1\text{-}Cre\text{-}flox/flox}$ mice we have the possibility to assess whether depressive-like behaviour is present in animals with disruptions in cholinergic signaling from the PPT.

Depressive-like behaviour was evaluated by using the forced swim test (FST) and the tail suspension test (Figure 19). These tests are pharmacologically validated methods of assessing behavioural despair or depressive-like behaviour in animals. Immobility is interpreted as hopelessness and depressive-like behaviour since rodents given antidepressants will swim longer and spend less time immobile. The time spent immobile, as well as the total distance swam, in the last 4 minutes of the test were measured. For the tail suspension test, animals will move to escape the aversive situation, but a mouse showing increased depressive-like traits will stop struggling and hang immobile. Here, the time spent immobile as well as the number of immobility episodes was measured.

VAChT$^{En1\text{-}Cre\text{-}flox/flox}$ mice spent significantly less time immobile than controls in both tests (forced swimming $t(16) = 2.233$, $p = 0.0402$; tail suspension $t(24) = 0.0040$, $p = 0.0040$; Fig. 19a and Fig. 19c, respectively). However, the VAChT$^{En1\text{-}Cre\text{-}flox/flox}$ mice did not swim a greater distance than controls in the forced swim test ($t(17) = 1.551$, $p = 0.1394$; Fig. 19b) or have a greater number of immobility episodes in the tail suspension test ($t(24) = 0.05978$, $p = 0.9528$; Fig. 19d).

In summary, the VAChT$^{En1\text{-}Cre\text{-}flox/flox}$ mice demonstrate anti-depressive-like behaviour in both the forced swim test and tail suspension tests, suggesting that the cholinergic signaling from the PPT may be involved in regulating depressive symptoms.

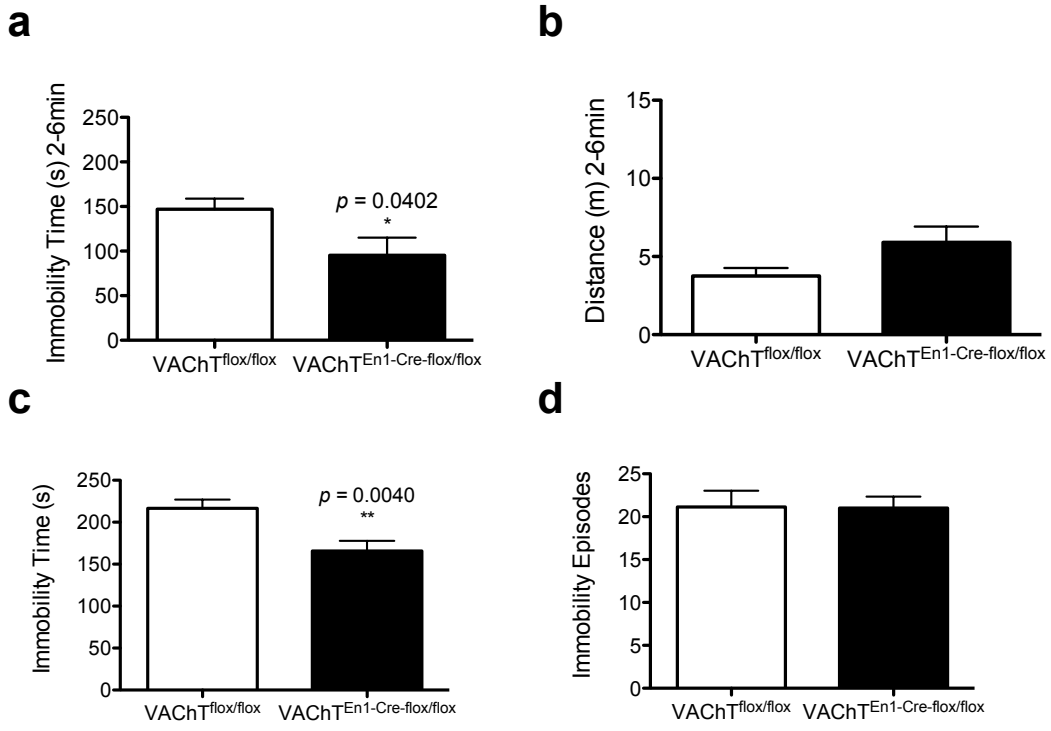

Figure 19. VAChT$^{En1\text{-}Cre\text{-}flox/flox}$ mice present antidepressive-like behaviour in the forced swimming test and the tail suspension test. (a) immobility time in the final four minutes of the forced swimming test and (b) total distance swam in the final four minutes of the forced swimming test. (c) the total immobility time and (d) the number of immobility episodes in the tail suspension test. Data expressed as mean ± SEM and analyzed using a Students' t test; *, p <0.05; **, p <0.01. (a-b) VAChT$^{flox/flox}$ n = 7, VAChT$^{En1\text{-}Cre\text{-}flox/flox}$ n = 12. (c-d) VAChT$^{flox/flox}$ n = 14, VAChT$^{En1\text{-}Cre\text{-}flox/flox}$ n = 12.

5.3.4.2 Anxiety

Since the VAChT$^{En1\text{-}Cre\text{-}flox/flox}$ mice showed an anti-depressive-like phenotype, we decided to test the animals for further psychiatric-like behaviours. We assessed anxiety-like behaviour using a number of tests. First, we used the elevated plus maze. In this test, the plus-shaped apparatus has two closed, dark arms and two bright open arms. The percentage of time spent on either the open or closed arms, or in the centre, was measured (Fig. 20a). Additionally, the number of entries into the open arm was quantified (Fig.

20b). Mice with increased anxiety traits will spend more time in the dark, closed arms of the maze.

In the elevated plus maze, VAChT$^{En1\text{-}Cre\text{-}flox/flox}$ mice did not differ from controls in the amount of time they spent in the closed arms, open arms, or the centre ($F_{(1,81)}$ = 0.001, p = 0.9400) or in the number of open arm entries (t(27) = 0.5215, p = 0.6063).

Next, anxiety-like behaviour was evaluated using the locomotor boxes. Mice are allowed to explore the boxes freely for a two-hour period. Mice with increased anxiety traits will spend more time in the corners of the box, whereas mice with less anxiety traits will explore the box and spend more time in the centre. Here, total time in the centre of the locomotor was measured (Fig. 20c). Likewise, when time spent in the centre of the locomotor boxes was measured, VAChT$^{En1\text{-}Cre\text{-}flox/flox}$ mice did not differ from controls (t(18) = 0.3276, p = 0.7470).

Finally, the light/dark place preference test was used as an additional measure of anxiety. In this test, a black box with a small entrance is placed inside the locomotor box to divide it into two halves: the open half and the dark covered half. The percent of time spent in the dark versus the light portion of the box was measured (Fig 20d). Surprisingly, in the light/dark place preference test, VAChT$^{En1\text{-}Cre\text{-}flox/flox}$ mice spent a significantly greater time in the dark than littermate controls (t(26) = 2.401, p = 0.0238).

In summary, results from the light/dark place preference task suggested that VAChT$^{En1\text{-}Cre\text{-}flox/flox}$ mice show increased anxiety-like behaviour phenotype, however, in the other two tests, the partial loss of cholinergic signaling from the PPT did not appear to affect anxiety-like behaviour. Together these results suggest that if VAChT$^{En1\text{-}Cre\text{-}flox/flox}$ mice show an anxiety phenotype, it does not seem to be a robust phenotype.

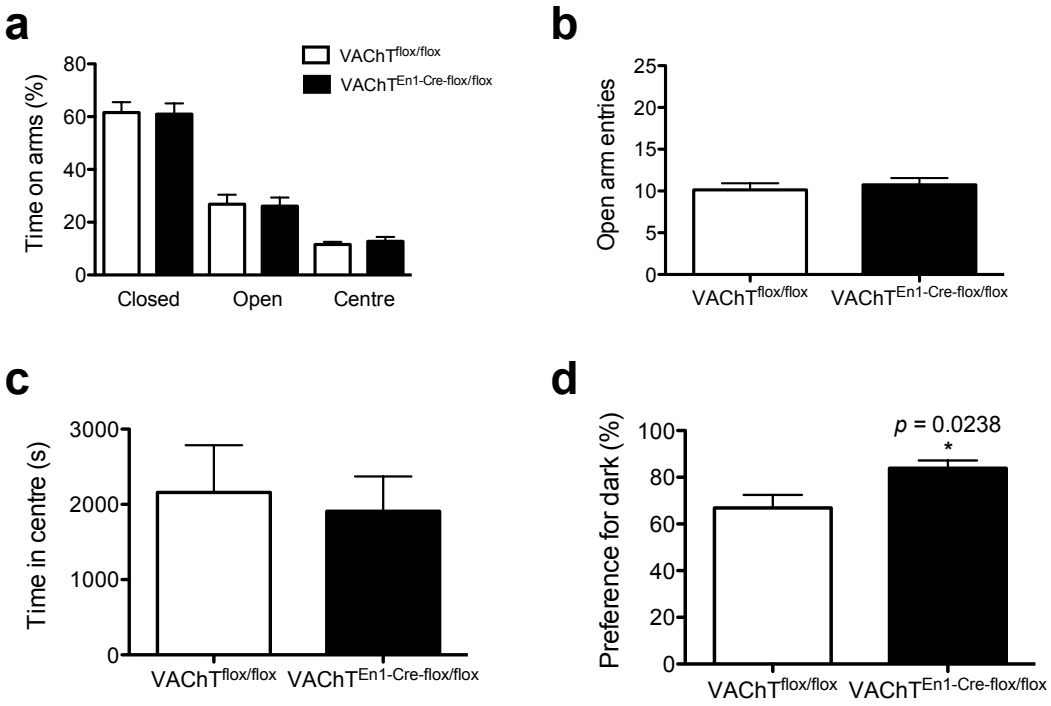

Figure 20. VAChT$^{En1\text{-}Cre\text{-}flox/flox}$ mice demonstrate an anxiety-like phenotype in the light/dark place preference test. (a) Percentage of time spent on the closed or open arms or the centre of the elevated plus maze and (b) the number of entries into the open arm of the elevated plus maze. (c) Total time spent in the centre of a locomotor box during a two-hour period. (d) Percentage of time spent in the dark chamber during the light/dark place preference test. (a) Data expressed as mean ± SEM and analyzed using a two-way ANOVA and (b-d) data analyzed using a Students' t test; *, $p < 0.05$. (a-b) VAChT$^{flox/flox}$ $n = 14$, VAChT$^{En1\text{-}Cre\text{-}flox/flox}$ $n = 15$. (c) VAChT$^{flox/flox}$ $n = 8$, VAChT$^{En1\text{-}Cre\text{-}flox/flox}$ $n = 12$. (d) VAChT$^{flox/flox}$ $n = 16$, VAChT$^{En1\text{-}Cre\text{-}flox/flox}$ $n = 12$.

5.3.4.3 Compulsivity

To further characterize potential psychiatric-like behaviours of these VAChT$^{En1\text{-}Cre\text{-}flox/flox}$ mice, we next assessed compulsivity or repetitive behaviours using the marble burying task (Fig. 21). Here, twenty marbles are even spaced on top of two inches of clean bedding in a novel cage. Mice were place in the cage for fifteen minutes and the number of marbles buried in the bedding was quantified. Mice that buried a greater number of marbles were considered to have more perseverative behaviour.

VAChT$^{En1\text{-}Cre\text{-}flox/flox}$ mice buried significantly less marbles then VAChT$^{flox/flox}$ control mice ($t(31) = 2.077$, $p = 0.0462$), suggesting that these mice show decreased compulsivity compared to controls.

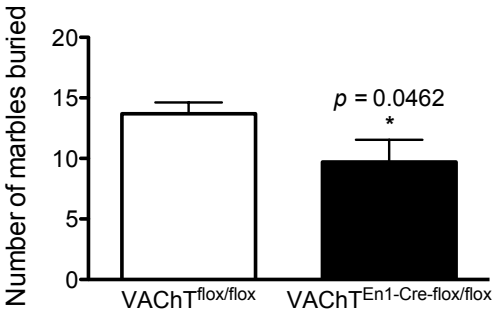

Figure 21. VAChT$^{En1\text{-}Cre\text{-}flox/flox}$ mice have decreased compulsive behaviours in the marble burying task. VAChT$^{En1\text{-}Cre\text{-}flox/flox}$ mice buried less marbles than controls in the marble burying task. Data expressed as mean ± SEM and analyzed using a Student's t-test; *, $p < 0.05$. VAChT$^{flox/flox}$ $n = 19$, VAChT$^{En1\text{-}Cre\text{-}flox/flox}$ $n = 19$.

5.3.5 Learning and Memory

5.3.5.1 Spatial memory

We tested spatial learning and memory in the VAChT$^{En1\text{-}Cre\text{-}flox/flox}$ mice using the MWM (Fig. 22). For the spatial version of this test, mice undergo 4 days of training (the acquisition phase) to learn the location of a hidden platform. On the fifth day, the probe trial occurs and the amount of time spent in each quadrant of the tank with the platform removed is quantified.

During the course of acquisition, performance of VAChT$^{En1\text{-}Cre\text{-}flox/flox}$ mice was significantly different from that of controls in terms of latency to find the target ($F_{(1,22)} = 5.33$, $p = 0.0307$; Fig. 22a). Bonferroni *post* hoc test analysis demonstrated that the VAChT$^{En1\text{-}Cre\text{-}flox/flox}$ mice did not improve their latency to find the target on days 3 and 4 during the acquision phase. VAChT$^{En1\text{-}Cre\text{-}flox/flox}$ mice took the same time to find the hidden platform across the four acquisition days, whereas VAChT$^{flox/flox}$ control mice were able to find the platform more quickly each successive day. These results indicated that VAChT$^{En1\text{-}Cre\text{-}flox/flox}$ mice had deficits in learning the location of the platform. On the

probe trial day, VAChT$^{En1\text{-}Cre\text{-}flox/flox}$ mice showed no preference for the target quadrant of the pool whereas the Tukey *post hoc* test demonstrated that the VAChT$^{flox/flox}$ control mice spent significantly more time in the target quadrant ($r = 0.4666$, $p < 0.0001$) (Fig. 22b). The occupancy plots for the probe trial show that the controls remembered where the platform should be and spent the majority of their time in this quadrant (Fig. 22c). In contrast, VAChT$^{En1\text{-}Cre\text{-}flox/flox}$ mice did not seem to recall this location during the probe trial and primarily spent their time in thigmotaxis or passive floating (Fig. 22d).

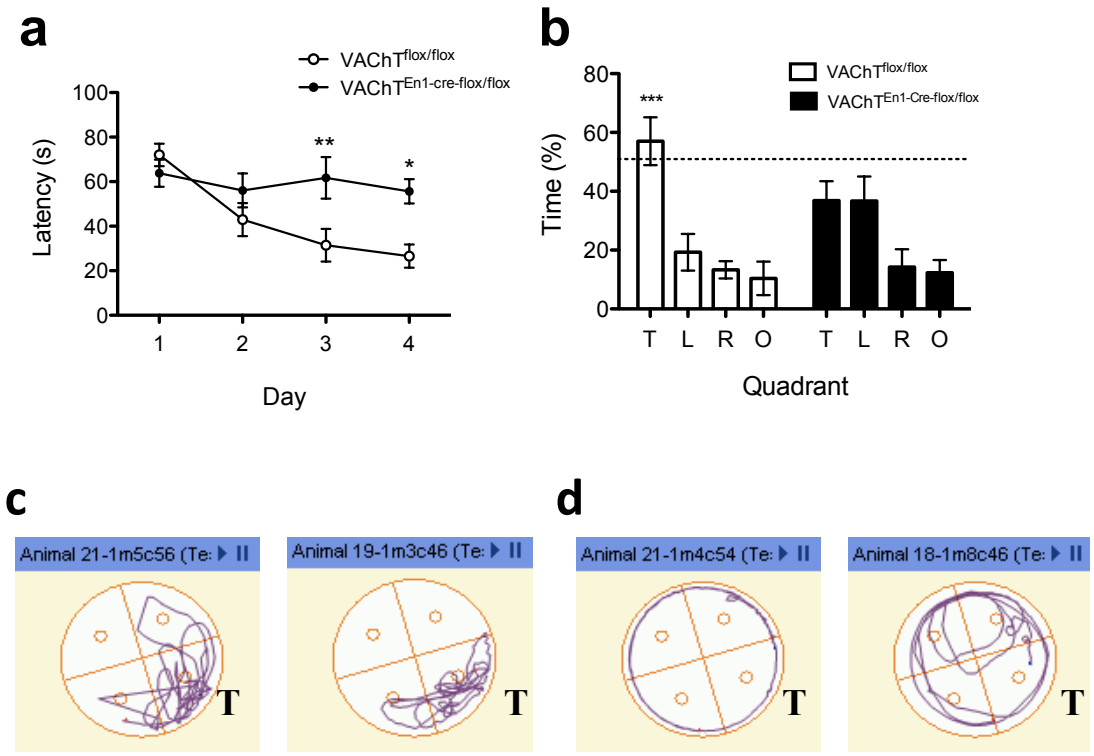

Figure 22. VAChT$^{En1\text{-}Cre\text{-}flox/flox}$ mice show deficits in learning and memory in the spatial version of the Morris water maze. (a) Latency to find hidden platform over 4 training days during of the spatial Morris water maze and (b) time spent in each quadrant during probe trial; T=target, L=left of target, R=right of target and O=opposite from target. (c) Representative plots of flox/flox mice during the probe trial and (d) representative plots of VAChT$^{En1\text{-}Cre\text{-}flox/flox}$ mice during the probe trial. The target quadrant is the bottom right segment of the path tracing images. Data expressed as mean ± SEM and analyzed using a two-way ANOVA; *, $p < 0.05$, **, $p < 0.01$, ***, $p < 0.0001$. VAChT$^{flox/flox}$ $n = 12$, VAChT$^{En1\text{-}Cre\text{-}flox/flox}$ $n = 12$.

5.3.5.2 Goal-directed learning

We next assessed the ability of VAChT$^{En1\text{-}Cre\text{-}flox/flox}$ mice to learn and remember the location of a visible platform that was further indicated by a large cue (Vorhees and Williams, 2006). In the cued version of the Morris water maze, mice undergo 8 trials on Day 1 (the acquisition phase) to learn to swim to the visible platform, and the location of the platform and their starting point changes in each trial. On Day 2, the mice undergo two trials but with platform location and starting point combinations they did not experience on Day 1.

During the acquisition day VAChT$^{En1\text{-}Cre\text{-}flox/flox}$ mice were significantly different from controls ($t(14) = 2.611$, $p = 0.0205$) in terms of latency to find the target platform (Fig. 23a). This deficit was even more pronounced during the probe trial where VAChT$^{flox/flox}$ mice decreased their latency to find the cued platform and VAChT$^{En1\text{-}Cre\text{-}flox/flox}$ mice did not ($t(14) = 4.653$, $p = 0.004$; Fig. 23b). Examination of the path traces confirmed that VAChT$^{flox/flox}$ mice swam almost directly to the platform (Fig 23c) whereas VAChT$^{En1\text{-}Cre\text{-}flox/flox}$ mice do not appear to use the cue to find the target on the second day (Fig. 23d).

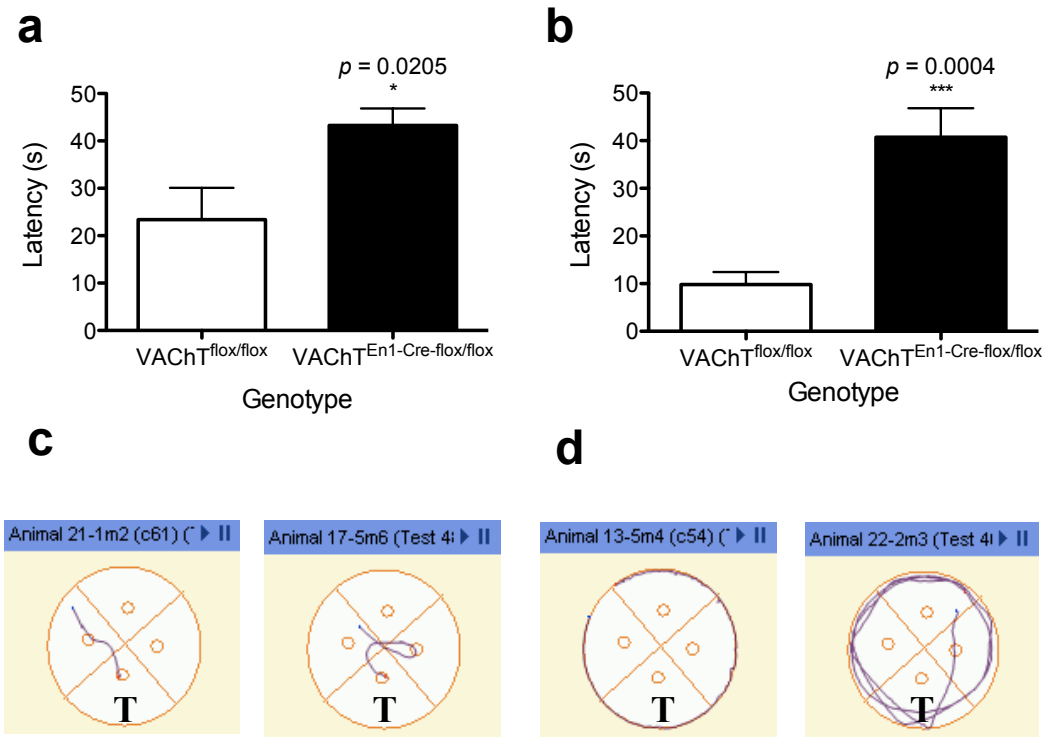

Figure 23. VAChT$^{En1\text{-}Cre\text{-}flox/flox}$ mice show deficits in learning and memory in the cue-directed version of the Morris water maze. (a) Latency to find the visible platform during the cued Morris water maze training day (8 trials) and (b) latency to find the visible platform during the probe trial (2 trials). (c) Representative plots of VAChT$^{flox/flox}$ mice during the probe trial and (d) representative plots of VAChT$^{En1\text{-}Cre\text{-}flox/flox}$ mice during the probe trial. The target quadrant is the bottom segment of the path tracing images; T= Target. Data expressed as mean ± SEM and analyzed using a Student's t-test; *, $p < 0.05$; **, $p < 0.01$; ***, $p < 0.0001$. VAChT$^{flox/flox}$ $n = 8$, VAChT$^{En1\text{-}Cre\text{-}flox/flox}$ $n = 8$.

5.3.5.3 Working memory

To further characterize the learning and memory deficits that result from a deficiency of cholinergic signaling in the PPT, we used the spontaneous alternations Y-Maze to evaluate working memory in these animals (Fig. 24) (de Castro et al., 2009).

VAChT$^{En1\text{-}Cre\text{-}flox/flox}$ mice and control mice had the same number of spontaneous alternations ($t(23) = 1.912$, $p = 0.0684$; Fig. 24) in the Y maze. Performance of both genotypes was above chance (> 50%) regarding alternations, suggesting that these mice have no working memory deficit.

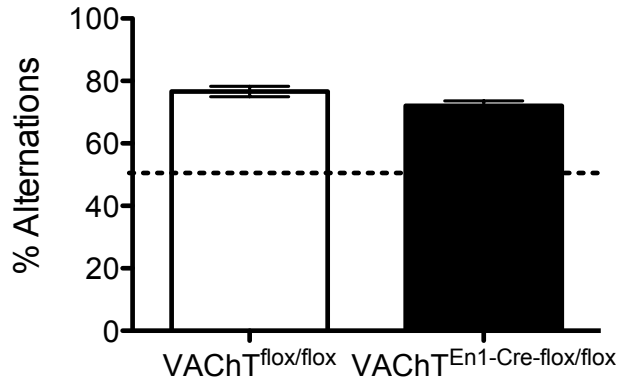

Figure 24. VAChT$^{En1\text{-}Cre\text{-}flox/flox}$ mice have normal working memory in the spontaneous alternations Y-maze task. The percent of alternation is shown. Both genotypes performed about chance, as indicated by the dashed line. Data expressed as mean ± SEM and analyzed using a Students' t-test. VAChT$^{flox/flox}$ *n* = 14, VAChT$^{En1\text{-}Cre\text{-}flox/flox}$ *n* = 11.

5.3.6 Attention

To determine whether VAChT$^{En1\text{-}Cre\text{-}flox/flox}$ mice are affected in other cognitive domains that are sensitive to cholinergic tone from the PPT, we used the 5-choice serial reaction time task (5-CSRTT) (Romberg et al., 2011). During the training phase, VAChT$^{En1\text{-}Cre\text{-}flox/flox}$ mice did not differ from controls in terms of number of training sessions needed to achieve criterion ($F_{(1,10)}$ = 0.18, p = 0.6819) with a main effect of training phase ($F_{(2,20)}$ = 7.12, p = 0.0046; Fig. 25). It should be noted that one mouse of each genotype never completed the training phase and thus were removed from the experiment and were not subjected to the 5-CSRT task. Mice were first trained using a 4 s stimulus duration and then we proceeded to 2 s stimulus duration for the 5-CSRT task training. VAChT$^{En1\text{-}Cre\text{-}flox/flox}$ mice were able to acquire the task, reaching the criteria at both stimulus durations (2 and 4 s) in the same number of sessions as controls ($F_{(1,10)}$ = 0.18, p = 0.6819) with a main effect of training phase ($F_{(2,20)}$ = 7.12, p = 0.0046; Fig. 25). During the 5CSRTT training phase, two VAChT$^{flox/flox}$ control mice and one VAChT$^{En1\text{-}Cre\text{-}flox/flox}$ mouse were removed from the test due to their inability to pass the 2s stimulus duration phase even after all other mice had completed the 5CSRTT probe trial.

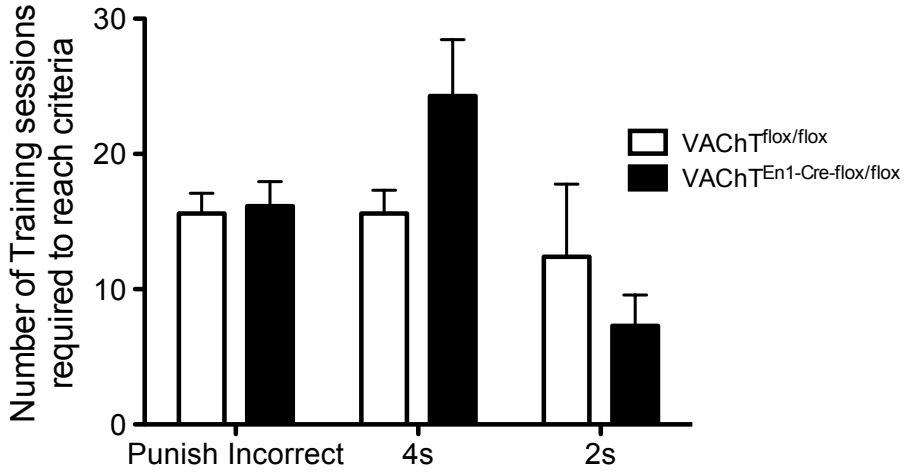

Figure 25. Sessions to reach criteria. Number of training sessions required to meet the criteria to pass the punish incorrect training phase, the 4s stimulus duration training phase or the 2s stimulus duration training phase. Data expressed as mean ± SEM and analyzed using a repeated measures two-way ANOVA. VAChT$^{flox/flox}$ *n* = 6, VAChT$^{En1\text{-}Cre\text{-}flox/flox}$ *n* = 7.

For the probe trial, we increased the attentional demand by decreasing the stimulus durations to 1.5 s, 1.0 s, 0.8 s and finally 0.6 s. During the probe trials, VAChT$^{En1\text{-}Cre\text{-}flox/flox}$ mice did not differ from controls in choice accuracy ($F_{(1,10)} = 0.02$, $p = 0.8970$) and there was a significant effect of stimulus duration ($F_{(3,30)} = 6.45$, $p = 0.0017$; Fig. 26a). The rate of omissions for VAChT$^{En1\text{-}Cre\text{-}flox/flox}$ mice was unaffected ($F_{(1,10)} = 0.14$, $p = 0.7154$) and there was a significant effect of stimulus duration ($F_{(3,20)} = 34.32$, $p < 0.0001$; Fig. 26b). As for premature responses, again VAChT$^{En1\text{-}Cre\text{-}flox/flox}$ mice were not different from controls ($F_{(1,1o)} = 0.81$, $p = 0.3896$; Fig. 26e). No change in perseverative responses was observed in VAChT$^{En1\text{-}Cre\text{-}flox/flox}$ mice ($F_{(1,10)} = 1.04$, $p = 0.3314$; Fig. 26f). Additionally, VAChT$^{En1\text{-}Cre\text{-}flox/flox}$ mice did not differ from controls in terms of their correct response latency ($F_{(1,10)} = 0.16$, $p = 0.6950$; Fig. 26c). There were also no differences between genotypes in terms of reward collection latency ($F_{(1,10)} = 0.12$, $p = 0.7376$; Fig. 26d).

In summary, decreased cholinergic signaling from the PPT did not have a significant affect on the attentional capacities of these animals as measured by the 5-CSRTT.

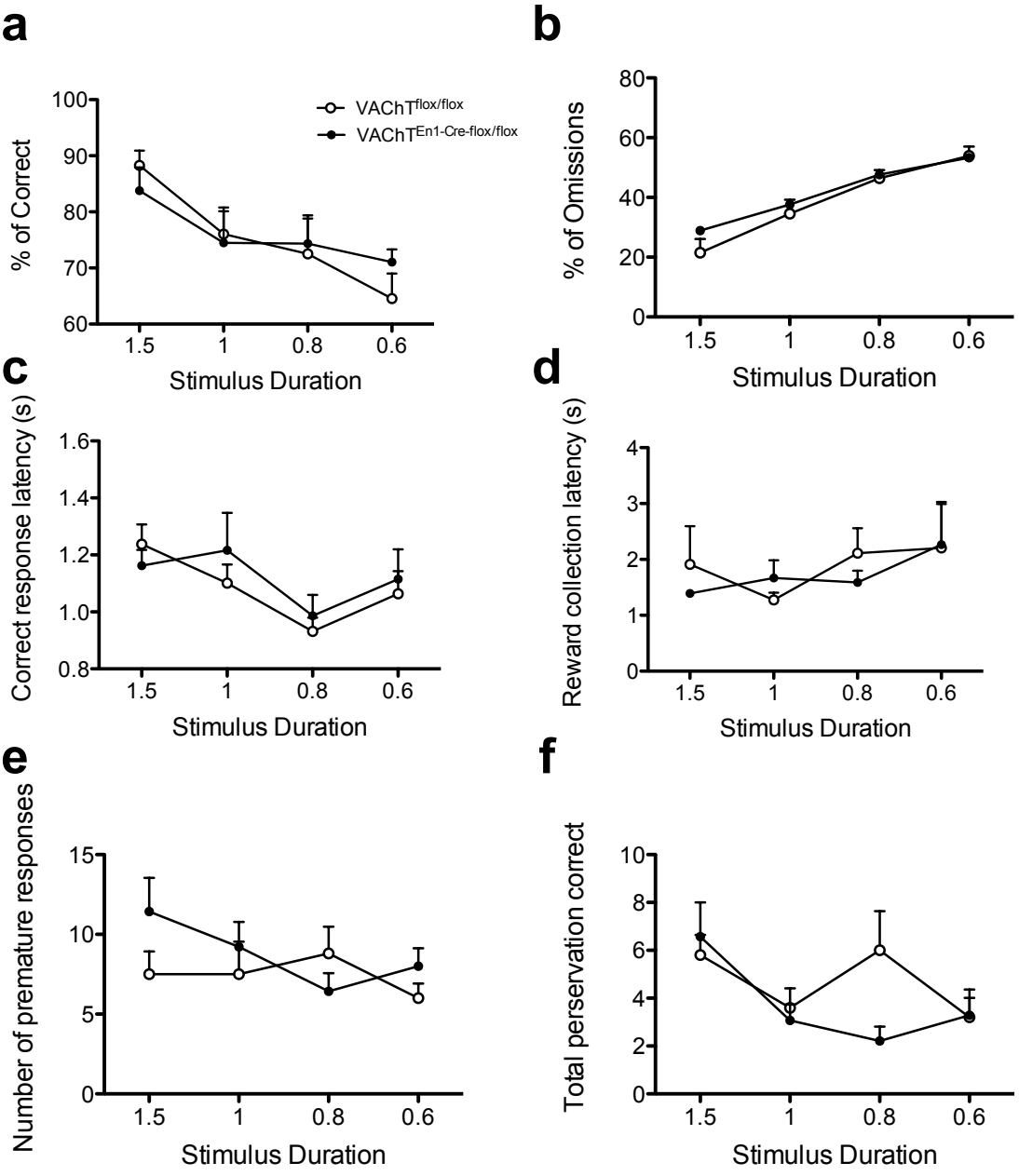

Figure 26. VAChT$^{En1\text{-}Cre\text{-}flox/flox}$ mice do not show attentional deficits in the 5-choice serial reaction time task. (a) Percent correct, (b) percent of omissions, (c) correct response latency, (d) reward collection latency, (e) number of premature responses and (f) total preservative correct. Data expressed as mean ± SEM and analyzed using a two-way ANOVA. VAChT$^{flox/flox}$ *n* = 6, VAChT$^{En1\text{-}Cre\text{-}flox/flox}$ *n* = 7.

Chapter 3

6 Discussion

Here we investigated the role of ACh release from PPT cholinergic neurons. Decreased cholinergic signaling from the PPT appeared to have no affect on spontaneous locomotor activity, neuromuscular functioning, metabolism, working memory or attention. A small but significant effect on gait and sleep was observed. VAChT$^{En1\text{-}Cre\text{-}flox/flox}$ mice had strong deficits in learning spatial cues in the Morris water maze and showed deficits in goal-directed behaviours. Additionally, an antidepressive-like behaviour, a slight anxiety-like behaviour and reduced compulsivity were observed in these animals. These results suggest that ACh has an important role in the modulation of several of the physiological functions regulated by the PPT.

6.1 Analysis of VAChT$^{En1\text{-}Cre\text{-}flox/flox}$ mice

We used the Rosa26-tdTomato reporter mice to elucidate the pattern of expression of Cre recombinase driven by the En1 promoter. Our immunohistological analysis of brain slices of these reporter mice revealed expression patterns of Cre recombinase that varied slightly from those previously reported by Patel et al. (2012). These authors found Cre-expression under the En1-Cre driver restricted to the rostral brainstem, and crossing of En1-Cre mice with ChAT$^{flox/flox}$ mice resulted in a complete loss of ChAT mRNA expression in the PPT and LDT, as measured by *in-situ* hybridization. Here, we found that approximately 40% of CHT1-labelled cholinergic neurons colocalized with neurons expressing tdTomato, suggesting that around 40% of cholinergic neurons within the PPT would have a loss of VAChT and subsequently be unable to release ACh, in contrast to the 100% decrease in ChAT mRNA observed in the En1-Cre;ChAT$^{flox/flox}$ mice. Additionally, we did observe that approximately 10% of cholinergic neurons in the Mo5 motor nuclei colocalized with neurons expressing tdTomato, while Patel and colleagues (2012) reportated that Mo5 was unaffected. Importantly, these authors created En1-Cre;Tau reporter mouse line to determine the neuronal populations affected by Cre-recombinase. One En1-Cre;Tau sagittal brain section from one mouse was stained by

immunohistochemistry for nuclear β –galactosidase (nLacZ) and VAChT. The image was included, however no quantification of colocalization between nLacZ- and VAChT-labelling was provided, and visual examination of the image indicates much less than 100% of the VAChT-labelled neurons colocalize with the nLacZ-labelled neurons, as was observed in our immunohistological analysis Importantly, Patel et al., (2012) did not investigate the protein levels of ChAT in the PPT and the neuronal populations it innervates to indirectly quantify the extent of Cre-mediated recombination. Our Western blot analysis showed that the thalamus, the primary output centre of the PPT, had an almost 100% decrease in VAChT levels. As projections from the PPT are the major source of ACh to the thalamus (Kotegal et al., 2012), these results strongly indicate that most cholinergic projections from the PPT to the thalamus did not have VAChT in their nerve terminals. While the Western blot analysis supports that the decrease in VAChT expression is restricted to the rostral brain, the immunohistological analysis indicates that these mice have only a partial decrease in VAChT expression, and subsequently cholinergic signaling, in the PPT.

6.1.1 Locomotion and gait

$VAChT^{En1\text{-}Cre\text{-}flox/flox}$ mice showed normal spontaneous locomotor activity in an open field, no muscular weakness in the grip strength or wire hang test, and their performance in the rotarod task was not significantly different from controls, indicating that these mutants were physically fit. These data indicate that the release of ACh from the cholinergic neurons of the PPT is not required for spontaneous locomotor activity or neuromuscular functioning.

Previous studies using lesions of the PPT to examine the effects of PPT signaling on spontaneous locomotion have found similar results. Steiniger and Kretschmer (2004) found that bilateral lesions of the PPT had no effect on spontaneous motor behaviour in rats. Hernandez-Chan et al. (2011) also found that bilateral lesions of the PPT with quinolinic acid failed to produce changes in motor activity. However, these lesions eliminated not only cholinergic, but also glutamatergic and GABAergic neurons from the PPT. Different from our results, Patel and colleagues (2012) who evaluated locomotor activity in conditional ChAT knockout mice using the En1-Cre driver, suggested that the

$En1^{Cre}$; $ChAT^{flox/flox}$ mice were hypoactive. Like the $VAChT^{En1\text{-}Cre\text{-}flox/flox}$ mice, the $En1^{Cre}$; $ChAT^{flox/flox}$ mice showed loss of cholinergic activity in the PPT (Patel et al., 2012). One possible explanation for the hypolocomotion phenotype observed in $En1^{Cre}$; $ChAT^{flox/flox}$mice is the different background. Although Patel et al. (2012) did not report the background of the mice they used in their studies, it is possible that they were mainly 129S1/SvImJ, as the $En1^{Cre}$ mice (Jax stock# 007916) are provided from Jax Laboratories in this background. Mice on a different 129 background, including 129S1/SvImJ, 129S6/SvEvTac, and 129X1/SvJ, have been reported to be hypoactive when compared to mice in C57Bl/6 background (Thomsen et al., 2011). For our studies, we initially backcrossed the $En1^{Cre}$ mice twice to a C57Bl/6 background before we crossed them to the $VAChT^{flox/flox}$ mice. Thus, in the $VAChT^{En1\text{-}Cre\text{-}flox/flox}$ mice the C57Bl/6 background predominates over the 129S1. Additionally, our experiments with the $VAChT^{En1\text{-}Cre\text{-}flox/flox}$ mice indicate that these mice travel 300 m in the first 10 minutes of the spontaneous locomotion in an open field test, which is the same distance travelled for the $En1^{Cre}$; $ChAT^{flox/flox}$ in the first 10 minutes of the open field test that Patel et al. (2012) performed. It is possible that the reason the $En1^{Cre}$; $ChAT^{flox/flox}$ mice are hypoactive compared to controls is that the authors used an unknown combination of $Nkx2.1^{Cre}$, $En1^{Cre}$ and $ChAT^{flox/+}$ mice as controls. It has been shown in our lab that $Nkx2.1^{Cre}$ mice have greater spontaneous locomotor activity than the $En1^{Cre}$ mice (unpublished data).

Our finding that cholinergic tone from the PPT does not influence neuromuscular functioning, as measured by the rotarod task, is supported by a study by Machold (2013). Machold (2013) tested $En1^{Cre}$; $ChAT^{flox/flox}$ mice on an accelerating rotarod , and found no significant difference btween these mice and controls in the latency to fall off the rotarod over the two consecutive days of training. As these $En1^{Cre}$; $ChAT^{flox/flox}$ mice also have a deficit in cholinergic signaling from the PPT, these data support our finding that ACh release from the PPT is not involved in motor control.

The PPT is thought to have a role in the initiation and maintenance of gait (Garcia-Rill 1991; Winn 2006; Karachi et al., 2010) and lesions of the PPT cause abnormalities in gait (Karachi et al., 2010). Importantly, PD and PSP are accompanied by approximately 40% cholinergic neuron loss in the PPN (Hirsch et al., 1987, Zweig et al., 1989), and

different studies have suggested that a loss of cholinergic signaling from the PPN causes physical abnormalities in PD and PSP patients. For instance, PET studies of PD patients with several postural instability leading to falls had significantly less cholinergic innervation in the thalamus from the PPN than non-fallers (Bohnen et al., 2009; 2012). PSP patients have an even greater loss of thalamic cholinergic activity in combination with more severe balance impairments and falls than PD patients (Hirsch et al., 1987; Wenning et al, 1999). The motor symptoms of PD (gait freezing and postural instability) remain unaffected by dopamine replacement therapy with levodopa suggesting that these symptoms are not a result of the loss of dopaminergic signaling in these individuals (Pahapill and Lozano, 2000; Fernandez 2012). On the other hand, the anticholinesterase inhibitor donepezil reduced the number of falls in frequently falling PD patients (Chung et al., 2010). We observed deficits on gait parameters in VAChT$^{En1\text{-}Cre\text{-}flox/flox}$ mice using the CatWalk gait analysis system. In both young mice (3-6 months of age) and old mice (12 month of age), the animals walked with a decreased paw area. This is indicative of a slight postural instability as a decreased paw area could suggest that the VAChT$^{En1\text{-}Cre\text{-}flox/flox}$ mice are walking on the sides of their paws or on their toes. Thus, our data give further support to the hypothesis that cholinergic signaling from the PPT is important for modulation of gait.

6.2 Psychiatric-like phenotypes

The cholinergic system has long been thought to play an important role in the etiology of depression (Janowsky 1972). This hypothesis has been supported by a number of animal and clinical studies. For instance, Mineur et al. (2013) showed that physostigmine-injected mice spent significantly more time immobile in the tail suspension test than controls, suggesting that the increased cholinergic tone in the brain resulted in this depressive-like behaviour. Physostigmine, is a AChE inhibitor used to increase cholinergic tone in the brain. In contrast, administration of nAChR antagonists (such as mecamylamine) to mice to cause a global decrease in cholinergic tone in the brain, results in an antidepressive-like phenotype in both the forced swim test and the tail suspension test (Andreasen 2008). Additionally, knockout mice lacking β2 subunit-containing nAChRs spend less time immobile in the tail suspension test and forced

swimming test, indicating that decreased cholinergic signaling via nAChRs may contribute to an antidepressive-like phenotype in mice (Caldarone et al., 2004). In all, it is clear that brain cholinergic tone is involved in depressive-like behaviour, but the mechanisms and specific cholinergic nuclei involved are not known. Our results suggest that ACh released from the PPT, at least in part, might be mediating the effects of depression. In both the forced swim test and the tail suspension test, the VAChT$^{En1\text{-}Cre\text{-}flox/flox}$ mice spent significantly less time immobile than the VAChT$^{flox/flox}$ control mice. This decrease in immobility time is indicative of an antidepressive-like phenotype in these animals. This suggests that the decreased cholinergic signaling from the PPT is responsible for the antidepression-like behaviour in these animals.

Interestingly, previous PPT lesion studies have revealed a surprising connection between the PPT and another psychiatric-like behaviour: anxiety. Several studies have reported increased anxiety-like behaviour in rodents after PPT lesions. Anxiety in animals is evaluated by comparing their avoidance behaviour in the presence of putative anxiogenic stimuli (for example walled vs. open arms and dark vs. light compartments) (Dere et al., 2002). NMDA-induced PPT lesions, as well as bilateral electrolytic lesions of the PPT have produced increased anxiety-like behaviours in the elevated plus maze test (Leri and Franklin 1998; Podhorna and Franklin 1999). In contrast, Homs-Ormo et al (2002) tested bilateral electrolytic lesions of the PPT on the behaviour of rats in the elevated plus maze and found that there was no difference between the lesioned animals and the sham animals during this task. The contrasting results obtained in these lesion studies are likely due to the differing populations of neurons targeted by the lesion, and to date, no studies have specifically isolated the role of ACh release from the PPT on murine anxiety. In this study, we observed that cholinergic signaling from the PPT do not seem to have strong influence in the regulation of anxiety as deletion of VAChT in the PPT led to deficits in the light/dark place preference test, but did not lead to deficits in the elevated plus maze or the time in spent in the centre of the open field arena.

In the literature, the marble-burying assay has been used to evaluate either anxiety-like and/or repetitive-like behaviours (Thomas et al., 2009). Interpretation of this test can consider the burying behaviour as an anxiety-like behaviour in response to a novel

stimuli, or as a obsessive/compulsive-like behaviour (Thomas et al., 2009). If viewed through through the anxiety-like behavior paradigm, these data suggest that the decrease in cholinergic tone from the PPT results in decreased anxiety-like behaviour in this test. While this result is in contrast to the results obtained in other measures of anxiety-like behaviour in this study, it has been shown that antidepressants decrease marble burying behaviour (Li et al., 2006), so its possible that this phenotype is an artifact of the antidepressive-like behaviour seen in the VAChT$^{En1\text{-}Cre\text{-}flox/flox}$ animals. Thomas et al. (2009) propose that marble burying reflects a perseverative behaviour more than novelty-induced anxiety. If considered in this manner, the loss of cholinergic tone in the PPT results in decreased repetitive behaviours. In terms of the role of cholinergic signaling from the PPT in compulsivity or perseverative behaviours, little is known. The present finding that mice lacking cholinergic signaling from the PPT have a decreased compulsive-like phenotype in the marble burying task is novel. Ahmari and collegues (2013) used optogenetics in mice to stimulate the ventral striatum and hyperactivate the cortico-striatal-thalamic-cortico (CSTC) circuit, and found that this resulted in a persistent increase in grooming, which is a mouse behaviour related to OCD. The PPT has direct influence on this circuitry (Winn 1998), so it is possible that the loss of cholinergic input to the CSTC results in the decreased compulsive-like behaviours seen in the VAChT$^{En1\text{-}Cre\text{-}flox/flox}$ animals during the marble burying task. Additionally, a feature of the 5-choice serial reaction time task is that it also provides a means of evaluating perseverative behaviour in the animals. During the probe trial with a 0.8 s stimulus, the VAChT$^{En1\text{-}Cre\text{-}flox/flox}$ mice show a strong trend towards a decreased perseverative response compared to controls. However, the 5-CSRTT does not adequately measure attention and compulsivity simultaneously. This trend requires further investigation as changing the parameters of the 5-CSRTT and increasing the number of mice used in the study may reveal a decreased-compulsivity phenotype in these animals that would support the results seen in the marble burying task.

6.3 Attention, sleep and cognition

The PPT has very strong reciprocal connections to the corticostriatal circuits, so it is often thought to be involved in many higher cognitive functions such as learning, memory and attention (Mena-Segovia et al., 2004).

It has been shown that the PPT has an important role in the regulation of working memory (Keating and Winn 2002; Taylor et al. 2004). Taylor et al. (2004) used the delayed spatial win-shift (DSWS) radial maze task to evaluate working memory and found that rats with bilateral electrolytic PPT lesions performed significantly worse than the sham lesion rats, making about four errors per test compared to the average rate of less than one error per test for the sham operated rats. VAChT$^{En1\text{-}Cre\text{-}flox/flox}$ mice did not show any differences in performance from the littermate controls when we evaluated working memory using the spontaneous alternations Y-Maze, suggesting that the PPT cholinergic tone is not important for working memory function. Taken together, these results indicate that the working memory deficits observed in studies using PPT lesions (Keating and Winn 2002; Taylor et al. 2004) are due to the loss of glutamatergic and GABAergic signaling from the PPT. Alternatively, since the VAChT ablation is not in 100% of PPT cholinergic neurons, there is the possibility that some of the specific cholinergic neurons involved in working memory have not been affected by Cre-mediated recombination and thus working memory is not affected in these animals.

When spatial learning and memory was evaluated using the spatial version of the Morris water maze (MWM), VAChT$^{En1\text{-}Cre\text{-}flox/flox}$ mice showed a strong impairment in spatial navigation during the spatial version of the MWM, with a greater latency to find the platform than controls during the acquisition phase, and no preference for the target zone during the probe trial. Stackman and Lora et al. (2012) showed that inactivation of the anterior thalamic nuclei with muscimol resulted in deficits in the performance of mice in the spatial MWM. The PPT has direct cholinergic afferents to the ATN (Gonzalo-Ruiz et al., 1995) and with the cholinergic signaling from the PPT to the thalamus almost abolished in the VAChT$^{En1\text{-}Cre\text{-}flox/flox}$ mice, its possible that the cholinergic input to the thalamus from the PPT is necessary for spatial memory. Another possible interpretation of deficits of the VAChT$^{En1\text{-}Cre\text{-}flox/flox}$ mice in the spatial MWM is that the cholinergic

signaling from the PPT is important for learning. The DSWS maze used by Taylor and colleagues (2004) was used to evaluate working memory, but this test is also very challenging to an animal's ability to use spatial cues. In the first stage of training in the DSWS maze, all four arms of the maze are open and there is no reward, there is no impairment of the lesioned animals' performance (Taylor et al., 2004). This apparatus is similar to the Y-maze used in this study, where there are three open arms of the maze for the animal to explore. It is only when the difficulty of the DSWS task is increased (by changing the arms of the maze that contain the reward) that the lesioned animals present impairments (Taylor et al., 2004). This suggests that it may not be working memory that is affected by the PPT lesion, but their ability to learn. This explanation accounts for a normal working memory in the Y-maze (where no training is involved) but impaired learning of the location of the escape platform in the MWM in the VAChT$^{En1\text{-}Cre\text{-}flox/flox}$ mice.

To explore goal-directed learning in the VAChT$^{En1\text{-}Cre\text{-}flox/flox}$ mice further, the goal-directed version of the Morris water maze was used. This version of the Morris water maze uses a similar paradigm to the DSWS task where animals must swim to a platform indicated by a cue in 8 different positions to receive the reward of being removed from the tank of water. On the testing day, the combination of the animal's starting location and the location of the cued-platform was one that was not used during the acquisition phase. Here, we saw significant deficits in goal-directed learning in the cued version of the MWM. Mice lacking cholinergic tone in the PPT showed significantly greater latencies to find the platform during the acquisition phase than the control mice, and an even greater deficit during the testing phase. This deficit in goal-directed behaviour was further emphasized by the VAChT$^{En1\text{-}Cre\text{-}flox/flox}$ mouse their path traces, which indicate that the mice often swam in thigmotaxis, which is correlated with stress and anxiety in animals (Graziano et al., 2003). This swimming strategy was also observed in the spatial version of the MWM. Since the escape platform in this test is visible to the mice by a very obvious cue, the mice do not have to use their spatial learning and memory skills to locate it in the tank. The inability of the VAChT$^{En1\text{-}Cre\text{-}flox/flox}$ mice to learn the location of the platform in both the spatial and cued versions of the MWM strongly suggests that the release of ACh from the PPT is critical for learning.

Finally, attention was evaluated in these mice using the 5-CSRTT. Our data demonstrates that the VAChT$^{En1\text{-}Cre\text{-}floxflox}$ mice were unhindered in their ability to learn the conditions of each pre-training phase and subsequently required the same number of sessions to meet the criteria to pass the pre-training phase as the control mice did. While the VAChT$^{En1\text{-}Cre\text{-}flox/flox}$ mice are not significantly different from controls in their ability to learn the requirements of the 5-CSRTT training phases, there is a trend that the VAChT$^{En1\text{-}Cre\text{-}floxflox}$ mice required more training days to meet the criteria to pass the 4s stimulus training phase. Increasing the number of mice performing the 5-CSRTT may reveal a learning deficit at this training phase. During the 5-CSRTT probe trial, the mice did not demonstrate any attentional deficits as their accuracy and number of omissions were not significantly different from controls. Inglis et al (2000) reported global attentional deficits in rats with bilateral PPT lesions in the 5-CSRTT, which were alleviated by decreasing the attentional demands of the test. As our results suggest that cholinergic efferents from the PPT do not seem to be required for normal attention processes, it is possible that the glutamatergic and GABAergic neurons in the PPT that were lesioned in addition to cholinergic neurons were responsible for the deficits observed by Inglis and colleagues. It is also possible that a sub-population of cholinergic efferents spared in VAChT$^{En1\text{-}Cre\text{-}flox/flox}$ could be responsible for the intact attentional performance.

6.4 Limitations

The primary limitation of this study is that these animals are born with the decreased cholinergic tone in the PPT and as a result they may develop compensatory mechanisms in the brain during development. The engrailed (En) homeobox 1 transcription factor is crucial for the formation of the midbrain [mesencephalon (mes)] and anterior hindbrain [rhombomere (r1)] during embryonic development (Sgaier et al., 2007). En1 acts at the mid-hindbrain junction between embryonic day 8.5 and 13, so Cre-mediated recombination was occurring during the initial formation of this brain structure. In this study, it is not possible to determine if the observed altered behaviours are due singularly to the loss of cholinergic signaling from the PPT, or from the combination of compensatory changes that have occurred since birth.

6.5 Future directions

To further expand on the results from this study, it would be of value to continue to characterize the compulsive-like behaviours seen in the VAChT$^{En1\text{-}Cre\text{-}flox/flox}$ mice. By increasing the number of mice used in the 5-CSRTT and by changing the parameters of the test to test for perseverative behaviours, it would confirm if the trend towards a decreased perseverative behaviour is in fact a phenotype for the VAChT$^{En1\text{-}Cre\text{-}flox/flox}$ mice that reflects the decreased compulsive-like behaviours seen in these animals in the marble burying task.

Additionally, it is necessary to account for any compensatory mechanisms that may have occurred in the VAChT$^{En1\text{-}Cre\text{-}flox/flox}$ mice as the decrease in cholinergic tone was present since early embryonic development. For future studies, a Cre recombinase virus will be injected into the PPT of adult VAChT$^{flox/flox}$ mice and the behavioural tests will be repeated in order to identify any effects from this potential compensation.

Chapter 4

7 Conclusions

The present data provide evidence for the role of cholinergic signaling from the pedunculopontine tegmental nucleus as the mice used in this study provide a novel means of selectively reducing ACh release from the PPT without damaging the cholinergic neurons or altering their potential release of other neurotransmitters/modulators. The present findings from this study suggest that ACh signaling from the PPT is important for the mediation of depressive-like symptoms and learning and memory, and to a lesser extent, gait, anxiety-like symptoms, sleep and perseverative-like behaviours. These data contribute to our current understanding of depression, Parkinson's disease and progressive supranuclear palsy. While the idea that dysregulation of the cholinergic system may contribute to the etiology of major depressive disorder is not novel, to date, no specific cholinergic nuclei have been implicated. Here, we present data that implicates cholinergic signaling from the PPT, at least in part, in depressive symptoms. As such, pharmacological agents that limit ACh signaling from the PPT may have the potential to ameliorate some of the symptoms of major depressive disorder, and thus lead to the development of novel antidepressant medications.

Additionally, these data emphasize the role of the PPT in the pathophysiology of PD and PSP. Some of the symptoms of these neurodegenerative diseases, such as gait abnormalities, postural instability and falls are not improved by traditional DA treatment (Nandi et al., 2012). Our data suggest that it is possible that PPT degeneration is also responsible for some cognitive impairments of PD. For instance, motor symptoms of PD are often preceded by sleep disturbances (Takakusaki et al., 2011), which may be due to altereded PPT cholinergic signaling and subsequent alterations in sleep-wake cycles, as seen in the $VAChT^{En1\text{-}Cre\text{-}flox/flox}$ mice. PD patients also often experience dementia (Bohnen et al., 2011), which may be due to PPT degeneration, as the data from this study suggest that intact PPT ACh release is necessary for learning and memory. The findings from this study further support the role of decreased cholinergic signaling from the PPT

in the symptoms of PD, and indicate the PPT as a potential target for deep brain stimulation to treat some PD patients.

As the decrease in cholinergic tone was present in VAChT$^{En1\text{-}Cre\text{-}flox/flox}$ since early development it not possible to rule out the possibility that the effects observed result from compensatory changes. For future studies, a Cre recombinase virus will be injected into the PPT of adult VAChT$^{flox/flox}$ mice.

References

Ahmari SE, Spellman T, Douglass NL, Kheirbek MA, Simpson HB, Deisseroth K, Gordon JA, Hen R (2013) Repeated cortico-striatal stimulation generates persisten OCD-like behavior. Science 340:1234-1239.

Alderson HL, Latimer M, Winn P (2008) A functional dissociation of the anterior and posterior pedunculopontine tegmental nucleus: excitotoxic lesions have differential effects on locomotion and the response to nicotine. Brain Struct Funct 213:247-253.

Alfonso A, Grundahl K, McManus JR, Asbury JM, Rand JB (1994) Alternative splicing leads to two cholinergic proteins in *Caenorhabditis elegans*. J Mol Biol 241:627-630.

Allen LF and Winn P (1995) Excitotoxic lesions of the pedunculopontine tegmental nucleus disinhibit orofacial behaviours stimulated by micorinjections of d-amphetamine into rat ventrolateral caudate-putamen. Exp Brain Res 104:262-274.

Andreasen JT (2008) Antidepressant-like effects of nicotinic acetylcholine receptor antagonists, but not agonists, in the mouse forced swim and mouse tail suspension tests. Psychopharmacology 23:797-804.

Andreasen JT, Olsen GM, Wilborg O, Redrobe JP (2008) Antidepresseant-like effects of nicotinic acetylcholine receptor antagonists, but not agonists, in the mouse forced swim and mouse tail suspension tests. J Psychopharm 23:797-804.

Angoa-Perez M, Kane MJ, Briggs DI, Francescutti DM, Kuhn DM (2013) Marble burying and nestlet shredding as tests of repetitive, compulsive-like behaviors in mice. J Vis Exp 24:50978.

Aosaki T, Graybiel AM, Kimura M (1994) Effects of the nigrostriatal dopamine system on acquired neural responses in the striatum of behaving monkeys. Science 265:412-415.

Aosaki T, Tsubokawa H, Ishida A, Watanabe K, Graybiel AM, Kimura M (1994) Responses of tonically active neurons in the primate's striatum undergo systemic changes during sensorimotor conditioning. J Neurosci 14:3969-3984.

Aravamuthan BR, Stein JF and Aziz TZ (2008) Tbe anatomy and localization of the pedunculopontine nucleus determined using probabilistic diffusion tractography. Br J Neurosurg 22:25-32.

Barbosa J Jr, Ferreira LT, Martins-Silva C, Santos MS, Torres GE, Caron MG, Gomez MV, Ferguson SS, Prado MA, Prado VF (2002) Trafficking of the vesicular

acetylcholine transporter in SN56 cells: a dynamin-sensitive step and interaction with the AP-2 adaptor complex. J Neurochem 82:1221-1228.

Bari A, Dalley JW, Robbins TW (2008) The application of the 5-choice serial reaction time task for the assessment of visual attentional processes and impulse control in rats. Nat Protoc 3:759-767.

Benjanin S, Cervini R, Mallet J, Berrard S (1994) A unique gene organization for two cholinergic markers, choline acetyltransferase and a putative vesicular transporter of acetylcholine. J Biol Chem 269:21944-21947.

Bevan MD and Bolam JP (1995) Cholinergic, GABAergic, and glutamate-enriched inputs from the mesopontine tegmentum to the subthalamic nucleus in the rat. J Neurosci 15:7105-20.

Birks RI and MacIntosh FC (1961) Acetylcholine metabolism of a sympathetic ganglion. Can J Biochem Physiol 39:787-827.

Blaha CD and Winn P (1993) Modulation of dopamine efflux in the striatum following cholinergic stimulation of the substantia nigra in intact and pedunculopontine tegmental nucleus-lesioned rats.

Bohnen NI, Muller ML, Koeppe RA, Studenski SA, Kilbourn MA, Frey KA, et al. (2009) History of falls in Parkinson disease is associated with reduced cholinergic activity. Neurology 73:1670-1676.

Bohnen NI, Muller ML, Kotagal V, Koeppe RA, Kilbourn MR, Gilman S, et al. (2012) Heterogeneity of cholinergic denervation in Parkinson's disease without dementia. J Cereb Blood Flow Metab 32:1609-1617.

Bohnen NI and Albin RL (2009) Cholinergic denervation occurs early in Parkinson disease. Neurology 73:256-257.

Bohnen NI and Albin RL (2011) The cholinergic system and Parkinson disease. Brain Behav Res 221:564-573.

Bolam JP, Francis CM, Henderson Z (1991) Cholinergic input to dopaminergic neurons in the substantia nigra: A double immunocytochemical study. Neuroscience 41:483- 494.

Buisson B and Bertrand D (2002) Nicotine addiction: the possible role of functional upregulation. Trends Pharmacol Sci. 23:130-136.

Calbresi P, Lacey MG, North RA (1989) Nicotinic excitation of rat ventral tegmental neurons in vitro studied by intracellular recording. Br J Pharmacol 98:135-140.

Caldarone BJ et al. (2004) High-affinity nicotinic acetylcholine receptors are required for antidepressant effects of amitriptyline on behavior and hippocampal cell proliferation. Biol Psychiatry 56:657–664.

Changeux JP et al. (1998) Brain nicotinic receptors - structure and regulation, role in learning and reinforcement. Brain Res Rev 26:198–216.

Changeux JP and Edelstein SJ (2005) Allosteric mechanisms of signal transduction. Science 308:1424-1428.

Charara A, Parent A (1994) Brainstem dopaminergic, cholinergic and serotoninergic afferents to the pallidum in the squirrel monkey. Brain Research 640:155-170.

Charara A, Smith J, Parent A (1996) Glutamatergic inputs from the pedunculopontine nucleus to midbrain dopaminergic neurons in primates: *Phaseolus vulgaris*-leucoagglutinin antergrade labeling combined with postembedding glutamate and GABA immunohistochemistry. J Comp Neurol 364:254-266.

Chung KA, Lobb BM, Nut JG and Horak FB (2010) Effects of a central cholinesterase inhibitor on reducing falls in Parkinson disease. Neurology 75:1263-1269.

Condé H (1992) Organization and physiology of the substantia nigra. Exp Brain Res 88:233-48.

Cooke LJ and Rylett J (1997) Inhibitors of serinethreonine phosphatases increase membrane-bound choline acetyltransferase activity and enhance acetylcholine synthesis. Brain Res 751:232-238.

Dahan L, Husum H, Mnie-Filali O, Arnt J, Hertel P, Haddjeri N (2009) Effects of bifeprunox and aripiprazole on rat serotonin and dopamine neuronal activity and anxiolytic behavior. J Psychopharmacol 23:177-189.

Dautan D, Huerta-Ocampo I, Witten IB, Deisseroth K, Bolam JP, Gerdjikov T, Mena-Segovia J (2014) A major external source of cholinergic innervation of the striatum and nucleus accumbens originates in the brainstem. J Neurosci 34:4509-4518.

de Castro BM et al. (2009) Reduced expression of the vesicular acetylcholine transporter causes learning deficits in mice. Genes Brain Behav 8:23-35.

Deacon RM (2013) Measuring the strength of mice. J Vis Exp doi: 10.3791/2610.

Dere E et al. (2002) The graded anxiety test: a novel test of murine unconditioned anxiety based on the principles of the elevated plus-maze and light-dark test. J Neurosci Method 122:65.

Dobransky T (2001) Functional characterization of phosphorylation of 69-kDA human choline acetyltransferase at serine 440 by protein kinase C. J Biol Chem 276:22244-22250.

Edley SM and Graybiel AM (1983) The afferent and efferent connections of the feline nucleus tegmenti pedunculopontinus, pars compacta. J Comp Neurol 217:187-215.

Eiden LE (1998) The cholinergic gene locus. J Neurochem 70:2227-2240.

Erickson JD et al. (1994) Functional identification of a vesicular acetylcholine transporter and its expression from a "cholinergic" gene locus. J Biol Chem 269:21929-21932.

Erro E, Lanciego JL, Gimenez-Amaya JM (1999) Relationships between thalamostriatal neurons and pedunculopontine projections to the thalamus: a neuroanatomical tract-tracing study in the rat. Exp Brain Res 127:162-170.

Ferguson SM et al. (2003) Vesicular Localization and Activity-Dependent Trafficking of Presynaptic Choline Transporters. J Neurosci 23:9697-9709.

Fernandez HH (2012) Updates in the medical management of Parkison disease. Cleve Clin J Med 79:28-35.

Ferreira LT, Santos MS, Kolmakova NG, Koenen J, Barbosa J Jr, Gomez MV, Guatimosim C, Zhang X, Parsons SM, Prado VF, Prado MA (2005) Structural requirements for steady-state localization of the vesicular acetylcholine transporter. J Neurochem 94:957-969.

Ford B, Holmes CJ, Mainville L, Jones BE (1995) GABAergic neurons in the rat pontomesencephalic tegmentum: codistrobution with cholinergic and other tegmental neurons projecting to the posterior lateral hypothalamus. J Comp Neurol 363:177-96.

Fritz S, Wessler I, Breitling R, Rossmanith W, Ojeda SR, Dissen GA, Amsterdam A, Mayerhofer A (2001) Expression of muscarinic receptor types in the primate ovary and evidence for nonneuronal acetylcholine synthesis. J Clin Endocrinol Metab 86:349-354.

Futami T, Takakusaki K, Kitai ST (1995) Glutamatergic and cholinergic inputs from the pedunculopontine tegmental nucleus to dopamine neurons in the substantia nigra pars compacta. Neuroscience research 21: 331-342.

Garcia-Rill E (1991) The pedunculopontine nucleus. Prog Neurobiol 36:363-389.

Gilmor ML, Nash NR, Roghani A, Edwards RH, Yi H, Hersch SM, Levey AI (1996) Expression of putative vesicular acetylcholine transporter in rat brain and localization in cholinergic synaptic vesicles. J Neurosci 167:2179-2190.

Gonzalo RA, Sanz-Anguela MJ, and Lieberman AR (1995) Cholinergic projections to the anterior thalamic nuclei in the rat: a combined retrograde tracing and choline acetyltransferase immunohistochemical study. Anat Embryol 192:335-349.

Gotti C et al. (2007) Heterogeneity and complexity of native brain nicotinic receptors. Biochem Pharmacol 74:1102-1111.

Gotti C and Clementi F (2004) Neuronal nicotinic receptors: from structure to pathology. Prog Neurobiol 74:363-396.

Gras C et al. (2008) The vesicular glutamate transporter VGLUT3 synergizes striatal acetylcholine tone. Nat Neurosci 11:292-300.

Graziano A, Petrosini L, Bartoletti A (2003) Automatic recognition of explorative strategies in the Morris water maze. J Neurosci Method 130:33-44.

Guzman MS et al. (2011) Elimination of the vesicular acetylcholine transporter in the striatum reveals regulation of behavior by cholinergic-glutamatergic co-transmission. PLoS Biol. 9:e101194.

Haber SN, Lynd E, Klein C, Groenewegen HJ (1990) Topographic organization of the ventral striatal efferent projections in the rhesus monkey: an anterograde tracing study. J Comp Neurol 293:282-298.

Haga, T (1971) Synthesis and release of [14C]acetylcholine in synaptosomes. *J* Neurochem 18:781–798.

Hazrati LN and Parent A (1992) Projection from the deep cerebellar nuclei to the pedunculopontine nucleus in the squirrel monkey. Brain Research 585:267-271.

Hernández-Chan NG, Góngora-Alfaro JL, A Álvarez-Cervera FJ, Soli ís-Rodríguez FA, Heredia-López FJ and Arankowsky-Sandoval G (2011) Quinolinic acid lesions of the pedunculopontine nucleus impair sleep architecture, but not locomotion, exploration, emotionality or working memory in the rat. Behav Brain Res 225:482-490.

Hikida T, Kaneko S, Isobe T, Kitabatake Y, Watanabe D, Pastan I, Nakanishi S (2001) Increased sensitivity to cocaine by cholinergic cell ablation in nucleus accumbens. Proc Natl Acad Sci U S A 98:13351-4.

Hikosaka O, Takikawa Y, Kawogoe R (2000) Role of the basal ganglia in the control of purposive saccadic eye movements. Physiol Rev 80:953-978.

Hirsch EC, Graybiel AM, Duyckaerts C and Javoy-Agid F (1987) Neuronal loss in the pedunculopontine tegmental nucleus in Parkinson disease and in progressive supranuclear palsy. Proc Natl Acad Sci USA 84:5976-5980.

Hnasko TS and Robert HE (2012) Neurotransmitter corelease: mechanism and physiological role. Annu Rev Physiol 74:225-243.

Homs-Ormo S, Coll-Andreu M, Satorra-Marin N, Arevalo-Garcia R and Morgado-Bernal I (2002) Effects of pedunculopontine tegmental nucleus lesions on emotional reactivity and locomotion in rats. Brain Res Bull 59:495-503.

Hughes RN (2004) The value of spontaneous alternation behavior (SAB) as a test of retention in pharmacological investigations of memory. Neurosci Behav Rev 28:497-505.

Inglis WL, Allen LF, Whitelaw RB, Latimer MP, Brace HM, Winn P (1994) An investigation into the role of the pedunculopontine tegmental nucleus in the mediation of locomotion and orofacial stereotypy induced by d-amphetamine and apomorphine in the rat. Neuroscience 58:817-833.

Inglis WL, Olmstead MC, Robbins TW (2001) Selective deficits in attentional performance on the 5-choice serial reaction time task following pedunculoponitine tegmental nucleus lesions. Behav Brain Res 123:117-131.

Janowsky DS, el-Yousef MK, Davis JM, Sekerke HJ (1972) A cholinergic-adrenergic hypothesis of mania and depression. Lancet 2:632-635.

Jellinger K (1988) The pedunculopontine nucleus in Parkinson's disease, progressive supranuclear palsy and Alzheimer's disease. J Neurol Neurosurg Psychiatry 51:540-543.

Jenkinson N et al. (2009) Anatomy, physiology, and pathophysiology of the pedunculopontine nucleus. Mov Disord 24:319-328.

Jones IW and Wonnacott S (2004) Precise localization of alpha7 nicotinic acetylcholine receptors on glutamatergic axon terminals in the rat ventral tegmental area.J Neurosci 24:11244-11252.

Karachi C et al. (2010) Cholinergic mesencephalic neurons are incolved in gait and postural disorders in Parkinson disease. J Clin Invest 120:2745-2754.

Keating GL and Winn P (2002) Examination of the role of the pedunculopontine tegmental nucleus in radial maze tasks with or without a delay. Neuroscience 112:687-696.

Khare P, Mulakaluri A, Parsons SM (2010) Search for the acetylcholine and vesamicol binding sites in the vesicular acetylcholine transporter: the region around the luminal end of the transport channel. J Neurochem 115:984-993.

Kim MH, Lu M, Lim EJ, Chai YG, Hersh LB (1999) Mutational analysis of aspartate residues in the transmembrane regions and cytoplasmic loops of rat vesicular acetylcholine transporter. J Biol Chem 274:673-680.

Kimmel RA, Turnbell DH, Blanquet V, Wurst W, Loomis CA, Joyner AL (2000) Two lineage boundries coordinate vertebrate apical ectodermal ridge formation. Genes Dev 2000 14:1377-1389.

Kita T and Kita H (2011) Cholinergic and non-cholinergic mesopontine tegmental neurons projecting to the subthalamic nucleus in the rat. Eur J Neurosci 33:433-443.

Kitabatake Y, Hikida T, Watanabe D, Pastan I, Nakanishi S (2003) Impairment of reward-related learning by cholinergic cell ablation in the striatum. Proc Natl Acad Sci U S A 100:7965-7970.

Kitamoto T (1998) Structure and organization of the drosophila cholinergic locus. 273:2706-2713.

Kobayashi Y, Isa T (2002) Sensory-motor gating and cognitive control by the brainstem cholinergic system. Neural Networks 15:731-741.

Kobayashi S, Nakamura Y (2003) Synaptic organization of the rat parafascicular nucleus, with special reference to its afferents from the superior colliculus and the pedunculopontine tegmental nucleus. Brain Research 980:80-91.

Kolisnyk B et al. (2013) ChAT-ChR2-EYFP mice have enhanced motor endurance but sow deficits in attention and several additional cognitive domains. J Neurosci 33:10427-10438.

Koopmans GC, Deumens R, Honig WM, Hamers FP, Steinbusch HW, Joosten EA (2005)The assessment of locomotor function in spinal cord injured rats: the importance of objective analysis of coordination. J Neurotrauma 22:214-225.

Kotegal V, Müller ML, Kaufer DI, Koeppe RA, Bohnen NI (2012) Thalamic cholinergic innervation is spared in Alzheimer disease compared to parkinsonian disorders. Neurosci Lett 514:169-172.

Krantz DE et al. (2000) A phosphorylation site regulates sorting of the vesicular acetylcholine transporter to dense core vesicles. J Cell Biol 149:379-395.

Lacey MG, Calabresi P, North RA (1990) Muscarine depolarizes rat substantia nigra zona compacta and ventral tegmental neurons in vitro through M1-like receptors. Journal of Pharmacology and Experimental Therapeutics 253:395-400.

Lapper SR and Bolam JP (1992) Input from the frontal cortex and the parafascicular nucleus to cholinergic interneurons in the dorsal striatum of the rat. Neuroscience 51:533-545.

Lavoie B and Parent A (1994) Pedunculopontine nucleus in the squirrel monkey: distribution of cholinergic and monoaminergic neurons in the mesopontine tegmentum with evidence for the presence of glutamate in cholinergic neurons. J Comp Neurol 344:190-209.

Leri F and Franklin KBJ (1998) Learning impairments caused by lesions to the pedunculopontine tegmental nucleus: an artifact of anxiety? Brain Res 807:187-192.

Li X, Morrow D, Witkin JM (2006) Decreases in nestlet shredding of mice by serotonin uptake inhibitors: comparison with marble burying. Life Sci 78:1933–1939.

Lima MM, Andersen ML, Reksidler AB, Ferraz AC, Vital MA, Tufik S (2012) Paradoxical sleep deprivation modulates tyrosine hydroxylase expression in the nigrostriatal pathway and attenuates motor deficits induced by dopaminergic depletion. CNS Neurol Disord Drug Targets 11:359-368.

Losier BJ and Semba K (1993) Dual projections of single cholinergic and aminergic brainstem neurons to the thalamus and basal forebrain in the rat. Brain Res 604:41-52.

Machold RP (2013) Loss of rostral brainstem cholinergic activity results in decreased ultrasonic vocalization behavior and altered sensorimotor gating. Behav Brain Res 256:51-55.

Madisen L, Zwingman TA, Sunkin SM, Oh SW, Zariwala HA, Gu H, Ng LL, Palmiter RD, Hawrylycz MJ, Jones AR, Lein ES, Zeng H (2010) A robust and high-throughput Cre reporting and characterization system for the whole mouse brain. Nat Neurosci 13:133-140.

Mallet J et al. (1998) The cholinergic locus: ChAT and VAChT genes. J Physiol 92:145-147.

Martinez-Gonzalez C, Bolam JP and Mena-Segovia J (2011) Topographical organization of the pedunculopontine nucleus. Front Neuroanat 5:22.

Martinez-Gonzalez C, Wang HL, Micklem BR, Bolam JP, Mena-Segovia J (2012) Subpopulations of cholinergic, GABAergic and glutamatergic neurons in the

pedunculopontine nucleus contain calcium-binding proteins and are heterogeneously distributed. Eur J Neurosci 35:723-34.

Martyn AC1, De Jaeger X, Magalhães AC, Kesarwani R, Gonçalves DF, Raulic S, Guzman MS, Jackson MF, Izquierdo I, Macdonald JF, Prado MA, Prado VF (2012) Elimination of the vesicular acetylcholine transporter in the forebrain causes hyperactivity and deficits in spatial memory and long-term potentiation. Proc Natl Acad Sci U S A 109:17651-1765.

Matsumura M, Watanabe K, Ohye C (1997) Single-unit activity in the primate nucleus tegmenti pedunculopontinus related to voluntary arm movement. Neurosci Res 28:155-65.

Matsumura M, Nambu A, Yamaji Y, Watanabe K, Imai H, Inase M, Tokuno H, Takada M (2000) Organization of somatic motor inputs from the frontal lobe to the pedunculopontine tegmental nucleus in the macaque monkey. Neuroscience 98:97-110.

Matsumura M (2005) The pedunculopontine tegemental nucleus and experimental parkinsonism. J Neurol 252:5-12.

McCormick DA (1989) Cholinergic and noradrenergic modulation of thalamocortical processing. Trends Neurosci 12:215-221.

McCormick DA (1992) Cellular mechanisms underlying cholinergic and noradrenergic modulation of neuronal firing mode in the cat and guinea pig dorsal lateral geniculate nucleus. The Journal of Neuroscience 12:278-289.

Mena-Segovia J, Bolam JP, Magill PJ (2004) Pedunculopontine nucleus and basal ganglia: distinct relatives or part of the same family? Trends Neurosci 27:585-588.

Mena-Segovia J, Winn P, Bolam JP (2008) Cholinergic modulation of midbrain dopaminergic systems. Brain Res Rev 58:265-271.

Mena-Segovia J, Micklem BR, Nair-Roberts RG, Ungless MA, Bolam JP (2009) GABAergic neuron distribution in the pedunculopontine nucleus defines functionalsubterritories. In: The Journal of Comparative Neurology, pp 397-408: Wiley Subscription Services, Inc., A Wiley Company.

Mesulam MM, Rosen AD, Mufson EJ (1984) Regional variations in cortical cholinergic innervation: chemoarchitectonics of acetylcholinesterase-containing fibers in the macaque brain. Brain Res 311:245-58.

Mineur YS, and Picciotto MR (2010) Nictotine receptors and depression: revisiting and revising the cholinergic hypothesis. Cell 31:580-858.

Misawa H, Ishii K, Deguchi T (1992) Gene expression of mouse choline acetyltransferase. Alternative splicing and identification of a highly active promoter region. J Biol Chem 267:20392-20399.

Mitchell AS, Dalrymple-Alford JC, Christie MA (2002) Spatial working memory and the brainstem cholinergic innervation to the anterior thalamus. J Neurosci 22:1922-1928.

Moriizumi T and Hattori T (1992) Separate neuronal populations of the rat globus pallidus projecting to the subthalamic nucleus, auditory cortex and pedunculopontine tegmental area. Neuroscience 46:701-710.

Müller ML, Albin, RL, Kotagal V, Koeppe RA, Scott, PJ, Frey KA and Bohnen NI (2013) Thalamic cholinergic innervation and postural sensory integration function in Parkinson's disease. Brain 136:3282-3289.

Nakamura Y, Tokuno H, Morizumi T, Kitao Y, Kudo M (1989) Monosynaptic nigral inputs to the pedunculopontine tegmental nucleus neurons which send their axons to the medial reticular formation in the medulla oblongata. An electron microscopic study in the cat. Neuroscience letters 103:145-150.

Nakano K, Hasegawa Y, Tokushige A, Nakagawa S, Kayahara T, Mizuno N (1990) Topographical projections from the thalamus, subthalamic nucleus and pedunculopontine tegmental nucleus to the striatum in the Japanese monkey, Macaca fuscata. Brain Res 537:54-68.

Nandi D, Aziz TZ, Giladi N, Winter J and Stein JF (2002) Reversal of akinesia in experimental parkinsonism by GABA antagonist microinjections in the pedunculopontine nucleus. Brain 125:2418-2430.

Nauta HJ and Cole M (1978) Efferent projections of the subthalamic nucleus: an autoradiographic study in monkey and cat. J Comp Neurol 180:1-16.

Neuman M et al., (2009) Assessing gait impairment following experimental traumatic brain injury in mice. J Neurosci Methods 176:34-44.

Nickerson A, Guerci A, El Mestikawy S, Semba K (2006) Vesicular glutamate transporter 3 immunoreactivity is present in cholinergic basal forebrain neurons projecting to the basolateral amygdala in rat. J Comp Neurol 498:690-711.

Norton AW, Jo YS, Clark EW, Taylor CA, Mizumori SJY (2011) Independent neural coding of reward and movement by pedunculopontine tegmental nucleus neurons in freely navigating rats. Eur J Neurosci 33:1885-1896.

Nguyen ML, Cox GD, Parsons SM (1998) Kinetic parameters for the vesicular

acetylcholine transporter: two protons are exchanged for one acetylcholine. Biochem 37:13400-13410.

Oakman SA, Faris PL, Cozzari C, Hartman BK (1999) Characterization of the extent of pontomesencephalic cholinergic neurons' projections to the thalamus: comparison with projections to midbrain dopaminergic groups. Neuroscience 94:529-547.

Oda Y (1999) Choline acetyltransferase: The structure, distribution and pathologic changes in the central nervous system. Pathol Internat 49:921-937.

Okada K and Kobayashi Y (2009) Characterization of oculomotor and visual activities in the primate pedunculopontine tegmental nucleus during visually guided saccade tasks. Eur J Neurosci 30:2211-23.

Okada K, Nakamura K, Kobayashi Y (2011) A neural correlate of predicted and actual reward-value information in monkey pedunculopontine tegmental and dorsal raphe nucleus during saccade tasks. Neural Plasticity 2011:1-21.

Olmstead MC and Franklin KBJ (1993) Effects of pedunculopontine tegmental nucleus lesions on morphine-induced conditioned place preference and analgesia in the formalin test. Neuroscience 57:411-418.

Olmstead MC, Inglis WL, Bordeaux CP, Clarke EJ, Wallum NP, Everitt BJ, Robbins TW. (1993) Lesions of the pedunculopontine tegmental nucleus increase sucrose consumption but do not affect discrimination or contrast effects. Behav Neurosci 113:732-743

Pan WX and Hyland BI (2005) Pedunculopontine tegmental nucleus controls conditioned responses of midbrain dopamine neurons in behaving rats. J Neurosci 25:4725-32.

Papahill and Lozano (2000) The pedunculopontine nucleus and Parkinson's disease. Brain 123:1767-1783.

Parent A, Pare D, Smith Y, Steriade M (1988) Basal forebrain cholinergic and noncholinergic projections to the thalamus and brainstem in cats and monkeys. J Comp Neurol 277:281-301.

Parsons SM (2000) Transport mechanisms in acetylcholine and monoamine storage. FASEB J 14:2423-34.

Patel J, Rossignol E, Rice ME, Machold RP (2012) Opposing regulation of dopaminergic activity and exploratory motor behavior by forebrain and brainstem cholinergic circuits. Nat Comm 3:1172.

Petrovic J, Ciric J, Lazic K, Kalauzi A, Saponjic J (2013) Lesion of the pedunculopontine tegmental nucleus in rat augments cortical activation and disturbs sleep/wake state transitions structure. Exp Neurol 247:562-71.

Picciotto MR et al. (2001) Neuronal nicotinic acetylcholine receptor subunit knockout mice: physiological and behavioural phenotypes and possible clinical implications. Pharmacol Ther 92:89-108.

Picciotto MR, Higley MJ, Mineur YS (2012) Acetylcholine as a neuromodulator: cholinergic signaling shapes nervous system function and behavior. Neuron 76:116-129.

Picciotto MR, Caldarone BJ, King SL, Zachariou V (2000) Nicotinic receptors in the brain. Links between molecular biology and behavior. Neuropsychopharmacology 22:451-65.

Picciotto MR, Caldarone BJ, Brunzell DH, Zachariou V, Stevens TR, King SL (2001) Neuronal nicotinic acetylcholine receptor subunit knockout mice: physiological and behavioral phenotypes and possible clinical implications. Pharmacol Ther. 92:89-108.

Pierce RC and Kalivas PW (2007) Locomotor behavior. Curr Protoc Neurosci doi: 10.1002/0471142301.ns0801s40.

Podhorn J and Franklin KBJ (1999) Long-lasting increase in anxiety after electrolytic lesions of the pedunculopontine tegmental nucleus. Behav Neurosci 113:550-557.

Prado MAM, Reis RAM, Prado VF, Mello MC, Gomez MV, Mello FG (2002) Regulation of acetylcholine synthesis and storage. Neurochem Int 41:291-299.

Prado VF et al. (2006) Mice deficient for the vesicular acetylcholine transporter are myasthenic and have deficits in object and social recognition. Neuron 51:601-612.

Prado VF, Roy A, Kolisnyk B, Gros R, Prado MA (2013) Regulation of cholinergic activity by the vesicular acetylcholine transporter. Biochem J 450:265-274.

Raggi A and Ferri R (2010) Sleep disorders in neurodegenerative diseases. Eur J Neurol 17:1326-1338.

Ribeiro FM, Alves-Silva J, Volknandt W, Martins-Silva C, Mahmud H, Wilhelm A, Gomez MV, Rylett RJ, Ferguson SS, Prado VF, Prado MA (2003) The hemicholinium-3 sensitive high affinity choline transporter is internalized by clathrin-mediated endocytosis and is present in endosomes and synaptic vesicles. J Neurochem 87:136-146.

Ribeiro FM et al. (2006) Regulated recycling and plasma membrane recruitment of the high-affinity choline transporter. Eur J Neurosci 26:3437-2348.

RobbinsTW (2002) The 5-choice serial reaction time task: behavioural pharmacology and functional neurochemistry. Psychopharmacol 163:362-380.

Roghani A, Shirzadi A, Butcher LL, Edwards RH (1998) Distribution of the vesicular transporter for acetylcholine in the rat central nervous system. Neuroscience 82:1195-1212.

Rolland AS, Karachi C, Muriel MP, Hirsch EC, Francois C (2011) Internal pallidum and substantia nigra control different parts of the mesopontine reticular formation in primate. Mov Disord 26:1648-1656.

Romberg C, Mattson MP, Mughal MR, Bussey TJ, Saksida LM (2011) Impaired attention in the 3xTgAD model of Alzheimer's disease assessed using a translational touchscreen method for mice: rescue by donepezil (Aricept). J Neurosci 31:3500-3507.

Roni MA and Rahman S (2011) Neuronal nicotinic receptor antagonist reduces anxiety-like behaviour in mice. Neursci Lett 504:237-241.

Ros H, Magill PJ, Moss J, Bolam JP, Mena-Segovia J (2010) Distinct types of non-cholinergic pedunculopontine neurons are differentially modulated during global brain states. Neuroscience 170:78-91.

Rossato JI, Bevilaua LR, Medina JH, Izquierdo I, Cammarota M (2006) Retrieval induces hippocampal-dependent reconsolidation of spatial memory. Learn Mem 13:431-440.

Saper CB, Loewy AD (1982) Projections of the pedunculopontine tegmental nucleus in the rat: evidence for additional extrapyramidal circuitry. Brain Research 252:367-372.

Scarnati E and Florio T (1997) The pedunculopontine nucleus and related structures. Adv Neurol 74:97-110.

Schafer M (2002) Molecular cloning and functional identification of mouse vesicular glutamate transporter 3 and its expression in subsets of novel excitatory neurons. J Biol Chem 277:50734-50748.

Schliebs R and Arendt T (2006) The significance of the cholinergic system in the brain during aging and in Alzheimer's disease. J Neural Transm 113:1625-1644.

Schulz JM and Reynolds JNJ (2012) Oause and rebound: sensory control of cholinergic signaling in the striatum. Cell 36:41-50.

Schulz JM, Oswald MJ, Reynolds JN (2011) Visual-induced excitation leads to firing pauses in striatal cholinergic interneurons. J Neurosci 31:11133-11143.

Semba K and Fibiger HC (1992) Afferent connections of the laterodorsal and pedunculopontine tegmental nuclei in the rat: a retro- and antero-grade transport and immunohistochemical study. J Comp Neurol 323:387-410.

Semba K, Reiner PB, McGeer EG, Fibiger HC (1988) Brainstem afferents to the magnocellular basal forebrain studied by axonal transport, immunohistochemistry, and electrophysiology in the rat. J Comp Neurol 267:433-353.

Sgaier SK et al. (2007) Genetic subdivision of the tectum and cerebellum into functionally related regions based on differential sensitivity to engrailed proteins. Development 134:2325-2335.

Skinner RD, Kinjo N, Henderson V, Garcia-Rill E (1990) Locomotor projections from the pedunculopontine nucleus to the spinal cord. Neuroreport 1:183-186.

Smith LK and Carroll PT (1993) Membrane-bound choline-O-acetyltransferase in rat hippocampal tissue is anchored by glycosyl-phosphatidylinositol. Brain Res 605:155-163.

Song K, Ming G, Fon E, Bellocchio E, Edwards RH, Poo M (1997) Expression of a putative vesicular acetylcholine transporter facilitates quantal transmitter packaging. Cell Press 18:815-826.

Spann BM and Grofova I (1991) Nigropedunculopontine projection in the rat: an anterograde tracing study with phaseolus vulgarisleucoagglutinin (PHA-L). J Comp Neurol 311:375-388.

Stackman RW, Lora JC, Williams SB (2012) Directional responding of C57BL/6J mice in the Morris water maze is influenced by visual and vestibular cues and is dependent upon the anterior thalamic nuclei. J Neurosci 32:10211-10255.

Steckler T, Holsboer F (2001) Interaction between the cholinergic system and CRH in the modulation of spatial discrimination learning. Brain Res 906:46-59.

Steininger TL, Rye DB, Wainer BH (1992) Afferent projections to the cholinergic pedunculopontine tegmental nucleus and adjacent midbrain extrapyramidal area in the albino rat. I. Retrograde tracing studies. J Comp Neurol 321:515-543.

Steiniger and Kretschmer (2004) Effects of ibotenate pedunculopontine tegmental nucleus lesions on exploratory behavior in the open field. Behav Brain Res 151:17-23.

Steriade M, Pare D, Parent A, Smith Y (1988) Projections of cholinergic and non-cholinergic neurons of the brainstem core to relay and associational thalamic nuclei in the cat and macaque monkey. Neuroscience 25:47-67.

Sziklas V and Petrides M (1999) The effects of lesions to the anterior thalamic nuclei on object-place associations in rats. Eur J Neurosci 11:559-566.

Takakusaki K (2008) Forebrain control of locomotor behaviors. Brain Res Rev 57:192-198.

Takakusaki K, Shiroyama T, Yamamoto T, Kitai ST (1996) Cholinergic and noncholinergic tegmental pedunculopontine projection neurons in rats revealed by intracellular labeling. The Journal of comparative neurology 371:345-361.

Takakusaki K, Habaguchi T, Ohtinata-Sugimoto J, Saitoh K, Sakamoto T (2003) Basal ganglia efferents to the brainstem centres controlling postural muscle tone and locomotion: a new concept for understanding motor disorders in basal ganglia dysfunction. Neuroscience 119:293-308.

Taly A et al. (2009) Nicotinic receptors: allosteric transitions and therapeutic targets in the nervous system. Nat Rev Drug Discov 8:733-750.

Taylor CL, Kozak R, Latimer MP, Winn P (2004) Effects of changing reward on performance of the delayed spatial win-shift radial maze task in pedunculopontine tegmental nucleus lesioned rats. Behav Brain Res 153:431-438.

Thomas A et al. (2009) Marble burying reflects a repetitive and perseverative behavior more than novelty-induced anxiety. Psychopharmacol 204:361-373.

Thomsen M and Caine SB (2011) Psychomotor stimulant effects of cocaine in rates and 15 mouse strains. Exp Clin Psychopharmacol 19:321-341.

Tucek S (1985) Regulation of acetylcholine synthesis in the brain. J Neurochem 44:11-24.

Van Groen T and Wyss JM (1993) Projections from the anterodorsal and anteroventral nucleus of the thalamus to the limbic cortex in the rat. J Comp Neurol 358:584-604.

Vardy E, Arkin IT, Gottschalk KE, Kaback HR, Schuldiner S (2004) Structural conservation in the major facilitator superfamily as revealed by comparative modeling. Protein Sci 13:1832-1840.

Varoqui H and Erickson JD (1996) Active transport of acetylcholine by the human vesicular acetylcholine transporter. J Biol Chem 271:27229-27232.

Vorhees CV and Williams MT (2006) Morris water maze: procedures for assessing spatial and related forms of learning and memory. Nat Protoc 1:848-858.

Wang HL and Morales M (2009) Pedunculopontine and laterodorsal tegmental nuclei contain distinct populations of cholinergic, glutamatergic and GABAergic neurons in the rat. In: European Journal of Neuroscience, pp 340-358: Blackwell Publishing Ltd.

Warren NM, Piggott MA, Perry EK, Burn DJ (2005) Cholinergic systems in progressive supranuclear palsy. Brain 128:239-249.

Wenning GK, Ebersbach G, Verny M, Chaudhuri KR, Jellinger K, McKee A, et al. (1999) Progression of falls in postmortem-confirmed parkinsonian disorders. Mov Disord 14:947-950.

Wess J, Blin N, Yun J, Schoneberg T, Liu J (1996) Molecular aspects of muscarinic receptor assembly and function. Prog Brain Res 109:153-162.

Wess J, Duttaroy A, Zhang W, Gomeza J, Cui Y et al. (2003) M1-M5 muscarinic receptor knockout mice as novel tools to study the physiological roles of the muscarinic cholinergic system. Receptors Channels 9:279-290.

Wilson WL, Munn C, Ross RC, Harding JW, Wright JW (2009) The role of the AT4 and cholinergic systems in the Nucleus Basalis Magnocellularis (NBM): effects on spatial memory. Brain Res 1272:25-31.

Winn P, Brown VJ, Inglis WL (1997) On the relationships between the striatum and the pedunculopontine tegmental nucleus. Crit Rev Neurobiol 11:241-261.

Winn P (1998) Frontal syndrome as a consequence of lesions in the pedunculopontine tegmental nucleus: a short theoretical review. Brain Res Bull 47:551-563.

Winn P (2006) How best to consider the structure and function of the pedunculopontine tegmental nucleus: evidence from animal studies. Neurol Sci 248:234-250.

Woolf NJ and Butcher LL (1986) Cholinergic systems in the rat brain: III. Projections from the pontomesencephalic tegmentum to the thalamus, tectum, basal ganglia, and basal forebrain. Brain research bulletin 16:603-637.

Yamamura HI and Snyder SH (1972) Choline: high-affinity uptake by rat brain synaptosomes. Science 178:626–628.

Zaborszky L, Hoemke L, Mohlberg H, Schleicher A, Amunts K, Zilles K (2008) Stereotaxic probabilistic maps of the magnocellular cell groups in human basal forebrain. Neuroimage 42:1127-1141.

Zweig RM, Jankel WR, Hedreen JC, Mayeux R, Price DL (1989) The pedunculopontine nucleus in Parkinson's disease. Ann Neurol 26:41-46.

Curriculum Vitae

Name:	Kaie Rosborough
Post-secondary Education and Degrees:	The University of Western Ontario London, Ontario, Canada 2008-2012 B.Sc. The University of Western Ontario London, Ontario, Canada 2012-2014 M.Sc.
Honours and Awards:	Western Graduate Research Scholarship 2012-2013, 2013-2014 Nomination for Teaching Assistant Excellence Award for Oral Histology (Dentistry 5140) 2012-2013
Related Work Experience	Teaching Assistant for Oral Histology (Dentistry 5140) The University of Western Ontario 2012-2014
Papers	Understanding the role of cholinergic signaling from the PPT (In progress)
Posters	Understanding the role of cholinergic tone in the depression (2014) Robarts Research Retreat, London, ON. Understanding the role of cholinergic tone in the PPT (2014) London Health Research Day, London, ON. Understanding the role of cholinergic tone in the PPT (2014) Anatomy and Cell Biology Research Day, London, ON. Understanding the role of cholinergic signaling from the pedunculopontine tegmental nucleus on cognitive functioning through the selective elimination of the vesicular acetylcholine transporter (2013) Canadian Association for Neuroscience: Canadian Neuroscience Meeting, Toronto, ON.

Understanding the role of cholinergic signaling from the pedunculopontine tegmental nucleus on cognitive functioning through the selective elimination of the vesicular acetylcholine transporter (2013) London Health Research Day, London, ON.

Talks

The role of cholinergic signaling from the PPT in depression. (2014) Robarts Molecular Medicine Data Club, London, ON.